LYAPUNOV-BASED ROBUST AND ADAPTIVE CONTROL OF NONLINEAR SYSTEMS USING A NOVEL FEEDBACK STRUCTURE

By

PARAG PATRE

A DISSERTATION PRESENTED TO THE GRADUATE SCHOOL
OF THE UNIVERSITY OF FLORIDA IN PARTIAL FULFILLMENT
OF THE REQUIREMENTS FOR THE DEGREE OF
DOCTOR OF PHILOSOPHY

UNIVERSITY OF FLORIDA

2009

To my parents, Madhukar and Surekha Patre, and my sister, Aparna

ACKNOWLEDGMENTS

I would like to express sincere gratitude to my advisor, Dr. Warren E. Dixon, whose experience and motivation were instrumental in successful completion of my PhD. I appreciate his patience towards me and allowing me the freedom to work independently.

I would also like to extend my gratitude to my committee members Dr. Norman Fitz-Coy, Dr. Rick Lind, Dr. Pramod Khargonekar, and Dr. Frank Lewis for the time and help they provided.

I would like to thank my coworkers, family, and friends for their support and encouragement.

TABLE OF CONTENTS

LIST OF TABLES

LIST OF FIGURES

Abstract of Dissertation Presented to the Graduate School
of the University of Florida in Partial Fulfillment of the
Requirements for the Degree of Doctor of Philosophy

LYAPUNOV-BASED ROBUST AND ADAPTIVE CONTROL OF NONLINEAR SYSTEMS USING A NOVEL FEEDBACK STRUCTURE

By

Parag Patre

August 2009

Chair: Warren E. Dixon
Major: Mechanical Engineering

The focus of this research is an examination of the interplay between different intelligent feedforward mechanisms with a recently developed continuous robust feedback mechanism, coined Robust Integral of the Sign of the Error (RISE), to yield asymptotic tracking in the presence of generic disturbances. This result solves a decades long open problem of how to obtain asymptotic stability of nonlinear systems with general sufficiently smooth disturbances with a continuous control method. Further, it is shown that the developed technique can be fused with other feedforward methods such as function approximation and adaptive control methods. The addition of feedforward elements adds system knowledge in the control structure, which heuristically, yields better performance and reduces control effort. This heuristic notion is supported by experimental results in this research.

One key element in the development of the novel feedforward mechanisms presented in this dissertation is the modularity between the controller and update law. This modularity provides flexibility in the selection of different update laws that could be easier to implement or help to achieve faster parameter convergence and better tracking performance.

The efficacy of the feedforward mechanisms is further enhanced by including a prediction error in the learning process. The prediction error, which directly relates to

the actual function mismatch, is used along with the system tracking errors to develop a composite adaptation law.

Each result is supported through rigorous Lyapunov-based stability proofs and experimental demonstrations.

CHAPTER 1
INTRODUCTION

1.1 Motivation and Problem Statement

The control of systems with uncertain nonlinear dynamics has been a decades long mainstream area of focus. For systems with uncertainties that can be linear parameterized, a variety of adaptive (e.g., [1–3]) feedforward controllers can be utilized to achieve an asymptotic result. Some recent results have also targeted the application of adaptive controllers for systems that are not linear in the parameters [4]. Learning controllers have been developed for systems with periodic disturbances [5–7], and recent research has focused on the use of exosystems [8–11] to compensate for disturbances that are the solution of a linear time-invariant system with unknown coefficients. A variety of methods have also been proposed to compensate for systems with unstructured uncertainty including: various sliding mode controllers (e.g., [3, 12]), robust control schemes [13], and neural network and fuzzy logic controllers [14–18]. From a review of these approaches, a general trend is that controllers developed for systems with more unstructured uncertainty will require more control effort (i.e., high gain or high frequency feedback) and yield reduced performance (e.g., uniformly ultimately bounded stability).

Recently a new robust control strategy, coined Robust Integral of the Sign of the Error (RISE) in [19, 20], was developed in [21, 22] that can accommodate for sufficiently smooth bounded disturbances. A significant outcome of this new control structure is that asymptotic stability is obtained despite a fairly general uncertain disturbance. This technique was used in [23] to develop a tracking controller for nonlinear systems in the presence of additive disturbances and parametric uncertainties under the assumption that the disturbances are C^2 with bounded time derivatives. In [24], Xian et al. utilized this strategy to propose a new output feedback discontinuous tracking controller for a general class of second-order nonlinear systems whose uncertain dynamics are first-order differentiable. In [25], Zhang et al. combined the high gain feedback structure with a

high gain observer at the sacrifice of yielding a semi-global uniformly ultimately bounded result. This particular high gain feedback method has also been used as an identification technique. For example, the method has been applied to identify friction (e.g., [26]), for range identification in perspective and paracatadioptric vision systems (e.g., [27], [28]), and for fault detection and identification (e.g., [29]). The development in Chapter 2 is motivated by the desire to include some knowledge of the dynamics in the control design as a means to improve the performance and reduce the control effort. Specifically, for systems that include some dynamics that can be segregated into structured (i.e., linear parameterizable) and unstructured uncertainty, this chapter illustrates how a new controller, error system, and stability analysis can be crafted to include a model-based adaptive feedforward term in conjunction with the high gain RISE feedback technique to yield an asymptotic tracking result.

Another learning method that has been extensively investigated by control researchers over the last fifteen years is the use of neural networks (NNs) as a feedforward element in the control structure. The focus on NN-based control methods is spawned from the ramification of the fact that NNs are universal approximators [30]. That is, NNs can be used as a black-box estimator for a general class of systems. Examples include: nonlinear systems with parametric uncertainty that do not satisfy the linear-in-the-parameters assumption required in most adaptive control methods; systems with deadzones or discontinuities; and systems with backlash. Typically, NN-based controllers yield global uniformly ultimately bounded (UUB) stability results (e.g., see [15, 31, 32] for examples and reviews of literature) due to residual functional reconstruction inaccuracies and an inability to compensate for some system disturbances. Motivated by the desire to eliminate the residual steady-state errors, several researchers have obtained asymptotic tracking results by combining the NN feedforward element with discontinuous feedback methods such as variable structure controllers (VSC) (e.g., [33, 34]) or sliding mode (SM) controllers (e.g., [34, 35]). A clever VSC-like controller was also proposed in [36] where

the controller is not initially discontinuous, but exponentially becomes discontinuous as an exogenous control element exponentially vanishes. Well known limitations of VSC and SM controllers include a requirement for infinite control bandwidth and chattering. Unfortunately, ad hoc fixes for these effects result in a loss of asymptotic stability (i.e., UUB typically results). Motivated by issues associated with discontinuous controllers and the typical UUB stability result, an innovative continuous NN-based controller was recently developed in [37] to achieve partial asymptotic stability for a particular class of systems. The result in Chapter 3 is motivated by the question: *Can a NN feedforward controller be modified by a continuous feedback element to achieve an asymptotic tracking result for a general class of systems?* Despite the pervasive development of NN controllers in literature and the widespread use of NNs in industrial applications, the answer to this fundamental question has remained an open problem. To provide an answer to the fundamental motivating question, the result in Chapter 3 focuses on augmenting a multi-layer NN-based feedforward method with the RISE control strategy

Like most of the research in adaptive control, the results in Chapter 2 and 3 exploit Lyapunov-based techniques (i.e., the controller and the adaptive update law are designed based on a Lyapunov analysis); however, Lyapunov-based methods restrict the design of the adaptive update law. For example, many of the previous adaptive controllers are restricted to utilizing gradient update laws to cancel cross terms in a Lyapunov-based stability analysis. Gradient update laws can potentially exhibit slower parameter convergence which could lead to a degraded transient performance of the tracking error in comparison to other possible adaptive update laws (e.g., least-squares update law). Several results have been developed in literature that aim to augment the typical position/velocity tracking error-based gradient update law including: composite adaptive update laws [3, 38, 39]; prediction error-based update laws [1, 40–43]; and various least-squares update laws [44–46]. The adaptive update law in these results are all still designed to cancel cross terms in the Lyapunov-based stability analysis. In contrast to these results,

researchers have also developed a class of modular adaptive controllers (cf. [1, 40, 42, 43]) where a feedback mechanism is used to stabilize the error dynamics provided certain conditions are satisfied on the adaptive update law. For example, nonlinear damping [41, 47] is typically used to yield an input-to-state stability (ISS) result with respect to the parameter estimation error where it is assumed a priori that the update law yields bounded parameter estimates. Often the modular adaptive control development exploits a prediction error in the update law (e.g., see [3, 40–43]), where the prediction error is often required to be square integrable (e.g., [40, 42, 43]). A brief survey of modular adaptive control results is provided in [40]. Since the RISE feedback mechanism alone can yield an asymptotic result without a feedforward component to cancel cross terms in the stability analysis, the research in Chapter 4 is motivated by the following question: *Can the RISE control method be used to yield a new class of modular adaptive controllers?*

Typical adaptive, robust adaptive, and function approximation methods and the ones used in Chapters 2-4 use tracking error feedback to update the adaptive estimates. As mentioned earlier, the use of the tracking error is motivated by the need for the adaptive update law to cancel cross-terms in the closed-loop tracking error system within a Lyapunov-based analysis. As the tracking error converges, the rate of the update law also converges, but drawing conclusions about the convergent value (if any) of the parameter update law is problematic. Ideally, the adaptive update law would include some estimate of the parameter estimation error as a means to prove the parameter estimates converge to the actual values; however, the parameter estimate error is unknown. The desire to include some measurable form of the parameter estimation error in the adaptation law resulted in the development of adaptive update laws that are driven, in part, by a prediction error [3, 42, 48–50]. The prediction error is defined as the difference between the predicted parameter estimate value and the actual system uncertainty. Including feedback of the estimation error in the adaptive update law enables improved parameter estimation. For example, some classic results [1, 3, 41] have proven

the parameter estimation error is square integrable and that the parameter estimates may converge to the actual uncertain parameters. Since the prediction error depends on the unmeasurable system uncertainty, the swapping lemma [3, 42, 48–50] is central to the prediction error formulation. The swapping technique (also described as input or torque filtering in some literature) transforms a dynamic parametric model into a static form where standard parameter estimation techniques can be applied. In [1] and [41], a nonlinear extension of the swapping lemma was derived, which was used to develop the modular z-swapping and x-swapping identifiers via an input-to-state stable (ISS) controller for systems in parametric strict feedback form. The advantages provided by prediction error based adaptive update laws led to several results that use either the prediction error or a composite of the prediction error and the tracking error (cf. [43, 51–56] and the references within). Although prediction error based adaptive update laws have existed for approximately two decades, no stability result has been developed for systems with additive bounded disturbances. In general, the inclusion of disturbances reduces the steady-state performance of continuous controllers to a uniformly ultimately bounded (UUB) result. In addition to a UUB result, the inclusion of disturbances may cause unbounded growth of the parameter estimates [57] for tracking error-based adaptive update laws without the use of projection algorithms or other update law modifications such as σ-modification [58]. Problems associated with the inclusion of disturbances are magnified for control methods based on prediction error-based update laws because the formulation of the prediction error requires the swapping (or control filtering) method. Applying the swapping approach to dynamics with additive disturbances is problematic because the unknown disturbance terms also get filtered and included in the filtered control input. *This problem motivates the question of how can a prediction error-based adaptive update law be developed for systems with additive disturbances.* To address this motivating question, a general Euler-Lagrange-like MIMO system is considered in Chapter

5 with structured and unstructured uncertainties, and a gradient-based composite adaptive update law is developed that is driven by both the tracking error and the prediction error.

The swapping procedure used in standard adaptive control cannot be extended to NN controllers directly. The presence of a NN reconstruction error has impeded the development of composite adaptation laws for NNs. Specifically, the reconstruction error gets filtered and included in the prediction error destroying the typical prediction error formulation. Using the techniques developed in Chapter 5, the result in Chapter 6 presents the first ever attempt to develop a prediction error-based composite adaptive NN controller for an Euler-Lagrange second-order dynamic system using the RISE feedback.

A usual concern about the RISE feedback is the presence of high-gain and high-frequency components in the control structure. However, in contrast to a typical widely used discontinuous high-gain sliding mode controller, the RISE feedback offers a continuous alternative. Moreover, the proposed control designs are not purely high gain as an adaptive element is used as a feedforward component that learns and incorporates the knowledge of system dynamics in the control structure.

1.2 Contributions

This research focuses on combining various feedforward terms with the RISE feedback method for the control of uncertain nonlinear dynamic systems. The contributions of Chapters 2-6 are as follows.

Chapter 2: *Asymptotic Tracking for Systems with Structured and Unstructured Uncertainties*: The development in this chapter is motivated by the desire to include some knowledge of the dynamics in the control design as a means to improve the performance and reduce the control effort. Specifically, for systems that include some dynamics that can be segregated into structured (i.e., linear parameterizable) and unstructured uncertainty, this chapter illustrates how a new controller, error system, and stability analysis can be crafted to include a model-based adaptive feedforward term in conjunction with the RISE feedback technique to yield an asymptotic tracking result. This chapter

presents the first result that illustrates how the amalgamation of these compensation methods can be used to yield an asymptotic result.

Chapter 3: *Asymptotic Tracking for Uncertain Dynamic Systems via a Multilayer Neural Network Feedforward and RISE Feedback Control Structure*: The use of a NN as a feedforward control element to compensate for nonlinear system uncertainties has been investigated for over a decade. Typical NN-based controllers yield uniformly ultimately bounded (UUB) stability results due to residual functional reconstruction inaccuracies and an inability to compensate for some system disturbances. Several researchers have proposed discontinuous feedback controllers (e.g., variable structure or sliding mode controllers) to reject the residual errors and yield asymptotic results. The research in this chapter describes how the RISE feedback term can be incorporated with a NN-based feedforward term to achieve the first ever asymptotic tracking result. To achieve this result, the typical stability analysis for the RISE method is modified to enable the incorporation of the NN-based feedforward terms, and a projection algorithm is developed to guarantee bounded NN weight estimates. Experimental results are presented to demonstrate the performance of the proposed controller.

Chapter 4: *A New Class of Modular Adaptive Controllers*: A novel adaptive nonlinear control design is developed which achieves modularity between the controller and the adaptive update law. Modularity between the controller/update law design provides flexibility in the selection of different update laws that could potentially be easier to implement or used to obtain faster parameter convergence and/or better tracking performance. For a general class of linear-in-the-parameters (LP) uncertain multi-input multi-output systems subject to additive bounded non-LP disturbances, the developed controller uses a model-based feedforward adaptive term in conjunction with the RISE feedback term. Modularity in the adaptive feedforward term is made possible by considering a generic form of the adaptive update law and its corresponding parameter estimate. This generic form of the update law is used to develop a new closed-loop error

system and stability analysis that does not depend on nonlinear damping to yield the modular adaptive control result. The result is then extended by considering uncertain dynamic systems that are not necessarily LP, and have additive non-LP bounded disturbances. A multilayer NN structure is used in the non-LP extension as a feedforward element to compensate for the non-LP dynamics in conjunction with the RISE feedback term. A NN-based controller is developed with modularity in NN weight tuning laws and the control law. An extension is provided that describes how the control development for the general class of systems can be applied to a class of dynamic systems modeled by Euler-Lagrange formulation. Experimental results on a two-link robot are included to illustrate the concept.

Chapter 5: *Composite Adaptive Control for Systems with Additive Disturbances*: In a typical adaptive update law, the rate of adaptation is generally a function of the state feedback error. Ideally, the adaptive update law would also include some feedback of the parameter estimation error. The desire to include some measurable form of the parameter estimation error in the adaptation law resulted in the development of composite adaptive update laws that are functions of a prediction error and the state feedback. In all previous composite adaptive controllers, the formulation of the prediction error is predicated on the critical assumption that the system uncertainty is linear in the uncertain parameters (LP uncertainty). The presence of additive disturbances that are not LP would destroy the prediction error formulation and stability analysis arguments in previous results. In this chapter, a new prediction error formulation is constructed through the use of the RISE technique. The contribution of this design and associated stability analysis is that the prediction error can be developed even with disturbances that do not satisfy the LP assumption (e.g., additive bounded disturbances). A composite adaptive controller is developed for a general MIMO Euler-Lagrange system with mixed structured (i.e., LP) and unstructured uncertainties. A Lyapunov-based stability analysis is used to

derive sufficient gain conditions under which the proposed controller yields semi-global asymptotic tracking. Experimental results are presented to illustrate the approach.

Chapter 6: *Composite Adaptation for NN-Based Controllers*: With the motivation of using more information to update the parameter estimates, composite adaptation that uses both the system tracking errors and a prediction error containing parametric information to drive the update laws, has become widespread in adaptive control literature. However, despite its obvious benefits, composite adaptation has not been implemented in NN-based control, primarily due to the NN reconstruction error that destroys a typical prediction error formulation required for the composite adaptation. This chapter presents the first ever attempt to design a composite adaptation law for NNs by devising an innovative swapping procedure that uses the RISE feedback method. Semi-global asymptotic tracking for the system errors is proved, while all other signals and control input are shown to be bounded.

CHAPTER 2
ASYMPTOTIC TRACKING FOR SYSTEMS WITH STRUCTURED AND UNSTRUCTURED UNCERTAINTIES

2.1 Introduction

The development in this chapter is motivated by the desire to include some knowledge of the dynamics in the control design as a means to improve the performance and reduce the control effort. Specifically, for systems that include some dynamics that can be segregated into structured (i.e., linear parameterizable) and unstructured uncertainty, this chapter illustrates how a new controller and error system can be crafted to include a model-based adaptive feedforward term in conjunction with the RISE feedback technique to yield an asymptotic tracking result. This chapter presents the first result that illustrates how the amalgamation of these compensation methods can be used to yield an asymptotic result. Heuristically, the addition of the model-based adaptive feedforward term should reduce the overall control effort because some of the disturbance has been isolated and compensated for by a non-high gain feedforward element. Moreover, the addition of the adaptive feedforward term injects some knowledge of the dynamics in the control structure, which leads to improved performance. Experimental results are presented to reinforce these heuristic notions. Specifically, the presented controller was implemented on a simple rotating circular disk testbed and demonstrated reduced tracking error and control effort. For this testbed, the dynamics that were included in the feedforward term included the inertia of the linkage assembly, and the friction present in the system.

2.2 Dynamic Model

The class of nonlinear dynamic systems considered in this manuscript is assumed to be modeled by the following Euler-Lagrange formulation that describes the behavior of a large class of engineering systems:

$$M(q)\ddot{q} + V_m(q,\dot{q})\dot{q} + G(q) + f(\dot{q}) + \tau_d(t) = \tau(t). \tag{2–1}$$

In (2–1), $M(q) \in \mathbb{R}^{n \times n}$ denotes a generalized inertia matrix, $V_m(q, \dot{q}) \in \mathbb{R}^{n \times n}$ denotes a generalized centripetal-Coriolis matrix, $G(q) \in \mathbb{R}^n$ denotes a generalized gravity vector, $f(\dot{q}) \in \mathbb{R}^n$ denotes a generalized friction vector, $\tau_d(t) \in \mathbb{R}^n$ denotes a generalized nonlinear disturbance (e.g., unmodeled effects), $\tau(t) \in \mathbb{R}^n$ represents the generalized torque input control vector, and $q(t)$, $\dot{q}(t)$, $\ddot{q}(t) \in \mathbb{R}^n$ denote the generalized link position, velocity, and acceleration vectors, respectively. The friction term $f(\dot{q})$ in (2–1) is assumed to have the following form [26] and [59]:

$$f(\dot{q}) = \gamma_1(\tanh(\gamma_2\dot{q}) - \tanh(\gamma_3\dot{q})) + \gamma_4 \tanh(\gamma_5\dot{q}) + \gamma_6\dot{q}, \tag{2–2}$$

where $\gamma_i \in \mathbb{R}\ \forall i = 1, 2, ..., 6$ denote unknown positive constants. The friction model in (2–2) has the following properties: 1) it is symmetric about the origin, 2) it has a static coefficient of friction, 3) it exhibits the Stribeck effect where the friction coefficient decreases from the static coefficient of friction with increasing slip velocity near the origin, 4) it includes a viscous dissipation term, and 5) it has a Coulombic friction coefficient in the absence of viscous dissipation. To a good approximation, the static friction coefficient is given by $\gamma_1 + \gamma_4$, and the Stribeck effect is captured by $\tanh(\gamma_2\dot{q}) - \tanh(\gamma_3\dot{q})$. The Coulombic friction coefficient is given by $\gamma_4 \tanh(\gamma_5\dot{q})$, and the viscous dissipation is given by $\gamma_6\dot{q}$. For further details regarding the friction model, see [26] and [59]. The subsequent development is based on the assumption that $q(t)$ and $\dot{q}(t)$ are measurable and that $M(q)$, $V_m(q, \dot{q})$, $G(q)$, $f(\dot{q})$, and $\tau_d(t)$ are unknown. The error system systems utilized in this manuscript assume that the generalized coordinates, $q(t)$, of the Euler-Lagrange dynamics in (2–1) allow additive and not multiplicative errors. Moreover, the following assumptions will be exploited in the subsequent development:

Assumption 2-1: Symmetric and Positive-Definite Inertia Matrix

The inertia matrix $M(q)$ is symmetric, positive definite, and satisfies the following inequality $\forall \xi(t) \in \mathbb{R}^n$:

$$m_1 \|\xi\|^2 \leq \xi^T M(q) \xi \leq \bar{m}(q) \|\xi\|^2 \tag{2–3}$$

where $m_1 \in \mathbb{R}$ is a known positive constant, $\bar{m}(q) \in \mathbb{R}$ is a known positive function, and $\|\cdot\|$ denotes the standard Euclidean norm.

Assumption 2-2: If $q(t)$, $\dot{q}(t) \in \mathcal{L}_\infty$, then $V_m(q,\dot{q})$, $F(\dot{q})$ and $G(q)$ are bounded. Moreover, if $q(t)$, $\dot{q}(t) \in \mathcal{L}_\infty$, then the first and second partial derivatives of the elements of $M(q)$, $V_m(q,\dot{q})$, $G(q)$ with respect to $q(t)$ exist and are bounded, and the first and second partial derivatives of the elements of $V_m(q,\dot{q})$, $F(\dot{q})$ with respect to $\dot{q}(t)$ exist and are bounded.

Assumption 2-3: The nonlinear disturbance term and its first two time derivatives, i.e. $\tau_d(t)$, $\dot{\tau}_d(t)$, $\ddot{\tau}_d(t)$ are bounded by known constants.

Assumption 2-4: The desired trajectory is designed such that $q_d^{(i)}(t) \in \mathbb{R}^n$ $(i = 0, 1, ..., 4)$ exist and are bounded.

2.3 Error System Development

The control objective is to ensure that the system tracks a desired time-varying trajectory despite structured and unstructured uncertainties in the dynamic model. To quantify this objective, a position tracking error, denoted by $e_1(t) \in \mathbb{R}^n$, is defined as

$$e_1 = q_d - q. \tag{2–4}$$

To facilitate the subsequent analysis, filtered tracking errors, denoted by $e_2(t)$, $r(t) \in \mathbb{R}^n$, are also defined as

$$e_2 = \dot{e}_1 + \alpha_1 e_1 \tag{2–5}$$

$$r = \dot{e}_2 + \alpha_2 e_2, \tag{2–6}$$

where α_1, $\alpha_2 \in \mathbb{R}$ denote positive constants. The subsequent development is based on the assumption that $q(t)$ and $\dot{q}(t)$ are measurable, so the filtered tracking error $r(t)$ is not measurable since the expression in (2–6) depends on $\ddot{q}(t)$.

The open-loop tracking error system can be developed by premultiplying (2–6) by $M(q)$ and utilizing the expressions in (2–1)-(2–5) to obtain the following expression:

$$M(q)r = Y_d\theta + S + W_d + \tau_d(t) - \tau(t), \tag{2–7}$$

where $Y_d\left(q_d, \dot{q}_d, \ddot{q}_d\right)\theta \in \mathbb{R}^n$ is defined as

$$\begin{aligned} Y_d\theta \triangleq\ & M(q_d)\ddot{q}_d + V_m(q_d, \dot{q}_d)\dot{q}_d + G(q_d) + \gamma_1\left(\tanh\left(\bar{\gamma}_2\dot{q}_d\right) - \tanh\left(\bar{\gamma}_3\dot{q}_d\right)\right) \\ & + \gamma_4\tanh\left(\bar{\gamma}_5\dot{q}_d\right) + \gamma_6\dot{q}_d. \end{aligned} \tag{2–8}$$

In (2–8), $\theta \in \mathbb{R}^p$ contains the constant unknown system parameters, $Y_d\left(q_d, \dot{q}_d, \ddot{q}_d\right) \in \mathbb{R}^{n\times p}$ is the desired regression matrix that contains known functions of the desired link position, velocity, and acceleration, $q_d\left(t\right), \dot{q}_d\left(t\right), \ddot{q}_d\left(t\right) \in \mathbb{R}^n$, respectively, and $\bar{\gamma}_2$, $\bar{\gamma}_3$, $\bar{\gamma}_5 \in \mathbb{R}$ are the best guess estimates for γ_2, γ_3, and γ_5, respectively. In (2–7), the auxiliary function $S\left(q, \dot{q}, q_d, \dot{q}_d, \ddot{q}_d\right) \in \mathbb{R}^n$ is defined as

$$\begin{aligned} S \triangleq\ & M\left(q\right)\left(\alpha_1\dot{e}_1 + \alpha_2 e_2\right) + M\left(q\right)\ddot{q}_d - M(q_d)\ddot{q}_d + V_m(q, \dot{q})\dot{q} - V_m(q_d, \dot{q}_d)\dot{q}_d + G(q) - G(q_d) \\ & + \gamma_6\dot{q} - \gamma_6\dot{q}_d + \gamma_4\tanh\left(\gamma_5\dot{q}\right) - \gamma_4\tanh\left(\gamma_5\dot{q}_d\right) + \gamma_1\left(\tanh\left(\gamma_2\dot{q}\right) - \tanh\left(\gamma_3\dot{q}\right)\right) \\ & - \gamma_1\left(\tanh\left(\gamma_2\dot{q}_d\right) - \tanh\left(\gamma_3\dot{q}_d\right)\right), \end{aligned} \tag{2–9}$$

and the auxiliary function $W_d(\dot{q}_d) \in \mathbb{R}^n$ is defined as

$$\begin{aligned} W_d \triangleq\ & \gamma_4\tanh\left(\gamma_5\dot{q}_d\right) - \gamma_4\tanh\left(\bar{\gamma}_5\dot{q}_d\right) + \gamma_1\left(\tanh\left(\gamma_2\dot{q}_d\right) - \tanh\left(\gamma_3\dot{q}_d\right)\right) \\ & - \gamma_1\left(\tanh\left(\bar{\gamma}_2\dot{q}_d\right) - \tanh\left(\bar{\gamma}_3\dot{q}_d\right)\right). \end{aligned} \tag{2–10}$$

Based on the expression in (2–7), the control torque input is designed as

$$\tau = Y_d\hat{\theta} + \mu. \tag{2–11}$$

In (2–11), $\mu(t) \in \mathbb{R}^n$ denotes the RISE term defined as

$$\mu(t) \triangleq (k_s+1)e_2(t) - (k_s+1)e_2(0) + \int_0^t\left[(k_s+1)\alpha_2 e_2(\sigma) + \beta sgn(e_2(\sigma))\right]d\sigma, \tag{2–12}$$

where k_s, $\beta \in \mathbb{R}$ are positive, constant control gains, and $\hat{\theta}(t) \in \mathbb{R}^p$ denotes a parameter estimate vector generated on-line according to the following update law:

$$\dot{\hat{\theta}} = \Gamma \dot{Y}_d^T r \tag{2–13}$$

with $\Gamma \in \mathbb{R}^{p \times p}$ being a known, constant, diagonal, positive-definite adaptation gain matrix. Since $\dot{Y}_d(t)$ is only a function of the known desired time varying trajectory, (2–13) can be integrated by parts as follows:

$$\hat{\theta}(t) = \hat{\theta}(0) + \Gamma \dot{Y}_d^T e_2(\sigma)\Big|_0^t - \Gamma \int_0^t \left\{ \ddot{Y}_d^T e_2(\sigma) - \alpha_2 \dot{Y}_d^T e_2(\sigma) \right\} d\sigma \tag{2–14}$$

so that the parameter estimate vector $\hat{\theta}(t)$ implemented in (2–11) does not depend on the unmeasurable signal $r(t)$.

Remark 2.1. *The control design in (2–11) is similar to the results in [22]. However, previous designs based on [22] could only compensate for uncertainty in the system through the high gain RISE feedback term $\mu(t)$. Through the new development presented in the current result, an adaptive feedforward term can also be used to compensate for system uncertainty. This flexibility presents a significant advantage because it allows more system dynamics to be incorporated in the control design. Specifically, if some of the system uncertainty can be segregated into a linear parameterizable form, then the model-based adaptive feedforward term can be injected to compensate for the uncertainty instead of just relying on the non-model based high gain RISE feedback term. Heuristically, this contribution should improve the tracking performance and reduce the control effort. Experimental results on a simple one-link robot manipulator provide some validation of this heuristic idea.*

The closed-loop tracking error system can be developed by substituting (2–11) into (2–7) as

$$M(q)r = Y_d \tilde{\theta} + S + W_d + \tau_d - \mu(t), \tag{2–15}$$

where $\tilde{\theta}(t) \in \mathbb{R}^p$ represents the parameter estimation error vector defined as

$$\tilde{\theta} = \theta - \hat{\theta}. \tag{2–16}$$

To facilitate the subsequent stability analysis (and to illustrate some insight into the structure of the design for $\mu(t)$), the time derivative of (2–15) is determined as

$$M(q)\dot{r} = -\frac{1}{2}\dot{M}(q)r + \dot{Y}_d\tilde{\theta} + \tilde{N}(t) + N_d(t) - \dot{\mu}(t) - e_2, \tag{2–17}$$

where the unmeasurable auxiliary term $\tilde{N}(e_1, e_2, r) \in \mathbb{R}^n$ is defined as

$$\tilde{N}(t) \triangleq -Y_d\Gamma\dot{Y}_d^T r + \dot{S} - \frac{1}{2}\dot{M}(q)r + e_2, \tag{2–18}$$

where (2–13) was used. In (2–17), the unmeasurable auxiliary term $N_d(q_d, \dot{q}_d, \ddot{q}_d) \in \mathbb{R}^n$ is defined as

$$N_d(t) \triangleq \dot{W}_d + \dot{\tau}_d. \tag{2–19}$$

The time derivative of (2–12) is given as

$$\dot{\mu}(t) = (k_s + 1)r + \beta sgn(e_2). \tag{2–20}$$

In a similar manner as in [60], the Mean Value Theorem can be used to develop the following upper bound[1]

$$\left\|\tilde{N}(t)\right\| \leq \rho(\|z\|)\|z\|, \tag{2–21}$$

where $z(t) \in \mathbb{R}^{3n}$ is defined as

$$z(t) \triangleq \begin{bmatrix} e_1^T & e_2^T & r^T \end{bmatrix}^T. \tag{2–22}$$

The following inequalities can be developed based on the expression in (2–19) and its time derivative:

$$\|N_d(t)\| \leq \zeta_{N_d} \qquad \left\|\dot{N}_d(t)\right\| \leq \zeta_{N_{d2}}, \tag{2–23}$$

[1] See Lemma 1 of the Appendix for the proof of the inequality in (2–21).

where ζ_{N_d}, $\zeta_{N_{d2}} \in \mathbb{R}$ are known positive constants.

2.4 Stability Analysis

Theorem 2-1: The controller given in (2–11), (2–12), and (2–14) ensures that all system signals are bounded under closed-loop operation and that the position tracking error is regulated in the sense that

$$\|e_1(t)\| \to 0 \qquad \text{as} \qquad t \to \infty$$

provided the control gain k_s introduced in (2–12) is selected sufficiently large based on the initial conditions of the system (see the subsequent proof for details), α_1, α_2 are selected according to the following sufficient condition

$$\alpha_1 > \frac{1}{2}, \qquad \alpha_2 > 1 \tag{2–24}$$

and β is selected according to the following sufficient condition

$$\beta > \zeta_{N_d} + \frac{1}{\alpha_2}\zeta_{N_{d2}} \tag{2–25}$$

where ζ_{N_d} and $\zeta_{N_{d2}}$ are introduced in (2–23).

Proof: Let $\mathcal{D} \subset \mathbb{R}^{3n+p+1}$ be a domain containing $y(t) = 0$, where $y(t) \in \mathbb{R}^{3n+p+1}$ is defined as

$$y(t) \triangleq \left[z^T(t) \quad \tilde{\theta}^T(t) \quad \sqrt{P(t)} \right]^T \tag{2–26}$$

and the auxiliary function $P(t) \in \mathbb{R}$ is defined as

$$P(t) \triangleq \beta \sum_{i=1}^{n} |e_{2i}(0)| - e_2(0)^T N_d(0) - \int_0^t L(\tau) d\tau \tag{2–27}$$

where the subscript $i = 1, 2, .., n$ denotes the ith element of the vector. In (2–27), the auxiliary function $L(t) \in \mathbb{R}$ is defined as

$$L(t) \triangleq r^T \left(N_d(t) - \beta sgn(e_2) \right). \tag{2–28}$$

The derivative $\dot{P}(t) \in \mathbb{R}$ can be expressed as

$$\dot{P}(t) = -L(t) = -r^T(N_d(t) - \beta sgn(e_2)). \tag{2–29}$$

Provided the sufficient condition introduced in (2–25) is satisfied, the following inequality can be obtained[2] :

$$\int_0^t L(\tau)d\tau \leq \beta \sum_{i=1}^{n} |e_{2i}(0)| - e_2(0)^T N_d(0). \tag{2–30}$$

Hence, (2–30) can be used to conclude that $P(t) \geq 0$.

Let $V(y,t) : \mathcal{D} \times [0,\infty) \to \mathbb{R}$ be a continuously differentiable, positive definite function defined as

$$V(y,t) \triangleq e_1^T e_1 + \frac{1}{2} e_2^T e_2 + \frac{1}{2} r^T M(q) r + P + \frac{1}{2} \tilde{\theta}^T \Gamma^{-1} \tilde{\theta} \tag{2–31}$$

which satisfies the following inequalities:

$$U_1(y) \leq V(y,t) \leq U_2(y) \tag{2–32}$$

provided the sufficient condition introduced in (2–25) is satisfied. In (2–32), the continuous, positive definite functions $U_1(y)$, $U_2(y) \in \mathbb{R}$ are defined as

$$U_1(y) \triangleq \eta_1 \|y\|^2 \qquad U_2(y) \triangleq \eta_2(q) \|y\|^2 \tag{2–33}$$

where η_1, $\eta_2(q) \in \mathbb{R}$ are defined as

$$\eta_1 \triangleq \frac{1}{2} \min \left\{1, m_1, \lambda_{\min} \left\{\Gamma^{-1}\right\}\right\}$$
$$\eta_2(q) \triangleq \max \left\{\frac{1}{2}\bar{m}(q), \frac{1}{2}\lambda_{\max} \left\{\Gamma^{-1}\right\}, 1\right\}$$

where m_1, $\bar{m}(q)$ are introduced in (2–3) and $\lambda_{\min}\{\cdot\}$, $\lambda_{\max}\{\cdot\}$ denote the minimum and maximum eigenvalues, respectively, of the argument. After taking the time derivative of

[2] The inequality in (2–30) can be obtained in a similar manner as in Lemma 2 of the Appendix.

(2–31), $\dot{V}(y,t)$ can be expressed as

$$\dot{V}(y,t) = r^T M(q)\dot{r} + \frac{1}{2} r^T \dot{M}(q) r + e_2^T \dot{e}_2 + 2e_1^T \dot{e}_1 + \dot{P} - \tilde{\theta}^T \Gamma^{-1} \dot{\hat{\theta}}.$$

Remark 2.2. *From (2–17), (2–27) and (2–28), some of the differential equations describing the closed-loop system for which the stability analysis is being performed have discontinuous right-hand sides as*

$$M\dot{r} = -\frac{1}{2}\dot{M}(q)r + \dot{Y}_d\tilde{\theta} + \tilde{N}(t) + N_d(t) - (k_s+1)r - \beta_1 sgn(e_2) - e_2 \tag{2–34}$$

$$\dot{P}(t) = -L(t) = -r^T(N_d(t) - \beta sgn(e_2)) \tag{2–35}$$

Let $f(y,t) \in \mathbb{R}^{n+1}$ denote the right-hand side of (2–34)–(2–35). Since the subsequent analysis requires that a solution exists for $\dot{y} = f(y,t)$, it is important to show the existence and uniqueness of the solution to (2–34)–(2–35). As described in [13, 61], the existence of Filippov's generalized solution can be established for (2–34)–(2–35). First, note that $f(y,t)$ is continuous except in the set $\{(y,t) \,|\, e_2 = 0\}$. Let $\mathcal{F}(y,t)$ be a compact, convex, upper semicontinuous set-valued map that embeds the differential equation $\dot{y} = f(y,t)$ into the differential inclusions $\dot{y} \in \mathcal{F}(y,t)$. From Theorem 27 of [13], an absolute continuous solution exists to $\dot{y} \in \mathcal{F}(y,t)$ that is a generalized solution to $\dot{y} = f(y,t)$. A common choice for $\mathcal{F}(y,t)$ that satisfies the above conditions is the closed convex hull of $f(y,t)$ [13, 61]. A proof that this choice for $\mathcal{F}(y,t)$ is upper semicontinuous is given in [62]. Moreover, note that the differential equation describing the original closed-loop system (i.e., after substituting (2–11) into (2–1)) has a continuous right-hand side; thus, satisfying the condition for existence of classical solutions. Similar arguments are used for all the results in this dissertation.

After utilizing (2–5), (2–6), (2–13), (2–17), (2–20), and (2–29), $\dot{V}(y,t)$ can be simplified as

$$\dot{V}(y,t) = r^T \tilde{N}(t) - (k_s+1)\|r\|^2 - \alpha_2 \|e_2\|^2 - 2\alpha_1 \|e_1\|^2 + 2e_2^T e_1. \tag{2–36}$$

Because $e_2^T(t)e_1(t)$ can be upper bounded as

$$e_2^T e_1 \leq \frac{1}{2}\|e_1\|^2 + \frac{1}{2}\|e_2\|^2$$

$\dot{V}(y,t)$ can be upper bounded using the squares of the components of $z(t)$ as follows:

$$\dot{V}(y,t) \leq r^T \tilde{N}(t) - (k_s+1)\|r\|^2 - \alpha_2\|e_2\|^2 - 2\alpha_1\|e_1\|^2 + \|e_1\|^2 + \|e_2\|^2.$$

By using (2–21), the expression in (2–36) can be rewritten as follows:

$$\dot{V}(y,t) \leq -\eta_3\|z\|^2 - \left(k_s\|r\|^2 - \rho(\|z\|)\|r\|\|z\|\right) \tag{2–37}$$

where $\eta_3 \triangleq \min\{2\alpha_1 - 1, \alpha_2 - 1, 1\}$, and the bounding function $\rho(\|z\|) \in \mathbb{R}$ is a positive, globally invertible, nondecreasing function; hence, α_1, and α_2 must be chosen according to the sufficient conditions in (2–24). After completing the squares for the parenthetic terms in (2–37), the following expression can be obtained:

$$\dot{V}(y,t) \leq -\eta_3\|z\|^2 + \frac{\rho^2(\|z\|)\|z\|^2}{4k_s}. \tag{2–38}$$

The expression in (2–38) can be further upper bounded by a continuous, positive semi-definite function

$$\dot{V}(y,t) \leq -U(y) = -c\|z\|^2 \qquad \forall y \in \mathcal{D} \tag{2–39}$$

for some positive constant $c \in \mathbb{R}$, where

$$\mathcal{D} \triangleq \left\{ y \in \mathbb{R}^{3n+p+1} \mid \|y\| \leq \rho^{-1}\left(2\sqrt{\eta_3 k_s}\right)\right\}.$$

Larger values of k will expand the size of the domain $\mathcal{D}$. The inequalities in (2–32) and (2–39) can be used to show that $V(y,t) \in \mathcal{L}_\infty$ in $\mathcal{D}$; hence, $e_1(t)$, $e_2(t)$, $r(t)$, and $\tilde{\theta}(t) \in \mathcal{L}_\infty$ in $\mathcal{D}$. Given that $e_1(t)$, $e_2(t)$, and $r(t) \in \mathcal{L}_\infty$ in $\mathcal{D}$, standard linear analysis methods can be used to prove that $\dot{e}_1(t)$, $\dot{e}_2(t) \in \mathcal{L}_\infty$ in $\mathcal{D}$ from (2–5) and (2–6). Since $\theta \in \mathbb{R}^p$ contains the constant unknown system parameters and $\tilde{\theta}(t) \in \mathcal{L}_\infty$ in $\mathcal{D}$, (2–16) can be used to

prove that $\hat{\theta}(t) \in \mathcal{L}_\infty$ in $\mathcal{D}$. Since $e_1(t)$, $e_2(t)$, $r(t) \in \mathcal{L}_\infty$ in $\mathcal{D}$, the assumption that $q_d(t)$, $\dot{q}_d(t)$, $\ddot{q}_d(t)$ exist and are bounded can be used along with (2–4)-(2–6) to conclude that $q(t)$, $\dot{q}(t)$, $\ddot{q}(t) \in \mathcal{L}_\infty$ in $\mathcal{D}$. The assumption that $q_d(t)$, $\dot{q}_d(t)$, $\ddot{q}_d(t)$, $\dddot{q}_d(t)$, $\ddddot{q}_d(t)$ exist and are bounded along with (2–8) can be used to show that $Y_d\left(q_d, \dot{q}_d, \ddot{q}_d\right)$, $\dot{Y}_d\left(q_d, \dot{q}_d, \ddot{q}_d, \dddot{q}_d\right)$, and $\ddot{Y}_d\left(q_d, \dot{q}_d, \ddot{q}_d, \dddot{q}_d, \ddddot{q}_d\right) \in \mathcal{L}_\infty$ in $\mathcal{D}$. Since $q(t)$, $\dot{q}(t) \in \mathcal{L}_\infty$ in $\mathcal{D}$, Assumption 2-2 can be used to conclude that $M(q)$, $V_m(q, \dot{q})$, $G(q)$, and $F(\dot{q}) \in \mathcal{L}_\infty$ in $\mathcal{D}$. Thus from (2–1) and Assumption 2-3, we can show that $\tau(t) \in \mathcal{L}_\infty$ in $\mathcal{D}$. Given that $r(t) \in \mathcal{L}_\infty$ in $\mathcal{D}$, (2–20) can be used to show that $\dot{\mu}(t) \in \mathcal{L}_\infty$ in $\mathcal{D}$. Since $\dot{q}(t)$, $\ddot{q}(t) \in \mathcal{L}_\infty$ in $\mathcal{D}$, Assumption 2-2 can be used to show that $\dot{V}_m(q, \dot{q})$, $\dot{G}(q)$, $F(q)$ and $\dot{M}(q) \in \mathcal{L}_\infty$ in $\mathcal{D}$; hence, (2–17) can be used to show that $\dot{r}(t) \in \mathcal{L}_\infty$ in $\mathcal{D}$. Since $\dot{e}_1(t)$, $\dot{e}_2(t)$, $\dot{r}(t) \in \mathcal{L}_\infty$ in $\mathcal{D}$, the definitions for $U(y)$ and $z(t)$ can be used to prove that $U(y)$ is uniformly continuous in $\mathcal{D}$.

Let $\mathcal{S} \subset \mathcal{D}$ denote a set defined as follows:[3]

$$\mathcal{S} \triangleq \left\{ y(t) \in \mathcal{D} \mid U\left(y(t)\right) < \eta_1 \left(\rho^{-1} \left(2\sqrt{\eta_3 k_s} \right) \right)^2 \right\}. \tag{2–40}$$

Theorem 8.4 of [63] can now be invoked to state that

$$c \left\| z(t) \right\|^2 \to 0 \qquad \text{as} \qquad t \to \infty \qquad \forall y(0) \in \mathcal{S}. \tag{2–41}$$

Based on the definition of $z(t)$, (2–41) can be used to show that

$$\left\| e_1(t) \right\| \to 0 \qquad \text{as} \qquad t \to \infty \qquad \forall y(0) \in \mathcal{S}.$$

□

2.5 Experimental Results

The testbed depicted in Figure 2-1 was used to implement the developed controller. The testbed consists of a circular disc of unknown inertia mounted on a NSK direct-drive

[3] The region of attraction in (2–40) can be made arbitrarily large to include any initial conditions by increasing the control gain k_s (i.e., a semi-global type of stability result) [22].

Figure 2-1. The experimental testbed consists of a circular disk mounted on a NSK direct-drive switched reluctance motor.

switched reluctance motor (240.0 Nm Model YS5240-GN001). The NSK motor is controlled through power electronics operating in torque control mode. The motor resolver provides rotor position measurements with a resolution of $614,400$ pulses/revolution. A Pentium 2.8 GHz PC operating under QNX hosts the control algorithm, which was implemented via Qmotor 3.0, a graphical user-interface, to facilitate real-time graphing, data logging, and adjustment of control gains without recompiling the program (for further information on Qmotor 3.0, the reader is referred to [64]). Data acquisition and control implementation were performed at a frequency of 1.0 kHz using the ServoToGo I/O board. A rectangular nylon block was mounted on a pneumatic linear thruster to apply an external friction load to the rotating disk. A pneumatic regulator maintained a constant pressure of 20 pounds per square inch on the circular disk.

The dynamics for the testbed are given as follows:

$$J\ddot{q} + f(\dot{q}) + \tau_d(t) = \tau(t), \tag{2–42}$$

where $J \in \mathbb{R}$ denotes the combined inertia of the circular disk and rotor assembly, the friction torque $f(\dot{q}) \in \mathbb{R}$ is defined in (2–2), and $\tau_d(t) \in \mathbb{R}$ denotes a general nonlinear disturbance (e.g., unmodeled effects). The parameters γ_2, γ_3, γ_5 are embedded inside

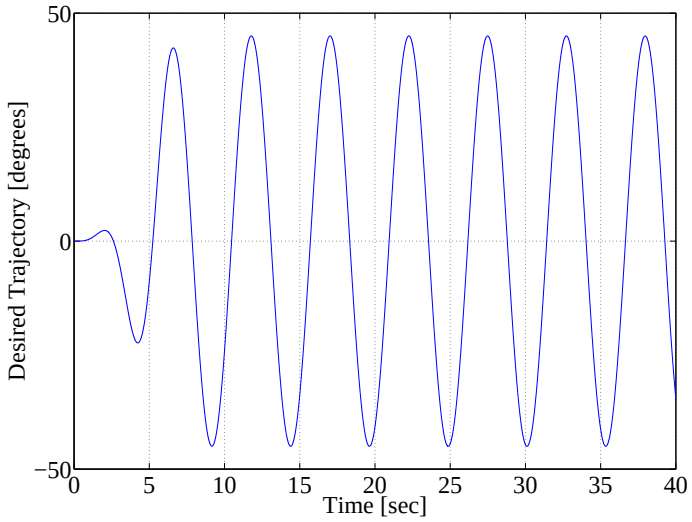

Figure 2-2. Desired trajectory used for the experiment.

the nonlinear hyperbolic tangent functions and hence cannot be linearly parameterized. Since these parameters cannot be compensated for by an adaptive algorithm, best-guess estimates $\bar{\gamma}_2 = 50$, $\bar{\gamma}_3 = 1$, $\bar{\gamma}_5 = 50$ are used. The values for $\bar{\gamma}_2$, $\bar{\gamma}_3$, $\bar{\gamma}_5$ are based on previous experiments concerned with friction identification. Significant errors in these static estimates could degrade the performance of the system. The control torque input $\tau(t)$ is given by (2–11), where $Y_d(\dot{q}_d, \ddot{q}_d) \in \mathbb{R}^{1\times 4}$ is the regression matrix defined as

$$Y_d \triangleq \left[\ddot{q}_d \quad \tanh(\bar{\gamma}_2\dot{q}_d) - \tanh(\bar{\gamma}_3\dot{q}_d) \quad \tanh(\bar{\gamma}_5\dot{q}_d) \quad \dot{q}_d\right],$$

and $\hat{\theta}(t) \in \mathbb{R}^4$ is the vector consisting of the unknown parameters defined as

$$\hat{\theta} \triangleq \left[\hat{J} \quad \hat{\gamma}_1 \quad \hat{\gamma}_4 \quad \hat{\gamma}_6\right]^T. \tag{2–43}$$

The parameter estimates vector in (2–43) is generated on-line using the adaptive update law in (2–14). The desired link trajectory (see Figure 2-2) was selected as follows (in degrees):

$$q_d(t) = 45.0\sin(1.2t)(1 - \exp(-0.01t^3)). \tag{2–44}$$

For all experiments, the rotor velocity signal is obtained by applying a standard

backwards difference algorithm to the position signal. The integral structure of the adaptive term in (2–14) and the RISE term in (2–12) was computed on-line via a standard trapezoidal algorithm. In addition, all the states and unknown parameters were initialized to zero. The signum function for the control scheme in (2–12) was defined as:

$$sgn(e_2(t)) = \begin{cases} 1 & e_2 > 0.0005 \\ 0 & -0.0005 < e_2 \leq 0.0005 \\ -1 & e_2 \leq -0.0005 \end{cases} .$$

The RISE controller is composed of proportional-integral-derivative (PID) elements and the integral of sign term. There are several tuning techniques available in the literature for the PID elements in the controller, however, the control gains were obtained by choosing gains and then adjusting based on performance. If the response exhibited a prolonged transient response (compared with the response obtained with other gains), the proportional and integral gains were adjusted. If the response exhibited overshoot, derivative gains were adjusted. To fine tune the performance, the adaptive gains were adjusted after the feedback gains were tuned as described to yield the best performance. In contrast to this approach of adjusting the control and adaptation gains, the control gains could potentially be adjusted using more methodical approaches. For example, the nonlinear system in [65] was linearized at several operating points and a linear controller was designed for each point, and the gains were chosen by interpolating, or scheduling the linear controllers. In [66], a neural network is used to tune the gains of a PID controller. In [67], a genetic algorithm was used to fine tune the gains after an initialization. Additionally, in [68], the tuning of a PID controller for robot manipulators is discussed.

Experiment 1

In the first experiment, the controller in (2–11) was implemented without including the adaptation term. Thus the control torque input given in (2–11) takes the following

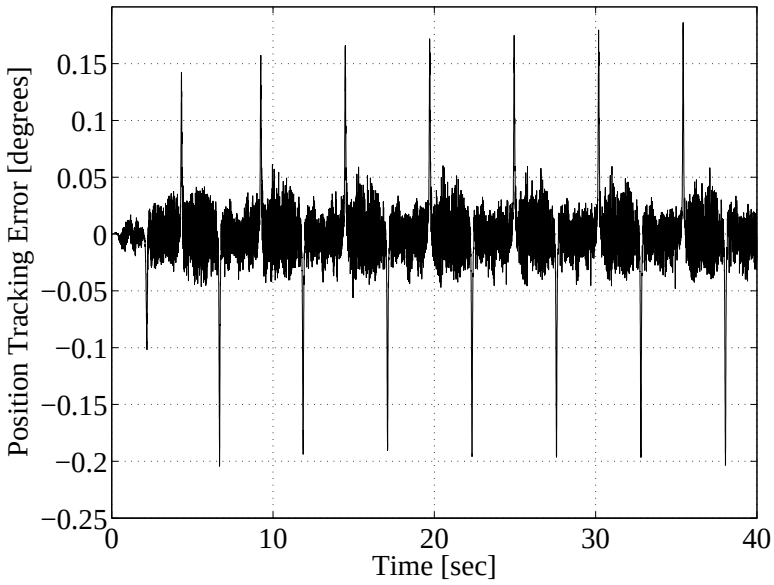

Figure 2-3. Position tracking error without the adaptive feedforward term.

form [22]:

$$\tau(t) = \mu(t).$$

The gains for the controller that yielded the best steady-state performance were determined as follows:

$$k_s = 100 \quad \beta = 115 \quad \alpha_1 = 40 \quad \alpha_2 = 30. \tag{2–45}$$

The position tracking error obtained from the controller is plotted in Figure 2-3, and the torque input by the controller is depicted in Figure 2-4.

Experiment 2

In the second experiment, the control input given in (2–11) was used. The update law defined in (2–14) was used to update the parameter estimates defined in (2–43). The following control gains and best guess estimates were used to implement the controller in (2–11):

$$k_s = 100 \quad \beta = 115 \quad \alpha_1 = 40 \quad \alpha_2 = 30 \quad \Gamma = diag\{10,\, 1,\, 1,\, 10\} \cdot$$

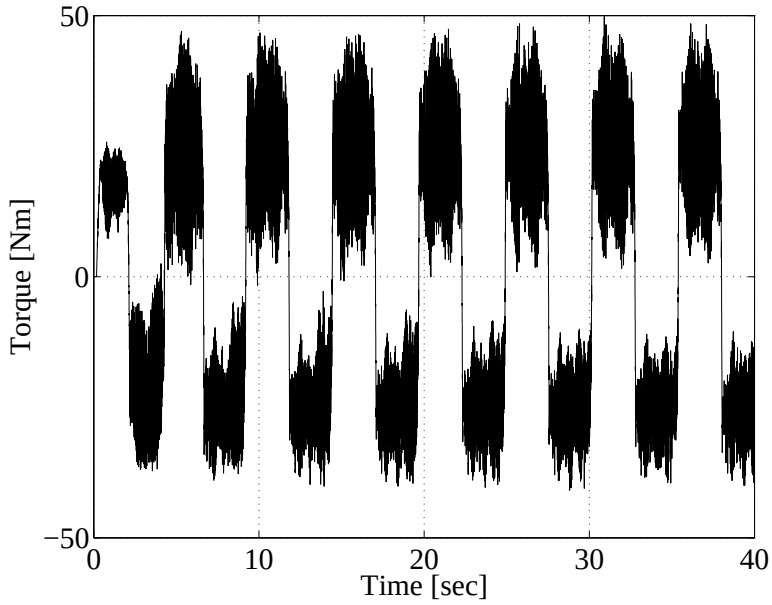

Figure 2-4. Torque input without the adaptive feedforward term.

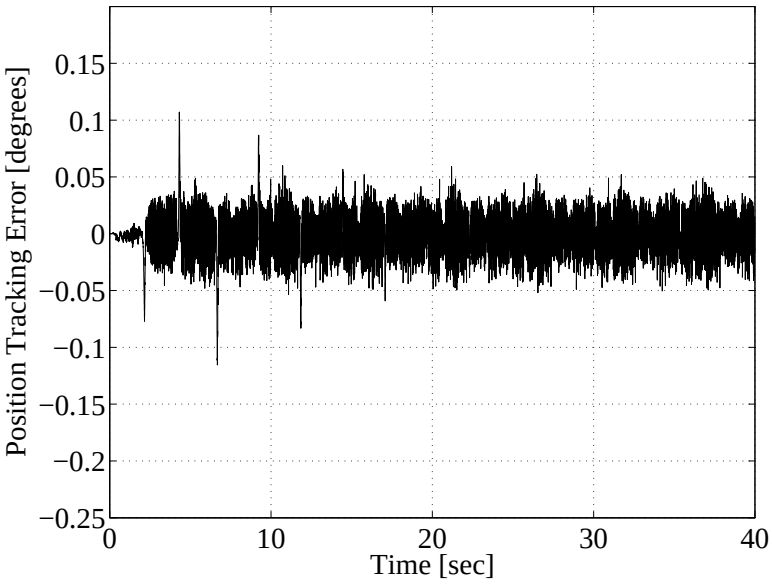

Figure 2-5. Position tracking error for the control structure that includes the adaptive feedforward term.

The position tracking error obtained from the controller is plotted in Figure 2-5, the parameter estimates are depicted in Figure 2-6, the contribution of the RISE term is shown in Figure 2-8, and the torque input by the controller is depicted in Figure 2-7.

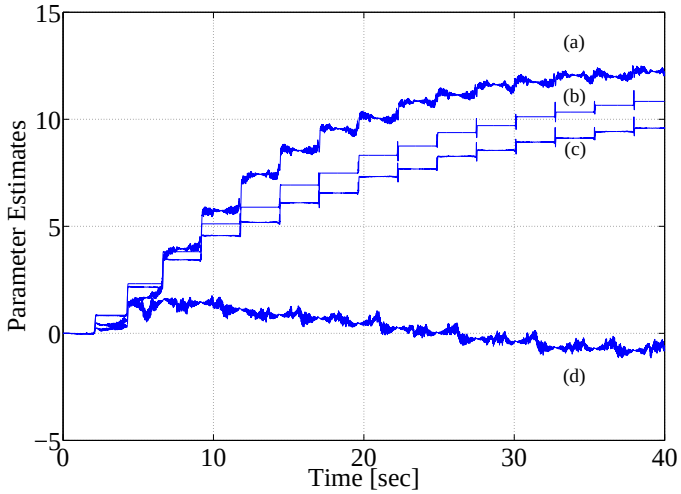

Figure 2-6. Parameter estimates of the adaptive feedforward component: (a) $\hat{\gamma}_1$, (b) $\hat{\gamma}_4$, (c) $\hat{\gamma}_6$, (d) $\hat{J}$.

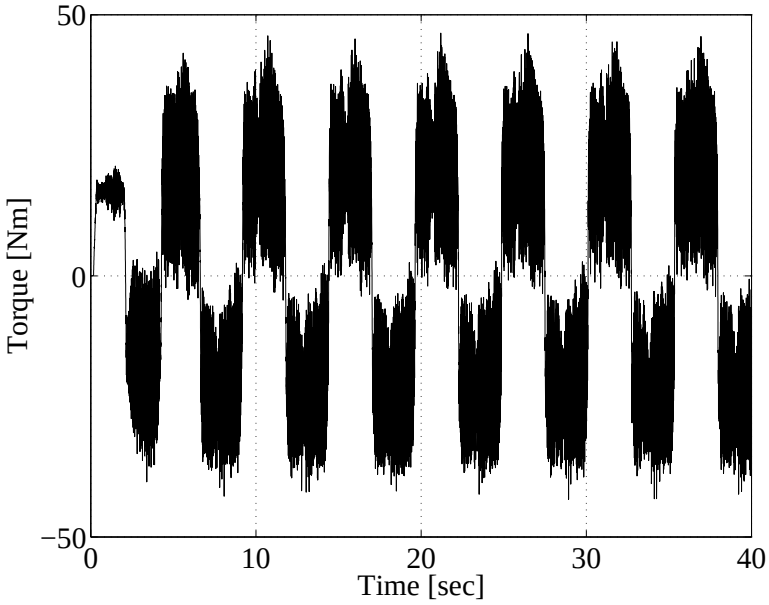

Figure 2-7. Torque input for the control structure that includes the adaptive feedforward term.

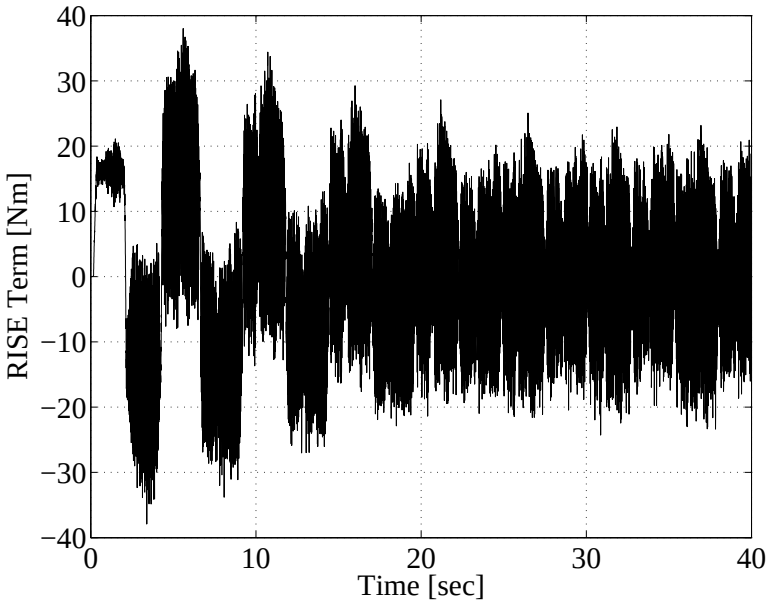

Figure 2-8. The contribution of the RISE term for the control structure that includes the adaptive feedforward term.

2.6 Discussion

Figure 2-5 illustrates that the incorporation of a model-based feedforward term eliminates the *spikes* present in Figure 2-3 that occur when the motor changes direction. The spikes are initially present in Figure 2-5, but reduce in magnitude and vanish as the adaptive update converges. These figures exactly illustrate how the addition of the adaptive feedforward element injects model knowledge into the control design to improve the overall performance. Figure 2-8 indicates that the contribution of the RISE term in the overall torque decreases with time as the feedforward adaptation term begins to compensate for part of the disturbances.

Both the experiments were repeated 10 consecutive times with the same gain values to check the repeatability and accuracy of the results. For each run, the root mean squared (RMS) values of the position tracking errors and torques are calculated. The average of these RMS values for the two cases (with adaptation and without adaptation) obtained over 10 sets are plotted in Figure 2-9, where the bars indicate the variance about the mean. An unpaired t-test assuming equal variances was performed using a statistical

package (Microsoft Office Excel 2003) with a significance level of $\alpha = 0.05$. The results of the t-test for the RMS error, and the RMS torque are shown in Table 2-1 and Table 2-2, respectively. Table 2-1 indicates that the P value obtained for the one-tailed test is less than the significance level α. Thus, the mean RMS error for case 2 is lower than that of case 1, and this difference is statistically significant. Similarly, from Table 2-2, the mean RMS torque for case 2 is lower than that of case 1. The results indicate that the mean RMS value of the position tracking error when the adaptive feedforward term is used is about 43.5% less than the case when no adaptation term is used. This improvement in performance by the proposed controller was obtained while using 17.6% less input torque as shown in Figure 2-9.

While the developed controller is a continuous controller, it can exhibit some high frequency content due to the presence of the integral sign function. However, the frequency content is finite unlike current discontinuous nonlinear control methods. The experimental results show some chattering in the input/output signals, but the mechanical system acts a low-pass filter because the actuator bandwidth is lower than the bandwidth produced by the controller. Also, the controller requires full-state feedback (i.e., both position and velocity measurements are needed), but as mentioned earlier, only the position is measured and the velocity is obtained by an unfiltered backward difference algorithm. The need for velocity feedback is also a source of noise, especially for the sub-degree errors that the controller yields.

2.7 Conclusions

A new class of asymptotic controllers is developed that contains an adaptive feedforward term to account for linear parameterizable uncertainty and a high gain feedback term which accounts for unstructured disturbances. In comparison with previous results that used a similar high gain feedback control structure, new control development, error systems and stability analysis arguments were required to include the additional adaptive feedforward term. The motivation for injecting the adaptive feedforward term is

Table 2-1. t-test: two samples assuming equal variances for RMS error

	RMS Error	
	Variable 1	Variable 2
Mean	3.214×10^{-2}	1.817×10^{-2}
Variance	1.044×10^{-5}	3.170×10^{-7}
Observations	10	10
Pooled Variance	5.378×10^{-6}	
Hypothesized Mean Difference	0	
df	18	
t Stat	13.47	
P(T<=t) one-tail	3.847×10^{-11}	
t Critical one-tail	1.734	
P(T<=t) two-tail	7.693×10^{-11}	
t Critical two-tail	2.101	

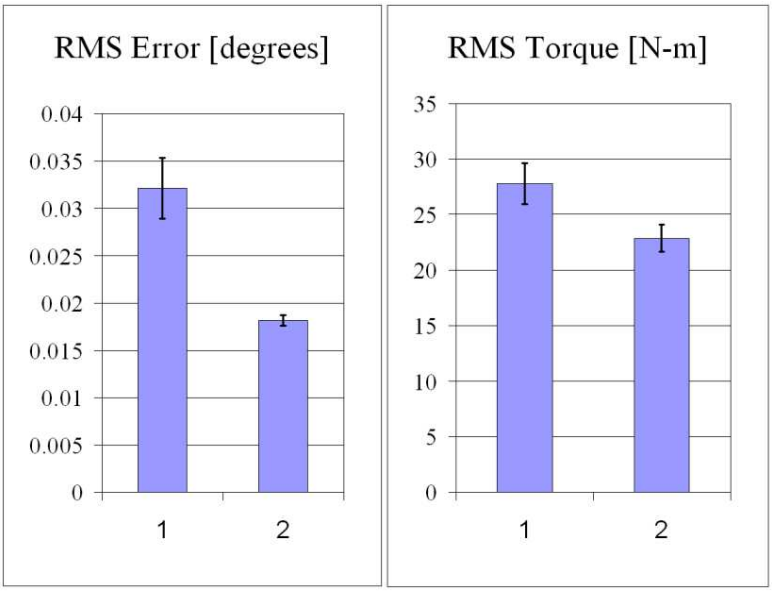

Figure 2-9. RMS position tracking errors and torques for the two cases - (1) without the adaptation term in the control input, (2) with the adaptation term in the control input.

Table 2-2. t-test: two samples assuming equal variances for RMS torque

	RMS Torque	
	Variable 1	Variable 2
Mean	27.79	22.90
Variance	3.452	1.474
Observations	10	10
Pooled Variance	2.463	
Hypothesized Mean Difference	0	
df	18	
t Stat	3.971	
P(T<=t) one-tail	8.208×10^{-7}	
t Critical one-tail	1.734	
P(T<=t) two-tail	1.642×10^{-6}	
t Critical two-tail	2.101	

that improved tracking performance and reduced control effort result from including more knowledge of the system dynamics in the control structure. This heuristic idea was verified by our experimental results that indicate reduced control effort and reduced RMS tracking errors.

CHAPTER 3
ASYMPTOTIC TRACKING FOR UNCERTAIN DYNAMIC SYSTEMS VIA A MULTILAYER NEURAL NETWORK FEEDFORWARD AND RISE FEEDBACK CONTROL STRUCTURE

3.1 Introduction

The contribution in this chapter is motivated by the question: *Can a NN feedforward controller be modified by a continuous feedback element to achieve an asymptotic tracking result for a general class of systems?* Despite the pervasive development of NN controllers in literature and the widespread use of NNs in industrial applications, the answer to this fundamental question has remained an open problem.

To provide an answer to the fundamental motivating question, the result in this chapter focuses on augmenting a multi-layer NN-based feedforward method with a recently developed [21] high gain control strategy coined the Robust Integral of the Sign of the Error (RISE) in [19, 20]. The RISE control structure is advantageous because it is a differentiable control method that can compensate for additive system disturbances and parametric uncertainties under the assumption that the disturbances are C^2 with bounded time derivatives. Due to the advantages of the RISE control structure a flurry of results have recently been developed (e.g., [22, 23, 25–27]).

A RISE feedback controller can be directly applied to yield asymptotic stability for the class of systems described in this chapter. However, the RISE method is a high-gain feedback tool, and hence, clear motivation exists (as with any other feedback controller) to combine a feedforward control element with the feedback controller for potential gains such as improved transient and steady-state performance, and reduced control effort. That is, it is well accepted that a feedforward component can be used to cancel out some dynamic effects without relying on high-gain feedback. Given this motivation, some results have already been developed that combine the RISE feedback element with feedforward terms. In [60], a remark is provided regarding the use of a constant best-guess feedforward component in conjunction with the RISE method to yield a UUB result. In [19, 20], the

RISE feedback controller was combined with a standard gradient feedforward term for systems that satisfy the linear-in-the-parameters assumption. The experimental results in [19] illustrate significant improvement in the root-mean-squared tracking error with reduced root-mean-squared control effort. However, for systems that do not satisfy the linear-in-the-parameters assumption, motivation exists to combine the RISE controller with a new feedforward method such as the NN.

To blend the NN and RISE methods, several technical challenges must be addressed. One (lesser) challenge is that the NN must be constructed in terms of the desired trajectory instead of the actual trajectory (i.e., a DCAL-based NN structure [36]) to remove the dependence on acceleration. The development of a DCAL-based NN structure is challenging for a multi-layer NN because the adaptation law for the weights is required to be state-dependent. Straightforward application of the RISE method would yield an acceleration dependent adaptation law. One method to resolve this issue is to use a "dirty derivative" (as in the UUB result in [69]; see also [25]). In lieu of a dirty derivative, the result in this chapter uses a Lyapunov-based stability analysis approach for the design of an adaptation law that is only velocity dependent. In comparison with the efforts in [19, 20], a more significant challenge arises from the fact that since a multi-layer NN includes the first layer weight estimate inside of a nonlinear activation function, the previous methods (e.g., [19, 20]) can not be applied. That is, because of the unique manner in which the NN weight estimates appear, the stability analysis and sufficient conditions developed in previous works are violated. Previous RISE methods have a restriction (encapsulated by a sufficient gain condition) that terms in the stability analysis that are upper bounded by a constant must also have time derivatives that are upper bounded by a constant (these terms are usually denoted by $N_d(t)$ in RISE control literature, see [60]). The norm of the NN weight estimates can be bounded by a constant (due to a projection algorithm) but the time derivative is state-dependent (i.e., the norm of $N_d(t)$ can be bounded by a constant but the norm of $\dot{N}_d(t)$ is state dependent). To

address this issue, modified RISE stability analysis techniques are developed that result in modified (but not more restrictive) sufficient gain conditions. By addressing this issue through stability analysis methods, the standard NN weight adaptation law does not need to be modified. Through unique modifications to the stability analysis that enable the RISE feedback controller to be combined with the NN feedforward term, the result in this chapter provides an affirmative answer for the first time to the aforementioned motivating question.

Since the NN and the RISE control structures are model independent (black box) methods, the resulting controller is a universal reusable controller [36] for continuous systems. Because of the manner in which the RISE technique is blended with the NN-based feedforward method, the structure of the NN is not altered from textbook examples [15] and can be considered a somewhat modular element in the control structure. Hence, the NN weights and thresholds are automatically adjusted on-line, with no off-line learning phase required. Compared to standard adaptive controllers, the current asymptotic result does not require linearity in the parameters or the development and evaluation of a regression matrix.

For systems with linear-in-the-parameters uncertainty, an adaptive feedforward controller has the desirable characteristics that the controller is continuous, can be proven to yield global asymptotic tracking, and includes the specific dynamics of the system in the feedforward path. Continuous feedback NN controllers don't include the specific dynamics in a regression matrix and have a degraded steady-state stability result (i.e., UUB tracking); however, they can be applied when the uncertainty in the system is unmodeled, can not be linearly parameterized, or the development and implementation of a regression matrix is impractical. Sliding mode feedback NN controllers have the advantage that they can achieve global asymptotic tracking at the expense of implementing a discontinuous feedback controller (i.e., infinite bandwidth, exciting structural modes, etc.). In comparison to these controllers, the development

in this chapter has the advantage of asymptotic tracking with a continuos feedback controller for a general class of uncertainty; however, these advantages are at the expense of semi-global tracking instead of the typical global tracking results.

3.2 Dynamic Model

The dynamic model and its properties are the same as in Chapter 2; however, the dynamics are not assumed to satisfy the linear-in-the-parameters assumption.

3.3 Control Objective

The control objective is to ensure that the system tracks a desired time-varying trajectory, denoted by $q_d(t) \in \mathbb{R}^n$, despite uncertainties in the dynamic model. To quantify this objective, a position tracking error, denoted by $e_1(t) \in \mathbb{R}^n$, is defined as

$$e_1 \triangleq q_d - q. \tag{3–1}$$

To facilitate the subsequent analysis, filtered tracking errors, denoted by $e_2(t)$, $r(t) \in \mathbb{R}^n$, are also defined as

$$e_2 \triangleq \dot{e}_1 + \alpha_1 e_1 \tag{3–2}$$

$$r \triangleq \dot{e}_2 + \alpha_2 e_2 \tag{3–3}$$

where α_1, $\alpha_2 \in \mathbb{R}$ denote positive constants. The filtered tracking error $r(t)$ is not measurable since the expression in (3–3) depends on $\ddot{q}(t)$.

3.4 Feedforward NN Estimation

NN-based estimation methods are well suited for control systems where the dynamic model contains unstructured nonlinear disturbances as in (2–1). The main feature that empowers NN-based controllers is the universal approximation property. Let $\mathbb{S}$ be a compact simply connected set of $\mathbb{R}^{N_1+1}$. With map $f : \mathbb{S} \to \mathbb{R}^n$, define $\mathbb{C}^n(\mathbb{S})$ as the space where f is continuous. There exist weights and thresholds such that some function $f(x) \in \mathbb{C}^n(\mathbb{S})$ can be represented by a three-layer NN as [15, 32]

$$f(x) = W^T \sigma\left(V^T x\right) + \varepsilon(x) \tag{3–4}$$

for some given input $x(t) \in \mathbb{R}^{N_1+1}$. In (3–4), $V \in \mathbb{R}^{(N_1+1)\times N_2}$ and $W \in \mathbb{R}^{(N_2+1)\times n}$ are bounded constant ideal weight matrices for the first-to-second and second-to-third layers respectively, where N_1 is the number of neurons in the input layer, N_2 is the number of neurons in the hidden layer, and n is the number of neurons in the third layer. The activation function[1] in (3–4) is denoted by $\sigma(\cdot) \in \mathbb{R}^{N_2+1}$, and $\varepsilon(x) \in \mathbb{R}^n$ is the functional reconstruction error. Note that, augmenting the input vector $x(t)$ and activation function $\sigma(\cdot)$ by "1" allows us to have thresholds as the first columns of the weight matrices [15, 32]. Thus, any tuning of W and V then includes tuning of thresholds as well. If $\varepsilon(x) = 0$, then $f(x)$ is in the functional range of the NN. In general for any positive constant real number $\varepsilon_N > 0$, $f(x)$ is within ε_N of the NN range if there exist finite hidden neurons N_2, and constant weights so that for all inputs in the compact set, the approximation holds with $\|\varepsilon\| < \varepsilon_N$. For various activation functions, results such as the Stone-Weierstrass theorem indicate that any sufficiently smooth function can be approximated by a suitable large network. Therefore, the fact that the approximation error $\varepsilon(x)$ is bounded follows from the *Universal Approximation Property* of the NNs [30].

Based on (3–4), the typical three-layer NN approximation for $f(x)$ is given as [15, 32]

$$\hat{f}(x) \triangleq \hat{W}^T \sigma(\hat{V}^T x) \tag{3–5}$$

where $\hat{V}(t) \in \mathbb{R}^{(N_1+1)\times N_2}$ and $\hat{W}(t) \in \mathbb{R}^{(N_2+1)\times n}$ are subsequently designed estimates of the ideal weight matrices. The estimate mismatch for the ideal weight matrices, denoted by $\tilde{V}(t) \in \mathbb{R}^{(N_1+1)\times N_2}$ and $\tilde{W}(t) \in \mathbb{R}^{(N_2+1)\times n}$, are defined as

$$\tilde{V} \triangleq V - \hat{V}, \qquad \tilde{W} \triangleq W - \hat{W}$$

[1] A variety of activation functions (e.g., sigmoid, hyperbolic tangent or radial basis) could be used for the control development in this dissertation.

and the mismatch for the hidden-layer output error for a given $x(t)$, denoted by $\tilde{\sigma}(x) \in \mathbb{R}^{N_2+1}$, is defined as

$$\tilde{\sigma} \triangleq \sigma - \hat{\sigma} = \sigma(V^T x) - \sigma(\hat{V}^T x). \tag{3–6}$$

The NN estimate has several properties that facilitate the subsequent development. These properties are described as follows.

Assumption 3-1: (*Boundedness of the Ideal Weights*) The ideal weights are assumed to exist and be bounded by known positive values so that

$$\|V\|_F^2 = tr\left(V^T V\right) = vec\,(V)^T\, vec\,(V) \leq \bar{V}_B \tag{3–7}$$

$$\|W\|_F^2 = tr\left(W^T W\right) = vec\,(W)^T\, vec\,(W) \leq \bar{W}_B, \tag{3–8}$$

where $\|\cdot\|_F$ is the Frobenius norm of a matrix, $tr\,(\cdot)$ is the trace of a matrix, and the operator $vec\,(\cdot)$ stacks the columns of a matrix $A \in \mathbb{R}^{m\times n}$ to form a vector $vec(A) \in \mathbb{R}^{mn}$ as

$$vec(A) \triangleq \left[\begin{array}{cccccccc} A_{11} & A_{21}... & A_{m1} & A_{12} & A_{22}... & A_{1n}... & A_{mn} \end{array}\right]^T.$$

Assumption 3-2: (*Convex Regions*) Based on (3–7) and (3–8), convex regions (e.g., see Section 4.3 of [70]) can be defined. Specifically, the convex region Λ_V can be defined as[2]

$$\Lambda_V \triangleq \left\{v : v^T v \leq \bar{V}_B\right\}, \tag{3–9}$$

where $\bar{V}_B$ was given in (3–7). In addition, the following definitions concerning the region Λ_V and the parameter estimate vector $vec\left(\hat{V}\right) \in \mathbb{R}^{(N_1+1)N_2}$ (i.e., the dynamic estimate of $vec\,(V) \in \Lambda_V$) are provided as follows: $int(\Lambda_V)$ denotes the interior of the region Λ_V, $\partial(\Lambda_V)$ denotes the boundary for the region Λ_V, $vec\left(\hat{V}\right)^{\perp} \in \mathbb{R}^{(N_1+1)N_2}$ is a unit vector normal to $\partial(\Lambda_V)$ at the point of intersection of the boundary surface $\partial(\Lambda_V)$ and $vec\left(\hat{V}\right)$ where the positive direction for $vec\left(\hat{V}\right)^{\perp}$ is defined as pointing away from $int(\Lambda_V)$ (note

[2] See Lemma 3 of the Appendix for the proof of convexity.

that $vec\left(\hat{V}\right)^{\perp}$ is only defined for $vec\left(\hat{V}\right) \in \partial(\Lambda_V)$), $P_r^t(\psi)$ is the component of the vector $\psi \in \mathbb{R}^{(N_1+1)N_2}$ that is tangent to $\partial(\Lambda_V)$ at the point of intersection of the boundary surface $\partial(\Lambda_V)$ and the vector $vec\left(\hat{V}\right)$, and

$$P_r^{\perp}(\psi) = \psi - P_r^t(\psi) \in \mathbb{R}^{(N_1+1)N_2} \tag{3–10}$$

is the component of the vector $\psi \in \mathbb{R}^{(N_1+1)N_2}$ that is perpendicular to $\partial(\Lambda_V)$ at the point of intersection of the boundary surface $\partial(\Lambda_V)$ and the vector $vec\left(\hat{V}\right)$. Similar to (3–9), the convex region Λ_W is defined as

$$\Lambda_W \triangleq \left\{ v : v^T v \leq \bar{W}_B \right\}, \tag{3–11}$$

where $\bar{W}_B$ was given in (3–8).

3.5 RISE Feedback Control Development

The contribution of this chapter is the control development and stability analysis that illustrates how the aforementioned textbook (e.g., [15]) NN feedforward estimation strategy can be fused with a RISE feedback control method as a means to achieve an asymptotic stability result for general Euler-Lagrange systems described by (2–1). In this section, the open-loop and closed-loop tracking error is developed for the combined control system.

3.5.1 Open-Loop Error System

The open-loop tracking error system can be developed by premultiplying (3–3) by $M(q)$ and utilizing the expressions in (2–1), (3–1), and (3–2) to obtain the following expression:

$$M(q)r = f_d + S + \tau_d - \tau \tag{3–12}$$

where the auxiliary function $f_d\left(q_d, \dot{q}_d, \ddot{q}_d\right) \in \mathbb{R}^n$ is defined as

$$f_d \triangleq M(q_d)\ddot{q}_d + V_m(q_d, \dot{q}_d)\dot{q}_d + G(q_d) + F\left(\dot{q}_d\right) \tag{3–13}$$

and the auxiliary function $S\left(q,\dot{q},q_d,\dot{q}_d,\ddot{q}_d\right)\in\mathbb{R}^n$ is defined as

$$S \triangleq M\left(q\right)\left(\alpha_1\dot{e}_1+\alpha_2 e_2\right)+M\left(q\right)\ddot{q}_d-M(q_d)\ddot{q}_d+V_m(q,\dot{q})\dot{q}-V_m(q_d,\dot{q}_d)\dot{q}_d \\ +G(q)-G(q_d)+F\left(\dot{q}\right)-F\left(\dot{q}_d\right). \tag{3–14}$$

The expression in (3–13) can be represented by a three-layer NN as

$$f_d = W^T\sigma(V^T x_d)+\varepsilon\left(x_d\right). \tag{3–15}$$

In (3–15), the input $x_d(t)\in\mathbb{R}^{3n+1}$ is defined as $x_d(t)\triangleq\left[1\ \ q_d^T(t)\ \ \dot{q}_d^T(t)\ \ \ddot{q}_d^T(t)\right]^T$ so that $N_1=3n$ where N_1 was introduced in (3–4). Based on the assumption that the desired trajectory is bounded, the following inequalities hold

$$\left\|\varepsilon\left(x_d\right)\right\|\leq\varepsilon_{b_1},\qquad \left\|\dot{\varepsilon}\left(x_d,\dot{x}_d\right)\right\|\leq\varepsilon_{b_2},\qquad \left\|\ddot{\varepsilon}\left(x_d,\dot{x}_d,\ddot{x}_d\right)\right\|\leq\varepsilon_{b_3} \tag{3–16}$$

where ε_{b_1} , ε_{b_2}, $\varepsilon_{b_3}\in\mathbb{R}$ are known positive constants.

3.5.2 Closed-Loop Error System

Based on the open-loop error system in (3–12), the control torque input is composed of a three-layer NN feedforward term plus the RISE feedback terms as

$$\tau \triangleq \hat{f}_d+\mu. \tag{3–17}$$

Specifically, the RISE feedback control term $\mu(t)\in\mathbb{R}^n$ is defined as [22]

$$\mu(t)\triangleq(k_s+1)e_2(t)-(k_s+1)e_2(0)+\int_0^t\left[(k_s+1)\alpha_2 e_2(\sigma)+\beta_1 sgn(e_2(\sigma))\right]d\sigma \tag{3–18}$$

where k_s, $\beta_1\in\mathbb{R}$ are positive constant control gains. The feedforward NN component in (3–17), denoted by $\hat{f}_d(t)\in\mathbb{R}^n$, is generated as

$$\hat{f}_d\triangleq\hat{W}^T\sigma(\hat{V}^T x_d). \tag{3–19}$$

The estimates for the NN weights in (3–19) are generated on-line (there is no off-line learning phase) using a smooth projection algorithm (e.g., see Section 4.3 of [70]) as

$$\dot{\hat{W}} = proj\left(\mu_1\right) = \begin{cases} \mu_1 & \text{if } vec\left(\hat{W}\right) \in int\left(\Lambda_W\right) \\ \mu_1 & \begin{cases} \text{if } vec\left(\hat{W}\right) \in \partial\left(\Lambda_W\right) \text{ and } vec\left(\mu_1\right)^T vec\left(\hat{W}\right)^{\perp} \leq 0 \end{cases} \\ P_{Mr}^{t}\left(\mu_1\right) & \begin{cases} \text{if } vec\left(\hat{W}\right) \in \partial\left(\Lambda_W\right) \text{ and } vec\left(\mu_1\right)^T vec\left(\hat{W}\right)^{\perp} > 0 \end{cases} \end{cases} \tag{3–20}$$

$$\dot{\hat{V}} = proj\left(\mu_2\right) = \begin{cases} \mu_2 & \text{if } vec\left(\hat{V}\right) \in int\left(\Lambda_V\right) \\ \mu_2 & \begin{cases} \text{if } vec\left(\hat{V}\right) \in \partial\left(\Lambda_V\right) \text{ and } vec\left(\mu_2\right)^T vec\left(\hat{V}\right)^{\perp} \leq 0 \end{cases} \\ P_{Mr}^{t}\left(\mu_2\right) & \begin{cases} \text{if } vec\left(\hat{V}\right) \in \partial\left(\Lambda_V\right) \text{ and } vec\left(\mu_2\right)^T vec\left(\hat{V}\right)^{\perp} > 0 \end{cases} \end{cases} \tag{3–21}$$

where

$$vec\left(\hat{W}\left(0\right)\right) \in int\left(\Lambda_W\right), \quad vec\left(\hat{V}\left(0\right)\right) \in int\left(\Lambda_V\right)$$

and the auxiliary terms $\mu_1(t) \in \mathbb{R}^{(N_2+1)\times n}$, $\mu_2(t) \in \mathbb{R}^{(N_1+1)\times N_2}$ are defined as

$$\mu_1 \triangleq \Gamma_1 \hat{\sigma}' \hat{V}^T \dot{x}_d e_2^T, \qquad \mu_2 \triangleq \Gamma_2 \dot{x}_d (\hat{\sigma}'^T \hat{W} e_2)^T \tag{3–22}$$

where $\Gamma_1 \in \mathbb{R}^{(N_2+1)\times(N_2+1)}$, $\Gamma_2 \in \mathbb{R}^{(N_1+1)\times(N_1+1)}$ are constant, positive definite, symmetric matrices. In (3–20) and (3–21), $P_{Mr}^{t}\left(A\right) = devec\left(P_r^t\left(vec\left(A\right)\right)\right)$ for a matrix A, where the operation $devec\left(\cdot\right)$ is the reverse of $vec\left(\cdot\right)$.

Remark 3.1. *The use of the projection algorithm in (3–20) and (3–21) is to ensure that $\hat{W}(t)$ and $\hat{V}(t)$ remain bounded inside the convex regions defined in (3–9), and (3–11). This fact will be exploited in the subsequent stability analysis.*

The closed-loop tracking error system can be developed by substituting (3–17) into (3–12) as

$$M(q)r = f_d - \hat{f}_d + S + \tau_d - \mu. \tag{3–23}$$

To facilitate the subsequent stability analysis, the time derivative of (3–23) is determined as

$$M(q)\dot{r} = -\dot{M}(q)r + \dot{f}_d - \dot{\hat{f}}_d + \dot{S} + \dot{\tau}_d - \dot{\mu}. \tag{3–24}$$

Taking the time derivative of the closed-loop error system is typical of the RISE stability analysis. In our case, the time differentiation also facilitates the design of NN weight adaptation laws instead of using the typical (as in [15, 32]) Taylor series approximation method to obtain a linear form for the estimation error $\tilde{V}$. Using (3–15) and (3–19), the closed-loop error system in (3–24) can be expressed as

$$\begin{aligned} M(q)\dot{r} = &-\dot{M}(q)r + W^T\sigma'\left(V^T x_d\right)V^T\dot{x}_d - \dot{\hat{W}}^T\sigma(\hat{V}^T x_d) \\ &- \hat{W}^T\sigma'(\hat{V}^T x_d)\dot{\hat{V}}^T x_d - \hat{W}^T\sigma'(\hat{V}^T x_d)\hat{V}^T\dot{x}_d + \dot{\varepsilon} + \dot{S} + \dot{\tau}_d - \dot{\mu} \end{aligned} \tag{3–25}$$

where $\sigma'(\hat{V}^T x) \equiv d\sigma\left(V^T x\right)/d\left(V^T x\right)|_{V^T x = \hat{V}^T x}$. After adding and subtracting the terms $W^T\hat{\sigma}'\hat{V}^T\dot{x}_d + \hat{W}^T\hat{\sigma}'\tilde{V}^T\dot{x}_d$ to (3–25), the following expression can be obtained:

$$\begin{aligned} M(q)\dot{r} = &-\dot{M}(q)r + \hat{W}^T\hat{\sigma}'\tilde{V}^T\dot{x}_d + \tilde{W}^T\hat{\sigma}'\hat{V}^T\dot{x}_d + W^T\sigma'V^T\dot{x}_d - W^T\hat{\sigma}'\hat{V}^T\dot{x}_d \\ &- \hat{W}^T\hat{\sigma}'\tilde{V}^T\dot{x}_d + \dot{S} - \dot{\hat{W}}^T\hat{\sigma} - \hat{W}^T\hat{\sigma}'\dot{\hat{V}}^T x_d + \dot{\tau}_d + \dot{\varepsilon} - \dot{\mu} \end{aligned} \tag{3–26}$$

where the notations $\hat{\sigma}$ and $\tilde{\sigma}$ are introduced in (3–6). Using the NN weight tuning laws in (3–20), (3–21), the expression in (3–26) can be rewritten as

$$M(q)\dot{r} = -\frac{1}{2}\dot{M}(q)r + \tilde{N} + N - e_2 - (k_s+1)r - \beta_1 sgn(e_2) \tag{3–27}$$

where the fact that the time derivative of (3–18) is given as

$$\dot{\mu}(t) = (k_s+1)r + \beta_1 sgn(e_2) \tag{3–28}$$

was utilized, and where the unmeasurable auxiliary terms $\tilde{N}(e_1, e_2, r, t)$, $N(\hat{W}, \hat{V}, x_d, \dot{x}_d, t) \in \mathbb{R}^n$ are defined as

$$\begin{aligned} \tilde{N}(t) \triangleq &-\frac{1}{2}\dot{M}(q)r - proj(\Gamma_1\hat{\sigma}'\hat{V}^T\dot{x}_d e_2^T)^T\hat{\sigma} \\ &- \hat{W}^T\hat{\sigma}'proj(\Gamma_2\dot{x}_d(\hat{\sigma}'^T\hat{W}e_2)^T)^T x_d + \dot{S} + e_2 \end{aligned} \tag{3–29}$$

and

$$N \triangleq N_d + N_B. \tag{3–30}$$

In (3–30), $N_d\left(x_d, \dot{x}_d, t\right) \in \mathbb{R}^n$ is defined as

$$N_d \triangleq W^T \sigma' V^T \dot{x}_d + \dot{\varepsilon} + \dot{\tau}_d \tag{3–31}$$

while $N_B(\hat{W}, \hat{V}, x_d, \dot{x}_d, t) \in \mathbb{R}^n$ is further segregated as

$$N_B \triangleq N_{B_1} + N_{B_2} \tag{3–32}$$

where $N_{B_1}(\hat{W}, \hat{V}, x_d, \dot{x}_d, t) \in \mathbb{R}^n$ is defined as

$$N_{B_1} \triangleq -W^T \hat{\sigma}' \hat{V}^T \dot{x}_d - \hat{W}^T \hat{\sigma}' \tilde{V}^T \dot{x}_d \tag{3–33}$$

and the term $N_{B_2}(\hat{W}, \hat{V}, x_d, \dot{x}_d, t) \in \mathbb{R}^n$ is defined as

$$N_{B_2} \triangleq \hat{W}^T \hat{\sigma}' \tilde{V}^T \dot{x}_d + \tilde{W}^T \hat{\sigma}' \hat{V}^T \dot{x}_d. \tag{3–34}$$

Motivation for segregating the terms in (3–30) is derived from the fact that the different components in (3–30) have different bounds. Segregating the terms as in (3–30)-(3–34) facilitates the development of the NN weight update laws and the subsequent stability analysis. For example, the terms in (3–31) are grouped together because the terms and their time derivatives can be upper bounded by a constant and rejected by the RISE feedback, whereas the terms grouped in (3–32) can be upper bounded by a constant but their derivatives are state dependent. The state dependency of the time derivatives of the terms in (3–32) violates the assumptions given in previous RISE-based controllers (e.g., [19, 20, 22, 23, 25–27]), and requires additional consideration in the adaptation law design and stability analysis. The terms in (3–32) are further segregated because $N_{B_1}(\hat{W}, \hat{V}, x_d)$ will be rejected by the RISE feedback, whereas $N_{B_2}(\hat{W}, \hat{V}, x_d)$ will be partially rejected by the RISE feedback and partially canceled by the adaptive update law for the NN weight estimates.

In a similar manner as in Chapter 2, the Mean Value Theorem can be used to develop the following upper bound

$$\left\| \tilde{N}(t) \right\| \leq \rho \left(\|z\| \right) \|z\| \tag{3–35}$$

where $z(t) \in \mathbb{R}^{3n}$ is defined as

$$z(t) \triangleq [e_1^T \quad e_2^T \quad r^T]^T \tag{3–36}$$

and the bounding function $\rho(\|z\|) \in \mathbb{R}$ is a positive globally invertible nondecreasing function. The following inequalities can be developed based on Assumption 2-3, (3–7), (3–8), (3–16), (3–32)-(3–34):

$$\|N_d\| \leq \zeta_1, \qquad \|N_{B_1}\| \leq \zeta_2, \qquad \|N_{B_2}\| \leq \zeta_3, \qquad \left\| \dot{N}_d \right\| \leq \zeta_4. \tag{3–37}$$

From (3–30), (3–32) and (3–37), the following bound can be developed

$$\|N_1\| \leq \|N_d\| + \|N_{1B}\| \leq \|N_d\| + \|N_{1B_a}\| + \|N_{1B_b}\| \leq \zeta_1 + \zeta_2 + \zeta_3. \tag{3–38}$$

By using (3–20), (3–21), the time derivative of $N_B(\hat{W}, \hat{V}, x_d)$ can be bounded as

$$\left\| \dot{N}_B \right\| \leq \zeta_5 + \zeta_6 \|e_2\|. \tag{3–39}$$

In (3–37) and (3–39), $\zeta_i \in \mathbb{R}$, $(i = 1, 2, ..., 6)$ are known positive constants.

3.6 Stability Analysis

Theorem 3-1: The combined NN and RISE controller given in (3–17)-(3–21) ensures that all system signals are bounded under closed-loop operation and that the position tracking error is regulated in the sense that

$$\|e_1(t)\| \to 0 \qquad \text{as} \qquad t \to \infty$$

provided the control gain k_s introduced in (3–18) is selected sufficiently large (see the subsequent proof), α_1, α_2 are selected according to the following sufficient condition

$$\alpha_1 > \frac{1}{2}, \qquad \alpha_2 > \beta_2 + 1, \tag{3–40}$$

and β_1 and β_2 are selected according to the following sufficient conditions:

$$\beta_1 > \max\left\{\zeta_1+\zeta_2+\zeta_3,\ \zeta_1+\zeta_2+\frac{\zeta_4}{\alpha_2}+\frac{\zeta_5}{\alpha_2}\right\},\quad \beta_3>\zeta_6 \tag{3–41}$$

where $\zeta_i \in \mathbb{R}$, $i = 1, 2,..., 5$ are introduced in (3–37)-(3–39) and β_2 is introduced in (3–44).

Proof: Let $\mathcal{D} \subset \mathbb{R}^{3n+2}$ be a domain containing $y(t) = 0$, where $y(t) \in \mathbb{R}^{3n+2}$ is defined as

$$y(t) \triangleq [z^T(t)\ \ \sqrt{P(t)}\ \ \sqrt{Q(t)}]^T. \tag{3–42}$$

In (3–42), the auxiliary function $P(t) \in \mathbb{R}$ is defined as

$$P(t) \triangleq \beta_1 \sum_{i=1}^{n} |e_{2i}(0)| - e_2(0)^T N(0) - \int_0^t L(\tau)d\tau \tag{3–43}$$

where the subscript $i = 1, 2, .., n$ denotes the ith element of the vector, and the auxiliary function $L(t) \in \mathbb{R}$ is defined as

$$L(t) \triangleq r^T(N_{B_1}(t) + N_d(t) - \beta_1 sgn(e_2)) + \dot{e}_2(t)^T N_{B_2}(t) - \beta_2 \|e_2(t)\|^2 \tag{3–44}$$

where $\beta_2 \in \mathbb{R}$ is a positive constant chosen according to the second sufficient condition in (3–41). The derivative $\dot{P}(t) \in \mathbb{R}$ can be expressed as

$$\dot{P}(t) = -L(t) = -r^T(N_{B_1}(t) + N_d(t) - \beta_1 sgn(e_2)) - \dot{e}_2(t)^T N_{B_2}(t) + \beta_2 \|e_2(t)\|^2. \tag{3–45}$$

Provided the sufficient conditions introduced in (3–41) are satisfied, the following inequality can be obtained in a similar fashion as in Lemma 2 of the Appendix

$$\int_0^t L(\tau)d\tau \le \beta_1 \sum_{i=1}^{n} |e_{2i}(0)| - e_2(0)^T N(0). \tag{3–46}$$

Hence, (3–46) can be used to conclude that $P(t) \ge 0$. The auxiliary function $Q(t) \in \mathbb{R}$ in (3–42) is defined as

$$Q(t) \triangleq \frac{\alpha_2}{2} tr(\tilde{W}^T \Gamma_1^{-1} \tilde{W}) + \frac{\alpha_2}{2} tr(\tilde{V}^T \Gamma_2^{-1} \tilde{V}). \tag{3–47}$$

Since Γ_1 and Γ_2 are constant, symmetric, and positive definite matrices and $\alpha_2 > 0$, it is straightforward that $Q(t) \ge 0$.

Let $V_L(y,t) : \mathcal{D} \times [0,\infty) \to \mathbb{R}$ be a continuously differentiable positive definite function defined as

$$V_L(y,t) \triangleq e_1^T e_1 + \frac{1}{2} e_2^T e_2 + \frac{1}{2} r^T M(q) r + P + Q \tag{3–48}$$

which satisfies the following inequalities:

$$U_1(y) \leq V_L(y,t) \leq U_2(y) \tag{3–49}$$

provided the sufficient conditions introduced in (3–41) are satisfied. In (3–49), the continuous positive definite functions $U_1(y)$, $U_2(y) \in \mathbb{R}$ are defined as

$$U_1(y) \triangleq \lambda_1 \|y\|^2 \ , \qquad U_2(y) \triangleq \lambda_2(q) \|y\|^2 \tag{3–50}$$

where λ_1, $\lambda_2(q) \in \mathbb{R}$ are defined as

$$\lambda_1 \triangleq \frac{1}{2} \min\{1, m_1\} \ , \qquad \lambda_2(q) \triangleq \max\{\frac{1}{2}\bar{m}(q), 1\}$$

where m_1, $\bar{m}(q)$ are introduced in (2–3). After utilizing (3–2), (3–3), (3–27), (3–28), the time derivative of (3–48) can be expressed as

$$\begin{aligned} \dot{V}_L(y,t) = & -2\alpha_1 \|e_1\|^2 + 2e_2^T e_1 + r^T \tilde{N}(t) - (k_s+1)\|r\|^2 - \alpha_2 \|e_2\|^2 \\ & + \beta_2 \|e_2\|^2 + \alpha_2 e_2^T \left[\hat{W}^T \hat{\sigma}' \tilde{V}^T \dot{x}_d + \tilde{W}^T \hat{\sigma}' \hat{V}^T \dot{x}_d\right] \\ & + tr(\alpha_2 \tilde{W}^T \Gamma_1^{-1} \dot{\tilde{W}}) + tr(\alpha_2 \tilde{V}^T \Gamma_2^{-1} \dot{\tilde{V}}). \end{aligned} \tag{3–51}$$

Based on the fact that

$$e_2^T e_1 \leq \frac{1}{2}\|e_1\|^2 + \frac{1}{2}\|e_2\|^2$$

and using (3–20), (3–21), the expression in (3–51) can be simplified as[3]

$$\dot{V}_L(y,t) \leq r^T \tilde{N}(t) - (k_s+1)\|r\|^2 - (2\alpha_1 - 1)\|e_1\|^2 - (\alpha_2 - \beta_2 - 1)\|e_2\|^2 . \tag{3–52}$$

[3] See Lemma 4 of the Appendix for the details of obtaining the inequality in (3–52).

By using (3–35), the expression in (3–52) can be further bounded as

$$\dot{V}_L(y,t) \leq -\lambda_3 \|z\|^2 - \left(k_s \|r\|^2 - \rho(\|z\|) \|r\| \|z\|\right) \tag{3–53}$$

where $\lambda_3 \triangleq \min\{2\alpha_1 - 1, \alpha_2 - \beta_2 - 1, 1\}$; hence, λ_3 is positive if α_1, α_2 are chosen according to the sufficient conditions in (3–40). After completing the squares for the second and third term in (3–53), the following expression can be obtained:

$$\dot{V}_L(y,t) \leq -\lambda_3 \|z\|^2 + \frac{\rho^2(z) \|z\|^2}{4k_s}. \tag{3–54}$$

The expression in (3–54) can be further upper bounded by a continuous, positive semi-definite function

$$\dot{V}_L(y,t) \leq -U(y) = -c \|z\|^2 \qquad \forall y \in \mathcal{D} \tag{3–55}$$

for some positive constant $c \in \mathbb{R}$, where

$$\mathcal{D} \triangleq \left\{ y \in \mathbb{R}^{3n+2} \mid \|y\| \leq \rho^{-1}\left(2\sqrt{\lambda_3 k_s}\right) \right\}.$$

Larger values of k will expand the size of the domain $\mathcal{D}$. The inequalities in (3–49) and (3–55) can be used to show that $V_L(y,t) \in \mathcal{L}_\infty$ in $\mathcal{D}$; hence, $e_1(t)$, $e_2(t)$, $r(t)$, $P(t)$, and $Q(t) \in \mathcal{L}_\infty$ in $\mathcal{D}$. Given that $e_1(t)$, $e_2(t)$, and $r(t) \in \mathcal{L}_\infty$ in $\mathcal{D}$, standard linear analysis methods can be used to prove that $\dot{e}_1(t)$, $\dot{e}_2(t) \in \mathcal{L}_\infty$ in $\mathcal{D}$ from (3–2) and (3–3). Since $e_1(t)$, $e_2(t)$, $r(t) \in \mathcal{L}_\infty$ in $\mathcal{D}$, the assumption that $q_d(t)$, $\dot{q}_d(t)$, $\ddot{q}_d(t)$ exist and are bounded can be used along with (3–1)-(3–3) to conclude that $q(t)$, $\dot{q}(t)$, $\ddot{q}(t) \in \mathcal{L}_\infty$ in $\mathcal{D}$. Since $q(t)$, $\dot{q}(t) \in \mathcal{L}_\infty$ in $\mathcal{D}$, Assumption 2-2 can be used to conclude that $M(q)$, $V_m(q,\dot{q})$, $G(q)$, and $F(\dot{q}) \in \mathcal{L}_\infty$ in $\mathcal{D}$. Therefore, from (2–1) and Assumption 2-3, we can show that $\tau(t) \in \mathcal{L}_\infty$ in $\mathcal{D}$. Given that $r(t) \in \mathcal{L}_\infty$ in $\mathcal{D}$, (3–28) can be used to show that $\dot{\mu}(t) \in \mathcal{L}_\infty$ in $\mathcal{D}$. Since $\dot{q}(t)$, $\ddot{q}(t) \in \mathcal{L}_\infty$ in $\mathcal{D}$, Assumption 2-2 can be used to show that $\dot{V}_m(q,\dot{q})$, $\dot{G}(q)$, $\dot{F}(q)$ and $\dot{M}(q) \in \mathcal{L}_\infty$ in $\mathcal{D}$; hence, (3–24) can be used to show that $\dot{r}(t) \in \mathcal{L}_\infty$ in $\mathcal{D}$. Since $\dot{e}_1(t)$,

$\dot{e}_2(t)$, $\dot{r}(t) \in \mathcal{L}_\infty$ in $\mathcal{D}$, the definitions for $U(y)$ and $z(t)$ can be used to prove that $U(y)$ is uniformly continuous in $\mathcal{D}$.

Let $\mathcal{S} \subset \mathcal{D}$ denote a set defined as follows:[4]

$$\mathcal{S} \triangleq \left\{ y(t) \in \mathcal{D} \mid U_2(y(t)) < \lambda_1 \left(\rho^{-1} \left(2\sqrt{\lambda_3 k_s} \right) \right)^2 \right\}. \tag{3–56}$$

Theorem 8.4 of [63] can now be invoked to state that

$$c \left\| z(t) \right\|^2 \to 0 \qquad \text{as} \qquad t \to \infty \qquad \forall y(0) \in \mathcal{S}. \tag{3–57}$$

Based on the definition of $z(t)$, (3–57) can be used to show that

$$\left\| e_1(t) \right\| \to 0 \qquad \text{as} \qquad t \to \infty \qquad \forall y(0) \in \mathcal{S}. \tag{3–58}$$

3.7 Experiment

As in Chapter 2, the testbed depicted in Figure 2-1 was used to implement the developed controller, however, no external friction is applied to the circular disk. The desired link trajectory is selected as follows (in degrees):

$$q_d(t) = 60.0 \sin(3.0t)(1 - \exp(-0.01t^3)). \tag{3–59}$$

For all experiments, the rotor velocity signal is obtained by applying a standard backwards difference algorithm to the position signal. The integral structure for the RISE term in (3–18) was computed on-line via a standard trapezoidal algorithm. The NN input vector $\bar{x}_d(t) \in \mathbb{R}^4$ is defined as

$$\bar{x}_d = [1 \quad q_d \quad \dot{q}_d \quad \ddot{q}_d]^T.$$

The initial values of $\hat{W}(0)$ were chosen to be a zero matrix; however, the initial values of $\hat{V}(0)$ were selected randomly between -1.0 and 1.0 to provide a basis [71]. A different

[4] The region of attraction in (3–56) can be made arbitrarily large to include any initial conditions by increasing the control gain k_s (i.e., a semi-global type of stability result) [22].

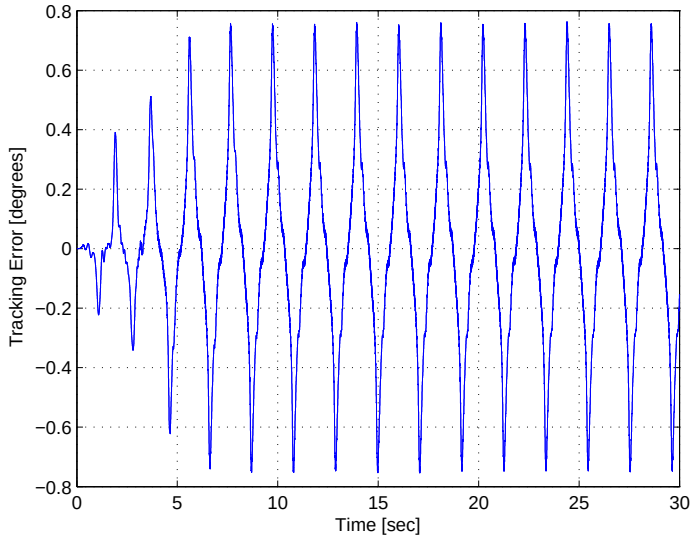

Figure 3-1. Tracking error for the RISE control law with no NN adaptation.

transient response could be obtained if the NN weights are initialized differently. Ten hidden layer neurons were chosen based on trial and error (i.e., $N_2 = 10$). In addition, all the states were initialized to zero. The following control gains were used to implement the controller in (3–17) in conjunction with the NN update laws in (3–20) and (3–22):

$$k_s = 30, \quad \beta_1 = 10, \quad \alpha_1 = 10, \quad \alpha_2 = 10, \quad \Gamma_1 = 5I_{11}, \quad \Gamma_2 = 0.05I_4. \tag{3–60}$$

3.7.1 Discussion

Two different experiments were conducted to demonstrate the efficacy of the proposed controller. The control gains were chosen to obtain an arbitrary tracking error accuracy (not necessarily the best performance). For each controller, the gains were not retuned (i.e., the common control gains remain the same for both controllers). For the first experiment, no adaptation was used and the controller with only the RISE feedback was implemented. The tracking error is shown in Figure 3-1, and the control torque is shown in Figure 3-2. For the second experiment, the proposed NN controller was used in (hereinafter denoted as RISE+NN). The tracking error is shown in Figure 3-3, and the

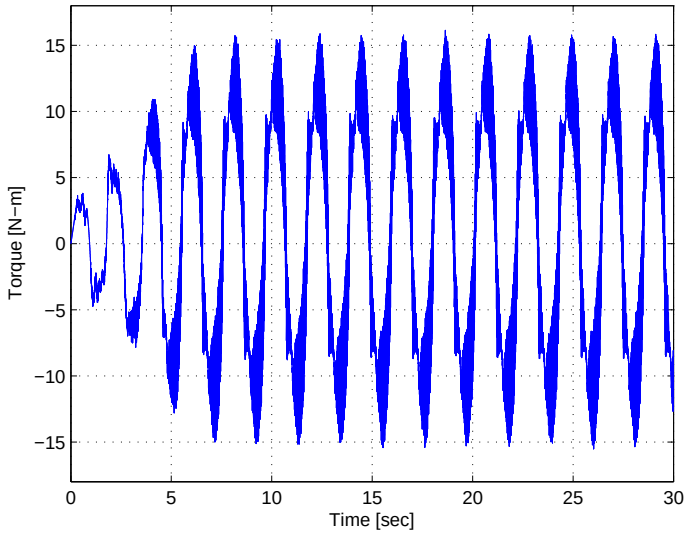

Figure 3-2. Control torque for the RISE control law with no NN adaptation.

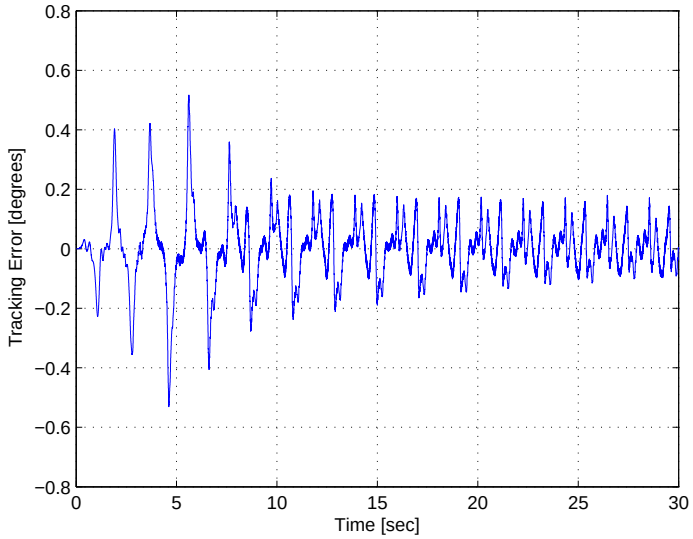

Figure 3-3. Tracking error for the proposed RISE+NN control law.

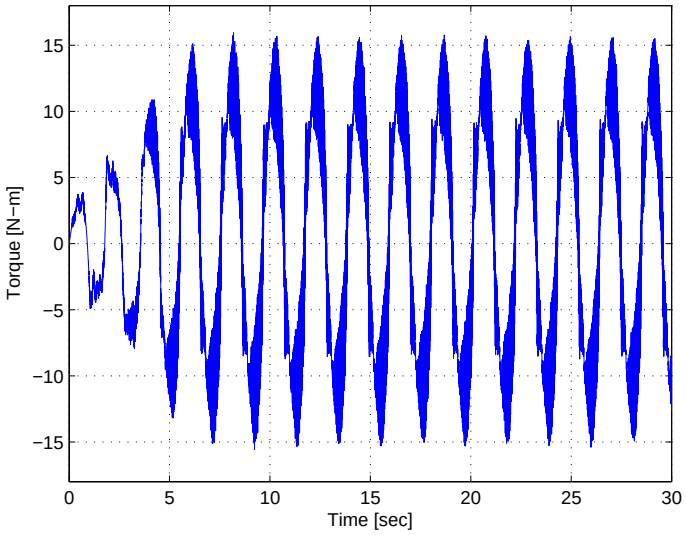

Figure 3-4. Control torque for the proposed RISE+NN control law.

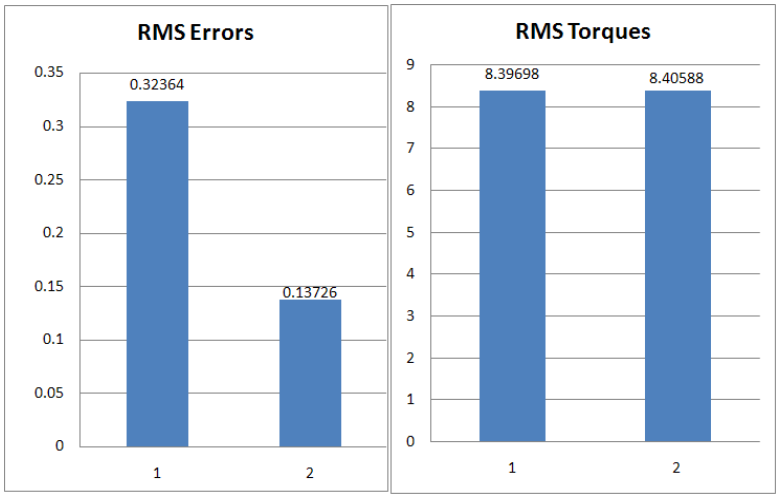

Figure 3-5. Average RMS errors (degrees) and torques (N-m). 1- RISE, 2- RISE+NN (proposed).

control torque is shown in Figure 3-4. Each experiment was performed five times and the average RMS error and torque values are shown in Figure 3-5, which indicate that the proposed RISE+NN controller yields a lower RMS error with a similar control effort.

3.8 Conclusions

The results in this chapter illustrate how a multilayer NN feedforward term can be fused with a RISE feedback term in a continuous controller to achieve semi-global

asymptotic tracking. Improved weight tuning laws are presented which guarantee boundedness of NN weights. To blend the NN and RISE methods, several technical challenges were addressed through Lyapunov-based techniques. These challenges include developing adaptive update laws for the NN weight estimates that do not depend on acceleration, and developing new RISE stability analysis methods and sufficient gain conditions to accommodate the incorporation of the NN adaptive updates in the RISE structure. Experimental results are presented that indicate reduced RMS tracking errors while requiring slightly higher RMS control effort.

CHAPTER 4
A NEW CLASS OF MODULAR ADAPTIVE CONTROLLERS

4.1 Introduction

The results in this chapter provide the first investigation of the ability to yield controller/update law modularity using the RISE feedback. First, we consider a general class of multi-input multi-output (MIMO) dynamic systems with structured (i.e., LP) and unstructured uncertainties and develop a controller with modularity between the controller/update law, where a model-based adaptive feedforward term is used in conjunction with the RISE feedback term [19]. The RISE-based modular adaptive approach is different than previous work (cf. [40, 41, 43]) in the sense that it does not rely on nonlinear damping. The use of the RISE method in lieu of nonlinear damping has several advantages that motivate this investigation including: an asymptotic modular adaptive tracking result can be obtained for nonlinear systems with non-LP additive bounded disturbances; the dual objectives of asymptotic tracking and controller/update law modularity are achieved in a single step unlike the two stage analysis required in some results (cf., [40, 43]); the development does not require that the adaptive estimates are a priori bounded; and the development does not require a positive definite estimate of the inertia matrix or a square integrable prediction error as in [40, 43]. Modularity in the adaptive feedforward term is made possible by considering a generic form of the adaptive update law and its corresponding parameter estimate. The general form of the adaptive update law includes examples such as gradient, least-squares, and etc. This generic form of the update law is used to develop a new closed-loop error system, and the typical RISE stability analysis is modified to accommodate the generic update law. New sufficient gain conditions are derived to prove an asymptotic tracking result.

The class of RISE-based modular adaptive controllers is then extended to include uncertain dynamic systems that do not satisfy the LP assumption. Neural networks (NNs) have gained popularity as a feedforward adaptive control method that can compensate

for non-LP uncertainty in nonlinear systems. A limiting factor in previous NN-based feedforward control results is that a residual function approximation error exists that limits the steady-state performance to a uniformly ultimately bounded result, rather than an asymptotic result. Some results (cf. [33–36, 72–74]) have been developed to augment the NN feedforward component with a discontinuous feedback element to achieve asymptotic tracking. Motivated by the practical limitations of discontinuous feedback, a multilayer NN-based controller was augmented by RISE feedback in [75] to yield the first asymptotic tracking result using a continuous controller. However, in most NN-based controllers, the NN adaptation is governed by a gradient update law to facilitate the Lyapunov-based stability analysis.

Since multilayer NNs are nonlinear in the weights, a challenge is to derive weight tuning laws in closed-loop feedback control systems that yield stability as well as bounded weights. The development in the current chapter illustrates how to extend the class of modular adaptive controllers for NNs. Specifically, the result allows the NN weight tuning laws to be determined from a developed generic update law (rather than be restricted to a gradient update law). We are not aware of any modular multilayer NN-based controller in literature with modularity in the tuning laws/controller. The NN feedforward structure adaptively compensates for the non-LP uncertain dynamics. For the tuning laws that could be used in this result, the NN weights can be initialized randomly, and no off-line training is required.

The modular adaptive control development for the general class of multi-input systems is then applied to a class of dynamic systems modeled by the Euler-Lagrange formulation. The Euler-Lagrange formulation describes the behavior of a large class of engineering systems (e.g., robot manipulators, satellites, vehicular systems). An experimental section is included that illustrates that different adaptation laws can be included with the feedback controller through examples including a gradient update law and a least squares update law for the LP dynamics case, and a common gradient weight

tuning law based on backpropagated error [76] and a simplified tuning law based on the Hebbian algorithm [77] for the non-LP dynamics case.

While the current result encompasses a large variety of adaptive update laws, an update law design based on the prediction error is not possible because the formulation of a prediction error requires the system dynamics to be completely LP. Future efforts can focus on developing a RISE-based adaptive controller for a completely LP system that could also use a prediction error/torque filtering approach. Also, one of the shortcomings of current work is that only a semi-global asymptotic stability is achieved, and further investigation is needed to achieve a global stability result. Inroads to solve the global tracking problem are provided in [78] under a set of assumptions.

4.2 Dynamic System

Consider a class of MIMO nonlinear systems of the following form:

$$x^{(m)} = f(x, \dot{x}, ..., x^{(m-1)}) + G(x, \dot{x}, ..., x^{(m-1)})u + h(t), \tag{4–1}$$

where $(\cdot)^{(i)}(t)$ denotes the i^{th} derivative with respect to time, $x^{(i)}(t) \in \mathbb{R}^n$, $i = 0, ..., m-1$ are the system states, $u(t) \in \mathbb{R}^n$ is the control input, $f(\cdot) \in \mathbb{R}^n$ and $G(\cdot) \in \mathbb{R}^{n \times n}$ are unknown nonlinear $\mathcal{C}^2$ functions, and $h(t) \in \mathbb{R}^n$ denotes a general nonlinear disturbance (e.g., unmodeled effects). The outputs of the system are the system states. Throughout the chapter $|\cdot|$ denotes the absolute value of the scalar argument, $\|\cdot\|$ denotes the standard Euclidean norm for a vector or the induced infinity norm for a matrix, and $\|\cdot\|_F$ denotes the Frobenius norm of a matrix.

The subsequent development is based on the assumption that all the system states are measurable. Moreover, the following properties and assumptions will be exploited in the subsequent development.

Assumption 4-1: $G(\cdot)$ is symmetric positive definite, and satisfies the following inequality $\forall y(t) \in \mathbb{R}^n$:

$$\underline{g} \|y\|^2 \leq y^T G^{-1}(\cdot) y \leq \bar{g}(x, \dot{x}, ..., x^{(m-1)}) \|y\|^2, \tag{4–2}$$

where $\underline{g} \in \mathbb{R}$ is a known positive constant, $\bar{g}(x, \dot{x}, ..., x^{(m-1)}) \in \mathbb{R}$ is a known positive function.

Assumption 4-2: The functions $G^{-1}(\cdot)$ and $f(\cdot)$ are second order differentiable such that $G^{-1}(\cdot)$, $\dot{G}^{-1}(\cdot)$, $\ddot{G}^{-1}(\cdot)$, $f(\cdot)$, $\dot{f}(\cdot)$, $\ddot{f}(\cdot) \in \mathcal{L}_\infty$ if $x^{(i)}(t) \in \mathcal{L}_\infty$, $i = 0, 1, ..., m+1$.

Assumption 4-3: The nonlinear disturbance term and its first two time derivatives (i.e., $h(t), \dot{h}(t), \ddot{h}(t)$) are bounded by known constants.

Assumption 4-4: The unknown nonlinearities $G^{-1}(\cdot)$ and $f(\cdot)$ are linear in terms of unknown constant system parameters (i.e., LP).

Assumption 4-5: The desired trajectory $x_d(t) \in \mathbb{R}^n$ is assumed to be designed such that $x_d^{(i)}(t) \in \mathcal{L}_\infty$, $i = 0, 1, ..., m+2$.

4.3 Control Objective

The objective is to design a continuous modular adaptive controller which ensures that the system tracks a desired time-varying trajectory $x_d(t)$ despite uncertainties and bounded disturbances in the dynamic model. To quantify this objective, a tracking error, denoted by $e_1(t) \in \mathbb{R}^n$, is defined as

$$e_1 \triangleq x_d - x. \tag{4–3}$$

To facilitate a compact presentation of the subsequent control development and stability analysis, auxiliary error signals denoted by $e_i(t) \in \mathbb{R}^n$, $i = 2, 3, ..., m$ are defined as

$$\begin{aligned} e_2 &\triangleq \dot{e}_1 + \alpha_1 e_1 \\ e_3 &\triangleq \dot{e}_2 + \alpha_2 e_2 + e_1 \\ e_4 &\triangleq \dot{e}_3 + \alpha_3 e_3 + e_2 \\ &\vdots \\ e_i &\triangleq \dot{e}_{i-1} + \alpha_{i-1} e_{i-1} + e_{i-2} \\ &\vdots \end{aligned} \tag{4–4}$$

$$e_m \triangleq \dot{e}_{m-1} + \alpha_{m-1} e_{m-1} + e_{m-2},$$

where $\alpha_i \in \mathbb{R}$, $i = 1, 2, ..., m-1$ denote constant positive control gains. The error signals $e_i(t)$, $i = 2, 3, ..., m$ can be expressed in terms of $e_1(t)$ and its time derivatives as

$$e_i = \sum_{j=0}^{i-1} a_{i,j} e_1^{(j)}, \tag{4–5}$$

where the constant coefficients $a_{i,j} \in \mathbb{R}$ can be evaluated by substituting (4–5) in (4–4), and comparing coefficients [79]. A filtered tracking error [57], denoted by $r(t) \in \mathbb{R}^n$, is also defined as

$$r \triangleq \dot{e}_m + \alpha_m e_m, \tag{4–6}$$

where $\alpha_m \in \mathbb{R}$ is a positive, constant control gain. The filtered tracking error $r(t)$ is not measurable since the expression in (4–6) depends on $x^{(m)}(t)$.

4.4 Control Development

The open-loop tracking error system is developed by premultiplying (4–6) by $G^{-1}\left(x, \dot{x}, ..., x^{(m-1)}\right)$ and utilizing the expressions in (4–1), (4–4), (4–5) as

$$G^{-1} r = Y_d \theta + S - G_d^{-1} h - u \tag{4–7}$$

where the fact that $a_{m,m-1} = 1$, was used. In (4–7), $Y_d\theta \in \mathbb{R}^n$ is defined as

$$Y_d \theta \triangleq G_d^{-1} x_d^{(m)} - G_d^{-1} f_d, \tag{4–8}$$

where $Y_d(x_d, \dot{x}_d, ..., x_d^{(m)}) \in \mathbb{R}^{n \times p}$ is a desired regression matrix, and $\theta \in \mathbb{R}^p$ contains the constant unknown system parameters. In (4–8), the functions $G_d^{-1}(x_d, \dot{x}_d, ..., x_d^{(m-1)}) \in \mathbb{R}^{n \times n}$, $f_d(x_d, \dot{x}_d, ..., x_d^{(m-1)}) \in \mathbb{R}^n$ are defined as

$$\begin{aligned} G_d^{-1} &\triangleq G^{-1}(x_d, \dot{x}_d, ..., x_d^{(m-1)}) \\ f_d &\triangleq f(x_d, \dot{x}_d, ..., x_d^{(m-1)}). \end{aligned} \tag{4–9}$$

Also in (4–7), the auxiliary function $S\left(x, \dot{x}, ..., x^{(m-1)}, t\right) \in \mathbb{R}^n$ is defined as

$$S \triangleq G^{-1}\left(\sum_{j=0}^{m-2} a_{m,j} e_1^{(j+1)} + \alpha_m e_m\right) + G^{-1} x_d^{(m)} - G_d^{-1} x_d^{(m)} - G^{-1} f + G_d^{-1} f_d - G^{-1} h + G_d^{-1} h. \tag{4–10}$$

Based on the open-loop error system in (4–7), the control input is composed of an adaptive feedforward term plus the RISE feedback term as

$$u \triangleq Y_d \hat{\theta} + \mu. \tag{4–11}$$

In (4–11), $\mu(t) \in \mathbb{R}^n$ denotes the RISE feedback term defined as [19, 22]

$$\mu\left(t\right) \triangleq (k_s + 1) e_m(t) - (k_s + 1) e_m(0) + \int_0^t \left[(k_s + 1)\alpha_m e_m(\sigma) + \beta_1 sgn(e_m(\sigma))\right] d\sigma, \tag{4–12}$$

where $k_s, \beta_1 \in \mathbb{R}$ are positive constant control gains, and $\alpha_m \in \mathbb{R}$ was introduced in (4–6). In (4–11), $\hat{\theta}\left(t\right) \in \mathbb{R}^p$ denotes a subsequently designed parameter estimate vector. The closed-loop tracking error system is developed by substituting (4–11) into (4–7) as

$$G^{-1} r = Y_d\left(\theta - \hat{\theta}\right) + S - G_d^{-1} h - \mu. \tag{4–13}$$

To facilitate the subsequent modular adaptive control development and stability analysis, the time derivative of (4–13) is expressed as

$$G^{-1}\dot{r} = -\frac{1}{2}\dot{G}^{-1} r + \tilde{N}(t) + N_B\left(t\right) - (k_s + 1) r - \beta_1 sgn(e_m) - e_m, \tag{4–14}$$

where the fact that the time derivative of (4–12) is given as

$$\dot{\mu}(t) = (k_s + 1) r + \beta_1 sgn(e_m) \tag{4–15}$$

was utilized. In (4–14), the unmeasurable/unknown auxiliary terms $\tilde{N}(e_1, e_2, ..., e_m, r, t)$, $N_B\left(t\right) \in \mathbb{R}^n$ are defined as

$$\tilde{N}(t) \triangleq -\frac{1}{2}\dot{G}^{-1} r + \dot{S} + e_m + \tilde{N}_0 \tag{4–16}$$

$$N_B(t) \triangleq N_{B_1}(t) + N_{B_2}(t), \tag{4–17}$$

where $N_{B_1}(t) \in \mathbb{R}^n$ is given by

$$N_{B_1} \triangleq \dot{Y}_d\theta - \dot{G}_d^{-1}h - G_d^{-1}\dot{h}, \tag{4–18}$$

and the sum of the auxiliary terms $\tilde{N}_0(t)$, $N_{B_2}(t) \in \mathbb{R}^n$ is given by

$$N_{B_2}(t) + \tilde{N}_0 = -\dot{Y}_d\hat{\theta} - Y_d\dot{\hat{\theta}}. \tag{4–19}$$

Specific definitions for $\tilde{N}_0(t)$, $N_{B_2}(t)$ are provided subsequently based on the definition of the adaptive update law for $\hat{\theta}(t)$. The structure of (4–14) and the introduction of the auxiliary terms in (4–16)-(4–19) is motivated by the desire to segregate terms that can be upper bounded by state-dependent terms and terms that can be upper bounded by constants. Specifically, depending on how the adaptive update law is designed, analysis is provided in the next section to upper bound $\tilde{N}(t)$ by state-dependent terms and $N_B(t)$ by a constant. The need to further segregate $N_B(t)$ is that some terms in $N_B(t)$ have time derivatives that are upper bounded by a constant, while other terms have time-derivatives that are upper-bounded by state dependent terms. The segregation of these terms based on the structure of the adaptive update law (see (4–19)) is key for the development of a stability analysis for the modular RISE-based adaptive update law/controller.

4.5 Modular Adaptive Update Law Development

A key difference between the traditional modular adaptive controllers that use nonlinear damping (cf., [1, 41, 63]) and the current RISE-based approach is that the RISE-based method does not exploit the ISS property with respect to the parameter estimation error. The current approach does not rely on nonlinear damping, but instead uses the ability of the RISE technique to compensate for smooth bounded disturbances. In general, previous nonlinear damping-based modular adaptive controllers first prove an ISS stability result provided the adaptive update law yields bounded parameter estimates (e.g., $\hat{\theta}(t) \in \mathcal{L}_\infty$ via a projection algorithm), and then use additional analysis along with

assumptions (PD estimate of the inertia matrix, square integrable prediction error, etc.) to conclude asymptotic convergence. In contrast, since the RISE-based modular adaptive control approach in this chapter does not exploit an ISS analysis, the assumptions regarding the parameter estimate are modified. The following development requires some general bounds on the structure of the adaptive update law $\dot{\hat{\theta}}(t)$ and the corresponding parameter estimate $\hat{\theta}(t)$ to segregate the components of the auxiliary terms introduced in (4–16)-(4–19). Specifically, instead of assuming that $\hat{\theta}(t) \in \mathcal{L}_\infty$, the subsequent development is based on the less restrictive assumption that the parameter estimate $\hat{\theta}(t)$ can be described as

$$\hat{\theta}(t) = f_1(t) + \Phi(x, \dot{x}, ..., x^{(m-1)}, e_1, e_2, ..., e_m, t). \tag{4–20}$$

In (4–20), $f_1(t) \in \mathbb{R}^p$ is a known function such that

$$\|f_1(t)\| \leq \gamma_1 \tag{4–21}$$

$$\left\|\dot{f}_1(t)\right\| \leq \gamma_2 + \sum_{i=1}^{m} \gamma_{i+2} \|e_i\| + \gamma_{m+3} \|r\|,$$

where $\gamma_i \in \mathbb{R}$, $i = 1, 2, ..., m+3$ are known non-negative constants (i.e., the constants can be set to zero for different update laws), and $\Phi\left(x, \dot{x}, ..., x^{(m-1)}, e_1, e_2, ..., e_m, t\right) \in \mathbb{R}^p$ is a known function that satisfies the following bound:

$$\|\Phi(t)\| \leq \rho_1(\|\bar{e}\|) \|\bar{e}\|, \tag{4–22}$$

where the bounding function $\rho_1(\cdot) \in \mathbb{R}$ is a positive, globally invertible, nondecreasing function, and $\bar{e}(t) \in \mathbb{R}^{nm}$ is defined as

$$\bar{e}(t) \triangleq \left[e_1^T \;\; e_2^T \;\; ... \;\; e_m^T\right]^T. \tag{4–23}$$

The estimate in (4–20) is assumed to be generated according to an update law of the following general form

$$\dot{\hat{\theta}}(t) = g_1(t) + \Omega(x, \dot{x}, ..., x^{(m-1)}, e_1, e_2, ..., e_m, r, t). \tag{4–24}$$

In (4–24), $g_1(t) \in \mathbb{R}^p$ is a known function such that

$$\|g_1(t)\| \leq \delta_1 \tag{4–25}$$

$$\|\dot{g}_1(t)\| \leq \delta_2 + \sum_{i=1}^{m} \delta_{i+2} \|e_i\| + \delta_{m+3} \|r\|,$$

where $\delta_i \in \mathbb{R}$, $i = 1, 2, ..., m+3$ are known non-negative constants, and $\Omega(x, \dot{x}, ..., x^{(m-1)}, e_1, e_2, ..., e_m, r, t) \in \mathbb{R}^p$ satisfies the following bound:

$$\|\Omega(t)\| \leq \rho_2(\|z\|)\|z\|, \tag{4–26}$$

where the bounding function $\rho_2(\cdot) \in \mathbb{R}$ is a positive, globally invertible, nondecreasing function, and $z(t) \in \mathbb{R}^{n(m+1)}$ is defined as

$$z(t) \triangleq \left[e_1^T \;\; e_2^T \;\; ... \;\; e_m^T \;\; r^T\right]^T. \tag{4–27}$$

Remark 4.1. *The update law in (4–24) depends on the unmeasurable signal $r(t)$. But it is assumed that the update law in (4–24) is of the form which upon integration yields an estimate $\hat{\theta}(t)$ that is independent of $r(t)$. Thus the controller needs only the measurable signals for implementation.*

The structure of the adaptive estimate and the adaptive update law is flexible in the sense that any of the terms in (4–20) and (4–24) can be removed for any specific update law and estimate. For example if all the error-dependent terms in (4–20) are removed, then the condition on $\hat{\theta}(t)$ is the same as in the standard nonlinear damping-based modular adaptive methods (i.e., $\hat{\theta}(t) \in \mathcal{L}_\infty$). In this sense, the ISS property with respect to the parameter estimation error is automatically proven by considering this special case of $\hat{\theta}(t)$. The results in this chapter are not proven for estimates or update

laws with additional terms that are not included in the generic structure in (4–20) and (4–24). For example, a standard gradient-based update law is of the form (4–24), but the corresponding estimate (obtained via integration by parts) is not of the form (4–20) due to the presence of some terms that are bounded by the integral of the error instead of being bounded by the error. However, the same gradient-based update law and its corresponding estimate can be used in (4–11) if a smooth projection algorithm is used that keeps the estimates bounded. As shown in [19], the standard gradient-based update law can be used in (4–11) without a projection algorithm, yet including this structure in the modular adaptive analysis is problematic because the integral of the error could be unbounded (so this update law could not be used in nonlinear damping-based modular adaptive laws without a projection either). Since the goal in this chapter is to develop a modular update law, a specific update law cannot be used to inject terms in the stability analysis to cancel the terms containing the parameter mismatch error. Instead, the terms containing the parameter mismatch error are segregated depending on whether they are state-dependent or bounded by a constant (see (4–19)).

Based on the development given in (4–20)-(4–25), the terms $\tilde{N}_0(t)$ and $N_{B_2}(t)$ introduced in (4–16)-(4–19) are defined as

$$\tilde{N}_0(t) \triangleq -\dot{Y}_d\Phi - Y_d\Omega \tag{4–28}$$

$$N_{B_2}(t) \triangleq -\dot{Y}_d f_1 - Y_d g_1. \tag{4–29}$$

In a similar manner as in Lemma 1 of the Appendix, by applying the Mean Value Theorem along with the inequalities in (4–22) and (4–26) yields an upper bound for the expression in (4–16) as

$$\left\|\tilde{N}(t)\right\| \leq \rho\left(\|z\|\right)\|z\|, \tag{4–30}$$

where the bounding function $\rho(\cdot) \in \mathbb{R}$ is a positive, globally invertible, nondecreasing function, and $z(t) \in \mathbb{R}^{n(m+1)}$ is defined in (4–27). The following inequalities are developed based on the expressions in (4–17), (4–18), (4–29), their time derivatives,

and the inequalities in (4–21) and (4–25):

$$\|N_B(t)\| \leq \zeta_1 \qquad \left\|\dot{N}_{B_1}(t)\right\| \leq \zeta_2 \tag{4–31}$$
$$\left\|\dot{N}_{B_2}(t)\right\| \leq \zeta_3 + \sum_{i=1}^{m} \zeta_{i+3} \|e_i\| + \zeta_{m+4} \|r\|,$$

where $\zeta_i \in \mathbb{R}$, $i = 1, 2, ..., m+4$ are known positive constants.

4.6 Stability Analysis

Theorem 4-1: The controller given in (4–11), (4–12), (4–20), and (4–24) ensures that all system signals are bounded under closed-loop operation and that the position tracking error is regulated in the sense that

$$\|e_1(t)\| \to 0 \qquad \text{as} \qquad t \to \infty$$

provided the control gain k_s introduced in (4–12) is selected sufficiently large (see the subsequent proof), α_i, $i = 1, 2, ..., m$ are selected according to the following conditions

$$\alpha_i > \frac{1}{2}\beta_{i+1}, \ i = 1, 2, ..., m-2 \qquad \alpha_{m-1} > \frac{1}{2}\beta_m + \frac{1}{2} \tag{4–32}$$
$$\alpha_m > \beta_{m+1} + \frac{1}{2}\beta_{m+2} + \frac{1}{2}\sum_{i=1}^{m-1}\beta_{i+1} + \frac{1}{2},$$

and β_i, $i = 1, 2, ..., m+2$ are selected according to the following sufficient conditions:

$$\beta_1 > \zeta_1 + \frac{1}{\alpha_m}\zeta_2 + \frac{1}{\alpha_m}\zeta_3 \tag{4–33}$$
$$\beta_{i+1} > \zeta_{i+3}, \ i = 1, 2, ..., m+1,$$

where β_1 was introduced in (4–12), and $\beta_2, ..., \beta_{m+2}$ are introduced in (4–36).

Proof: Let $\mathcal{D} \subset \mathbb{R}^{n(m+1)+1}$ be a domain containing $y(t) = 0$, where $y(t) \in \mathbb{R}^{n(m+1)+1}$ is defined as

$$y(t) \triangleq [z^T(t) \quad \sqrt{P(t)}]^T. \tag{4–34}$$

In (4–34), the auxiliary function $P(t) \in \mathbb{R}$ is defined as

$$P(t) \triangleq \beta_1 \sum_{i=1}^{n} |e_{mi}(0)| - e_m(0)^T N_B(0) - \int_0^t L(\tau) d\tau, \tag{4–35}$$

where $e_{mi}(0)$ denotes the ith element of the vector $e_m(0)$, and the auxiliary function $L(t) \in \mathbb{R}$ is defined as

$$L(t) \triangleq r^T (N_B(t) - \beta_1 sgn(e_m)) - \sum_{i=1}^{m} \beta_{i+1} \|e_i(t)\| \|e_m(t)\| - \beta_{m+2} \|e_m(t)\| \|r(t)\|, \tag{4–36}$$

where $\beta_i \in \mathbb{R}$, $i = 2, 3, ..., m+2$ are positive constants chosen according to the sufficient conditions in (4–33). Provided the sufficient conditions introduced in (4–33) are satisfied, the following inequality is obtained[1] :

$$\int_0^t L(\tau) d\tau \leq \beta_1 \sum_{i=1}^{n} |e_{mi}(0)| - e_m(0)^T N_B(0). \tag{4–37}$$

Hence, (4–37) indicates that $P(t) \geq 0$.

Let $V_L(y,t) : \mathcal{D} \times [0, \infty) \rightarrow \mathbb{R}$ be a continuously differentiable, positive definite function defined as

$$V_L(y,t) \triangleq \frac{1}{2} \sum_{i=1}^{m} e_i^T e_i + \frac{1}{2} r^T G^{-1} r + P, \tag{4–38}$$

which satisfies the following inequalities:

$$U_1(y) \leq V_L(y,t) \leq U_2(y) \tag{4–39}$$

provided the sufficient conditions introduced in (4–32)-(4–33) are satisfied. The Rayleigh-Ritz theorem was used to develop the inequalities in (4–39), where the continuous positive definite functions $U_1(y)$,$U_2(y) \in \mathbb{R}$ are defined as $U_1(y) \triangleq \lambda_1 \|y\|^2$ and $U_2(y) \triangleq \lambda_2(x, \dot{x}, ..., x^{(m-1)}) \|y\|^2$, where λ_1, $\lambda_2(x, \dot{x}, ..., x^{(m-1)}) \in \mathbb{R}$ are defined as

$$\lambda_1 \triangleq \frac{1}{2} \min \{1, \underline{g}\} \qquad \lambda_2(x, \dot{x}, ..., x^{(m-1)}) \triangleq \max\{\frac{1}{2} \bar{g}(x, \dot{x}, ..., x^{(m-1)}), 1\}, \tag{4–40}$$

[1] Details of the bound in (4–37) are provided in the Lemma 1 of the Appendix.

where $\underline{g}$, $\bar{g}(x, \dot{x}, ..., x^{(m-1)})$ are introduced in (4–2). After taking the time derivative of (4–38), $\dot{V}(y,t)$ is expressed as

$$\dot{V}_L(y,t) = r^T G^{-1}\dot{r} + \frac{1}{2} r^T \dot{G}^{-1} r + \sum_{i=1}^{m} e_i^T \dot{e}_i + \dot{P}.$$

The derivative $\dot{P}(t) \in \mathbb{R}$ is given by

$$\dot{P}(t) = -L(t) = -r^T(N_B(t) - \beta_1 sgn(e_m)) + \sum_{i=1}^{m} \beta_{i+1} \|e_i(t)\| \|e_m(t)\| + \beta_{m+2} \|e_m(t)\| \|r(t)\|. \tag{4–41}$$

After utilizing (4–4), (4–6), (4–14), (4–15), and (4–41), $\dot{V}(y,t)$ is expressed as

$$\begin{aligned}\dot{V}_L(y,t) = {} & \frac{1}{2} r^T \dot{G}^{-1} r - \sum_{i=1}^{m} \alpha_i e_i^T e_i + e_{m-1}^T e_m - \frac{1}{2} r^T \dot{G}^{-1} r \\ & + r^T \tilde{N} + r^T N_B - r^T r - k_s r^T r - \beta_1 r^T sgn(e_m) \\ & - r^T(N_B - \beta_1 sgn(e_m)) + \sum_{i=1}^{m} \beta_{i+1} \|e_i\| \|e_m\| + \beta_{m+2} \|e_m\| \|r\|.\end{aligned}$$

After canceling similar terms, $\dot{V}(y,t)$ is simplified as

$$\begin{aligned}\dot{V}_L(y,t) = {} & -\sum_{i=1}^{m} \alpha_i e_i^T e_i + e_{m-1}^T e_m - r^T r - k_s r^T r + r^T \tilde{N} \\ & + \sum_{i=1}^{m} \beta_{i+1} \|e_i\| \|e_m\| + \beta_{m+2} \|e_m\| \|r\|.\end{aligned}$$

Based on the fact that $a^T b \leq \frac{1}{2}(\|a\|^2 + \|b\|^2)$ for some $a, b \in \mathbb{R}^n$, $\dot{V}_L(y,t)$ is upper bounded using the squares of the components of $z(t)$ as

$$\begin{aligned}\dot{V}_L(y,t) \leq {} & -\sum_{i=1}^{m-2} (\alpha_i - \frac{1}{2}\beta_{i+1}) \|e_i\|^2 - (\alpha_{m-1} - \frac{1}{2}\beta_m - \frac{1}{2}) \|e_{m-1}\|^2 \\ & - (\alpha_m - \beta_{m+1} - \frac{1}{2}\beta_{m+2} - \frac{1}{2}\sum_{i=1}^{m-1} \beta_{i+1} - \frac{1}{2}) \|e_m\|^2 - \|r\|^2 \\ & - (k_s - \frac{1}{2}\beta_{m+2}) \|r\|^2 + r^T \tilde{N}.\end{aligned} \tag{4–42}$$

By using (4–30), the expression in (4–42) is rewritten as

$$\dot{V}_L(y,t) \leq -\lambda_3 \|z\|^2 - \left[(k_s - \frac{\beta_{m+2}}{2}) \|r\|^2 - \rho(\|z\|) \|r\| \|z\| \right], \tag{4–43}$$

where

$$\lambda_3 \triangleq \min\{\alpha_1 - \frac{1}{2}\beta_2, \alpha_2 - \frac{1}{2}\beta_3, ..., \alpha_{m-2} - \frac{1}{2}\beta_{m-1},$$
$$\alpha_{m-1} - \frac{1}{2}\beta_m - \frac{1}{2}, \alpha_m - \beta_{m+1} - \frac{1}{2}\beta_{m+2} - \frac{1}{2}\sum_{i=1}^{m-1}\beta_{i+1} - \frac{1}{2}, 1\}.$$

After completing the squares for the terms inside the brackets in (4–43), the following expression can be obtained, provided the sufficient gain conditions in (4–32) and (4–33) are satisfied:

$$\dot{V}_L(y,t) \leq -\lambda_3 \|z\|^2 + \frac{\rho^2(\|z\|) \|z\|^2}{4\left(k_s - \frac{\beta_{m+2}}{2}\right)}. \tag{4–44}$$

The expression in (4–44) can be further upper bounded by a continuous, positive semi-definite function

$$\dot{V}_L(y,t) \leq -U(y) = -c \|z\|^2 \qquad \forall y \in \mathcal{D} \tag{4–45}$$

for some positive constant $c \in \mathbb{R}$, where

$$\mathcal{D} \triangleq \left\{ y \in \mathbb{R}^{n(m+1)+1} \mid \|y\| \leq \rho^{-1}\left(2\sqrt{\lambda_3\left(k_s - \frac{\beta_{m+2}}{2}\right)}\right) \right\}.$$

Larger values of k will expand the size of the domain $\mathcal{D}$. The inequalities in (4–39) and (4–45) indicate that $V_L(y,t) \in \mathcal{L}_\infty$ in $\mathcal{D}$; hence, $e_i(t) \in \mathcal{L}_\infty$, and $r(t) \in \mathcal{L}_\infty$ in $\mathcal{D}$. Given that $e_i(t) \in \mathcal{L}_\infty$, and $r(t) \in \mathcal{L}_\infty$ in $\mathcal{D}$, then $\dot{e}_i(t) \in \mathcal{L}_\infty$ in $\mathcal{D}$ from (4–4) and (4–6). Since $e_i(t) \in \mathcal{L}_\infty$, and $r(t) \in \mathcal{L}_\infty$ in $\mathcal{D}$, the assumption that $x_d^{(i)}(t)$ exist and are bounded and (4–3)-(4–6) indicate that $x^{(i)}(t) \in \mathcal{L}_\infty$ in $\mathcal{D}$. Since $x^{(i)}(t) \in \mathcal{L}_\infty$ in $\mathcal{D}$, (4–20)-(4–25) indicate that $\hat{\theta}(t), \dot{\hat{\theta}}(t) \in \mathcal{L}_\infty$ in $\mathcal{D}$, and $G^{-1}(\cdot)$ and $f(\cdot) \in \mathcal{L}_\infty$ in $\mathcal{D}$ from Property 2. Thus, from (4–1) and Property 3, we can show that $u(t) \in \mathcal{L}_\infty$ in $\mathcal{D}$. Given that $r(t) \in \mathcal{L}_\infty$ in $\mathcal{D}$, (4–15) indicates that $\dot{\mu}(t) \in \mathcal{L}_\infty$ in $\mathcal{D}$. Since $x^{(i)}(t) \in \mathcal{L}_\infty$ in $\mathcal{D}$, then $\dot{G}^{-1}(\cdot)$ and $\dot{f}(\cdot) \in \mathcal{L}_\infty$

in $\mathcal{D}$ based on Property 2; hence, (4–14) indicates that $\dot{r}(t) \in \mathcal{L}_\infty$ in $\mathcal{D}$. Since $\dot{e}_i(t) \in \mathcal{L}_\infty$ and $\dot{r}(t) \in \mathcal{L}_\infty$ in $\mathcal{D}$, then $U(y)$ is uniformly continuous in $\mathcal{D}$ based on the definitions for $U(y)$ and $z(t)$.

Let $\mathcal{S} \subset \mathcal{D}$ denote a set defined as

$$\mathcal{S} \triangleq \left\{ y(t) \in \mathcal{D} \mid U_2(y(t)) < \lambda_1 \left(\rho^{-1} \left(2\sqrt{\lambda_3 \left(k_s - \frac{\beta_{m+2}}{2} \right)} \right) \right)^2 \right\}. \tag{4–46}$$

The region of attraction in (4–46) is arbitrarily large and can include any initial condition by increasing the control gain k_s (i.e., a semi-global stability result). By invoking Theorem 8.4 of [63]

$$c \left\| z(t) \right\|^2 \to 0 \qquad as \qquad t \to \infty \qquad \forall y(0) \in \mathcal{S}. \tag{4–47}$$

Based on the definition of $z(t)$, (4–47) indicates that

$$\left\| e_1(t) \right\| \to 0 \qquad as \qquad t \to \infty \qquad \forall y(0) \in \mathcal{S}. \tag{4–48}$$

4.7 Neural Network Extension to Non-LP Systems

The class of RISE-based modular adaptive controllers developed in the preceding sections are extended to include uncertain dynamic systems that do not satisfy the LP assumption (i.e., Assumption 4-4 is not satisfied). NN-based estimation methods are well suited for control systems where the dynamic model contains unstructured nonlinear disturbances as in (4–1). The main feature that empowers NN-based controllers is the universal approximation property as described in Section 3.4 of Chapter 3.

4.7.1 RISE Feedback Control Development

The modular control development and stability analysis is provided to illustrate how the aforementioned textbook (e.g., [15]) NN feedforward estimation strategy can be fused with a RISE feedback control method as a means to achieve asymptotic stability for general class of MIMO systems described by (4–1) while using generic NN weight update laws. The open-loop and closed-loop tracking error is developed for the combined control system.

Similar to (4–7), the open-loop tracking error system is developed by premultiplying (4–6) by G^{-1} and utilizing the expressions in (4–1) and (4–4) to obtain:

$$G^{-1}r = f_{NN} + S - G_d^{-1}h - u, \tag{4–49}$$

where the auxiliary function $f_{NN}(x_d, \dot{x}_d, ..., x_d^{(m)}) \in \mathbb{R}^n$ is defined as

$$f_{NN} \triangleq G_d^{-1}x_d^{(m)} - G_d^{-1}f_d, \tag{4–50}$$

where $G_d^{-1}(x_d, \dot{x}_d, ..., x_d^{(m-1)}) \in \mathbb{R}^{n\times n}$ and $f_d(x_d, \dot{x}_d, ..., x_d^{(m-1)}) \in \mathbb{R}^n$ are defined in (4–9). In (4–49), the auxiliary function $S\left(x, \dot{x}, ..., x^{(m-1)}, t\right) \in \mathbb{R}^n$ is defined similar to (4–10). The expression in (4–50) can be represented by a three-layer NN as

$$f_{NN} = W^T\sigma\left(V^T\bar{x}_d\right) + \varepsilon\left(\bar{x}_d\right). \tag{4–51}$$

In (4–51), the input $\bar{x}_d(t) \in \mathbb{R}^{(m+1)n+1}$ is defined as $\bar{x}_d(t) \triangleq [1 \;\; x_d^T(t) \;\; \dot{x}_d^T(t) \;\; ... \;\; x_d^{(m)T}(t)]^T$ so that $N_1 = (m+1)\,n$ where N_1 was introduced in (3–4). Based on the assumption that the desired trajectory is bounded, the inequalities in (3–16) hold. Based on the open-loop error system in (4–49), the control torque input is composed of a three-layer NN feedforward term plus the RISE feedback term as

$$u \triangleq \hat{f}_{NN} + \mu \tag{4–52}$$

where the RISE feedback term $\mu \in \mathbb{R}^n$ is defined in (4–12), and the feedforward NN component denoted by $\hat{f}_{NN}(t) \in \mathbb{R}^n$, is defined as

$$\hat{f}_{NN} \triangleq \hat{W}^T\sigma(\hat{V}^T\bar{x}_d). \tag{4–53}$$

4.7.2 Modular Tuning Law Development

The estimates for the NN weights in (4–53) are generated on-line (there is no off-line learning phase) using a smooth projection algorithm as

$$\dot{\hat{W}} \triangleq proj\left(\varrho_1\right) = \begin{cases} \varrho_1 & \text{if } vec(\hat{W}) \in int(\Lambda_W) \\ \varrho_1 & \text{if } vec(\hat{W}) \in \partial(\Lambda_W) \text{ and } vec\left(\varrho_1\right)^T vec(\hat{W})^{\perp} \leq 0 \\ P_{Mr}^{t}\left(\varrho_1\right) & \text{if } vec(\hat{W}) \in \partial(\Lambda_W) \text{ and } vec\left(\varrho_1\right)^T vec(\hat{W})^{\perp} > 0 \end{cases} \tag{4–54}$$

$$\dot{\hat{V}} \triangleq proj\left(\varrho_2\right) = \begin{cases} \varrho_2 & \text{if } vec(\hat{V}) \in int(\Lambda_V) \\ \varrho_2 & \text{if } vec(\hat{V}) \in \partial(\Lambda_V) \text{ and } vec\left(\varrho_2\right)^T vec(\hat{V})^{\perp} \leq 0 \\ P_{Mr}^{t}\left(\varrho_2\right) & \text{if } vec(\hat{V}) \in \partial(\Lambda_V) \text{ and } vec\left(\varrho_2\right)^T vec(\hat{V})^{\perp} > 0, \end{cases} \tag{4–55}$$

where $proj\left(\cdot\right)$ is the projection operator and

$$vec(\hat{W}\left(0\right)) \in int\left(\Lambda_W\right), \quad vec(\hat{V}\left(0\right)) \in int\left(\Lambda_V\right).$$

In (4–54) and (4–55), the auxiliary terms $\varrho_1(t) \in \mathbb{R}^{(N_2+1)\times n}$ and $\varrho_2(t) \in \mathbb{R}^{(N_1+1)\times N_2}$ denote adaptation rules of the following general form:

$$\begin{aligned} proj\left(\varrho_1\right) &= w_1\left(t\right) + \Xi_W(x, \dot{x}, ..., x^{(m-1)}, e_1, e_2, ..., e_m, r, t) \\ proj\left(\varrho_2\right) &= v_1\left(t\right) + \Xi_V(x, \dot{x}, ..., x^{(m-1)}, e_1, e_2, ..., e_m, r, t). \end{aligned} \tag{4–56}$$

In (4–56), $w_1\left(t\right) \in \mathbb{R}^{(N_2+1)\times n}$ and $v_1\left(t\right) \in \mathbb{R}^{(N_1+1)\times N_2}$ are known functions such that

$$\begin{aligned} \left\|w_1\left(t\right)\right\| &\leq \gamma_1 \\ \left\|\dot{w}_1\left(t\right)\right\| &\leq \gamma_2 + \sum_{i=1}^{m} \gamma_{i+2} \left\|e_i\right\| + \gamma_{m+3} \left\|r\right\| \end{aligned} \tag{4–57}$$

$$\begin{aligned} \left\|v_1\left(t\right)\right\| &\leq \delta_1 \\ \left\|\dot{v}_1\left(t\right)\right\| &\leq \delta_2 + \sum_{i=1}^{m} \delta_{i+2} \left\|e_i\right\| + \delta_{m+3} \left\|r\right\|, \end{aligned} \tag{4–58}$$

and $\Xi_W \in \mathbb{R}^{(N_2+1)\times n}$ and $\Xi_V \in \mathbb{R}^{(N_1+1)\times N_2}$ satisfy the following bounds:

$$\|\Xi_W(t)\| \leq \sum_{i=1}^{m} \gamma_{i+m+3} \|e_i\| + \gamma_{2m+4} \|r\| \tag{4–59}$$

$$\|\Xi_V(t)\| \leq \sum_{i=1}^{m} \delta_{i+m+3} \|e_i\| + \delta_{2m+4} \|r\|,$$

where $\gamma_i, \delta_i \in \mathbb{R}$, $i = 1, 2, ..., 2m+4$ are known non-negative constants (i.e., the constants can be set to zero for different update laws). In (4–54) and (4–55), $P_{Mr}^{t}(A) = devec(P_r^t(vec(A)))$ for a matrix A, where the operation $devec(\cdot)$ is the reverse of $vec(\cdot)$. The use of the projection algorithm in (4–54) and (4–55) is to ensure that $\hat{W}(t)$ and $\hat{V}(t)$ remain bounded inside the convex regions defined in (3–9) and (3–11). This fact will be exploited in the subsequent stability analysis. Thus, unlike the general form for parameter estimate $\hat{\theta}(t)$ in (4–20) for the LP case, the NN weight estimates are bounded by constants. The NN weight adaptation laws are restrictive compared to the adaptive laws for the parameter estimates in the LP case. This is because the first layer weight estimates $\hat{V}(t)$ are embedded inside the nonlinear activation function $\sigma(\cdot)$ (i.e., $\sigma(\hat{V}^T \bar{x}_d)$). Typically the NN activation functions are bounded over the entire domain; however, their time derivatives depend on the adaptation law $\dot{\hat{V}}(t)$, which could be state-dependent. Similar to the LP case, it is assumed that only the NN adaptation rules depend on the unmeasurable signal $r(t)$ but the corresponding weight estimate obtained after integration is independent of $r(t)$.

The closed-loop tracking error system can be developed by substituting (4–52) into (4–49) as

$$G^{-1} r = f_{NN} - \hat{f}_{NN} + S - G_d^{-1} h - \mu. \tag{4–60}$$

To facilitate the subsequent stability analysis, the time derivative of (4–60) is determined as

$$G^{-1}\dot{r} = -\dot{G}^{-1} r + \dot{f}_{NN} - \dot{\hat{f}}_{NN} + \dot{S} - \dot{G}_d^{-1} h - G_d^{-1} \dot{h} - \dot{\mu}. \tag{4–61}$$

Using (4–51), (4–53), the closed-loop error system in (4–61) can be expressed as

$$G^{-1}\dot{r} = -\dot{G}^{-1}r + W^T\sigma'\left(V^T\bar{x}_d\right)V^T\dot{\bar{x}}_d - \dot{\hat{W}}^T\sigma(\hat{V}^T\bar{x}_d) \tag{4–62}$$
$$- \hat{W}^T\sigma'(\hat{V}^T\bar{x}_d)(\dot{\hat{V}}^T\bar{x}_d + \hat{V}^T\dot{\bar{x}}_d) + \dot{\varepsilon} + \dot{S} - \dot{G}_d^{-1}h - G_d^{-1}\dot{h} - \dot{\mu},$$

where $\sigma'(\hat{V}^T\bar{x}) \equiv d\sigma\left(V^T\bar{x}\right)/d\left(V^T\bar{x}\right)|_{V^T\bar{x}=\hat{V}^T\bar{x}}$. After adding and subtracting the term $W^T\hat{\sigma}'\hat{V}^T\dot{\bar{x}}_d + \hat{W}^T\hat{\sigma}'\tilde{V}^T\dot{\bar{x}}_d$ to (4–62), the following expression can be obtained:

$$G^{-1}\dot{r} = -\dot{G}^{-1}r + \hat{W}^T\hat{\sigma}'\tilde{V}^T\dot{\bar{x}}_d + \tilde{W}^T\hat{\sigma}'\hat{V}^T\dot{\bar{x}}_d + W^T\sigma'V^T\dot{\bar{x}}_d - W^T\hat{\sigma}'\hat{V}^T\dot{\bar{x}}_d \tag{4–63}$$
$$- \hat{W}^T\hat{\sigma}'\tilde{V}^T\dot{\bar{x}}_d - \dot{\hat{W}}^T\hat{\sigma} - \hat{W}^T\hat{\sigma}'\dot{\hat{V}}^T\bar{x}_d + \dot{\varepsilon} + \dot{S} - \dot{G}_d^{-1}h - G_d^{-1}\dot{h} - \dot{\mu},$$

where the notations $\hat{\sigma}$ and $\tilde{\sigma}$ are introduced in (3–6). Substituting the NN weight adaptation laws in (4–54), (4–55) in (4–63) yields

$$G^{-1}\dot{r} = -\frac{1}{2}\dot{G}^{-1}r + \tilde{N} + N_B - e_m - (k_s+1)r - \beta_1 sgn(e_m), \tag{4–64}$$

where (4–15) was utilized, and the unmeasurable auxiliary terms $\tilde{N}(e_1, e_2, ..., e_m, r, t)$, $N_B(\hat{W}, \hat{V}, \bar{x}_d, \dot{\bar{x}}_d, t) \in \mathbb{R}^n$ are defined as

$$\tilde{N} \triangleq -\frac{1}{2}\dot{G}^{-1}r - \Xi_W^T\hat{\sigma} - \hat{W}^T\hat{\sigma}'\Xi_V^T\bar{x}_d + \dot{S} + e_m \tag{4–65}$$

$$N_B \triangleq N_{B_1} + N_{B_2}. \tag{4–66}$$

In (4–66), $N_{B_1}(\bar{x}_d, \dot{\bar{x}}_d, t)$, $N_{B_2}(\hat{W}, \hat{V}, \bar{x}_d, \dot{\bar{x}}_d, t) \in \mathbb{R}^n$ are given by

$$N_{B_1} = W^T\sigma'V^T\dot{\bar{x}}_d + \dot{\varepsilon} - \dot{G}_d^{-1}h - G_d^{-1}\dot{h} \tag{4–67}$$

$$N_{B_2} = \hat{W}^T\hat{\sigma}'\tilde{V}^T\dot{\bar{x}}_d + \tilde{W}^T\hat{\sigma}'\hat{V}^T\dot{\bar{x}}_d - w_1^T\hat{\sigma} - \hat{W}^T\hat{\sigma}'v_1^T\bar{x}_d \tag{4–68}$$

In a similar manner as before, application of the Mean Value Theorem will yield an upper bound for $\tilde{N}(t)$ as in (4–30). The following inequalities are developed based on Assumptions 4-2 and 4-3, (3–7), (3–8), (3–16), (4–56)-(4–59), and (4–66)-(4–68):

$$\|N_B\| \leq \zeta_1 \qquad \left\|\dot{N}_{B_1}\right\| \leq \zeta_2 \tag{4–69}$$

$$\left\| \dot{N}_{B_2} \right\| \leq \zeta_3 + \sum_{i=1}^{m} \zeta_{i+3} \left\| e_i \right\| + \zeta_{m+4} \left\| r \right\|, \tag{4–70}$$

where $\zeta_i \in \mathbb{R}$, $i = 1, 2, ..., m+4$ are known positive constants.

4.8 Stability Analysis

Theorem 4-2: The combined NN and RISE controller given in (4–52)-(4–55) ensures that all system signals are bounded under closed-loop operation and that the position tracking error is regulated in the sense that

$$\left\| e_1(t) \right\| \to 0 \qquad \text{as} \qquad t \to \infty$$

provided similar gains conditions as in Theorem 4-1 are satisfied. The proof of Theorem 4-2 is similar to Theorem 4-1.

4.9 Application to Euler-Lagrange Systems

The Euler-Lagrange formulation describes the behavior of a large class of engineering systems. In this section, the modular adaptive control development for the general class of MIMO dynamic systems is applied to dynamic systems modeled by the Euler-Lagrange formulation

$$M(q)\ddot{q} + V_m(q, \dot{q})\dot{q} + G(q) + F\left(\dot{q}\right) + \tau_d\left(t\right) = \tau(t). \tag{4–71}$$

In (4–71), $M(q) \in \mathbb{R}^{n \times n}$ denotes the inertia matrix, $V_m(q, \dot{q}) \in \mathbb{R}^{n \times n}$ denotes the centripetal-Coriolis matrix, $G(q) \in \mathbb{R}^n$ denotes the gravity vector, $F\left(\dot{q}\right) \in \mathbb{R}^n$ denotes friction, $\tau_d\left(t\right) \in \mathbb{R}^n$ denotes a general nonlinear disturbance (e.g., unmodeled effects), $\tau(t) \in \mathbb{R}^n$ represents the torque input control vector, and $q(t)$, $\dot{q}(t)$, $\ddot{q}(t) \in \mathbb{R}^n$ denote the link position, velocity, and acceleration vectors, respectively. The control development is based on the assumption that $q(t)$ and $\dot{q}(t)$ are measurable and that $M(q)$, $V_m(q, \dot{q})$, $G(q)$, $F\left(\dot{q}\right)$ and $\tau_d\left(t\right)$ are unknown. The modular adaptive controller developed in the earlier sections for the a general class of MIMO can be easily applied to Euler-Lagrange systems. Please see [80], [81] for complete details of the control development.

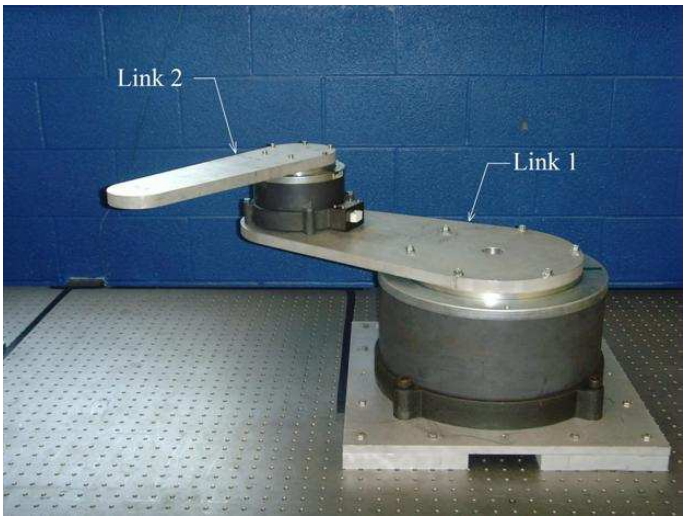

Figure 4-1. The experimental testbed consists of a two-link robot. The links are mounted on two NSK direct-drive switched reluctance motors.

4.10 Experiment

To investigate the performance of the modular controller developed in this chapter, an experiment was performed on a two-link robot testbed as depicted in Fig. 4-1. The testbed is composed of a two-link direct drive revolute robot consisting of two aluminum links, mounted on a 240.0 Nm (base joint) and 20.0 Nm (second joint) switched reluctance motors. The motors are controlled through power electronics operating in torque control mode. The motor resolvers provide rotor position measurements with a resolution of $614,400$ pulses/revolution, and a standard backwards difference algorithm is used to numerically determine velocity from the encoder readings. A Pentium 2.8 GHz PC operating under QNX hosts the control algorithm, which was implemented via a custom graphical user-interface [64], to facilitate real-time graphing, data logging, and the ability to adjust control gains without recompiling the program. Data acquisition and control implementation were performed at a frequency of 1.0 kHz using the ServoToGo I/O board.

The dynamics for the testbed are

$$\begin{bmatrix} \tau_1 \\ \tau_2 \end{bmatrix} = \begin{bmatrix} p_1 + 2p_3c_2 & p_2 + p_3c_2 \\ p_2 + p_3c_2 & p_2 \end{bmatrix} \begin{bmatrix} \ddot{q}_1 \\ \ddot{q}_2 \end{bmatrix} + \begin{bmatrix} -p_3s_2\dot{q}_2 & -p_3s_2\left(\dot{q}_1 + \dot{q}_2\right) \\ p_3s_2\dot{q}_2 & 0 \end{bmatrix} \begin{bmatrix} \dot{q}_1 \\ \dot{q}_2 \end{bmatrix} \tag{4–72}$$

$$+ f\left(\dot{q}\right) + \begin{bmatrix} \tau_{d_1} \\ \tau_{d_2} \end{bmatrix},$$

where the nonlinear friction term is assumed to be modeled as [19, 26]

$$f\left(\dot{q}\right) = \begin{bmatrix} \gamma_1\left(\tanh\left(\gamma_2\dot{q}_1\right) - \tanh\left(\gamma_3\dot{q}_1\right)\right) \\ \gamma_1\left(\tanh\left(\gamma_2\dot{q}_2\right) - \tanh\left(\gamma_3\dot{q}_2\right)\right) \end{bmatrix} + \begin{bmatrix} \gamma_4\tanh\left(\gamma_5\dot{q}_1\right) + \gamma_6\dot{q}_1 \\ \gamma_4\tanh\left(\gamma_5\dot{q}_2\right) + \gamma_6\dot{q}_2 \end{bmatrix}. \tag{4–73}$$

In (4–72) and (4–73), p_1, p_2, p_3, $\gamma_i \in \mathbb{R}$, $(i = 1, 2, ..., 6)$ are unknown positive constant parameters, c_2 denotes $cos(q_2)$, s_2 denotes $sin(q_2)$, and τ_{d_1}, $\tau_{d_2} \in \mathbb{R}$ denote general nonlinear disturbances (e.g., unmodeled effects). Part of the dynamics in (4–72) and (4–73) is linear in the following parameters:

$$\theta = \begin{bmatrix} p_1 & p_2 & p_3 & \gamma_1 & \gamma_4 & \gamma_6 \end{bmatrix}^T.$$

The parameters γ_2, γ_3, γ_5 are embedded inside the nonlinear hyperbolic tangent functions and hence cannot be linearly parameterized. Since these parameters cannot be compensated for by an adaptive algorithm, best-guess estimates $\bar{\gamma}_2 = 50$, $\bar{\gamma}_3 = 1$, $\bar{\gamma}_5 = 50$ are used. The values for $\bar{\gamma}_2$, $\bar{\gamma}_3$, $\bar{\gamma}_5$ are based on our previous experiments concerned with friction identification. Significant errors in these static estimates could degrade the performance of the system. An advantage of using the NN-based controller developed in non-LP extension section is that the NN can compensate for the non-LP dynamics. Specifically, for the NN-based controllers tested in this section, the NN is used to estimate the friction model, and the best guess values for $\bar{\gamma}_2$, $\bar{\gamma}_3$, $\bar{\gamma}_5$ are not required. The control objective is to track the desired time-varying trajectory by using the proposed

modular adaptive control law. Two different update laws were chosen for both the LP and non-LP cases. To achieve this control objective, the control gains α_1, α_2, k_s, and β_1, defined as scalars in (4–4), (4–6), and (4–12), were implemented (with non-consequential implications to the stability result) as diagonal gain matrices. Specifically, the control gains for both adaptive update laws for both the LP and non-LP cases were selected as

$$\begin{aligned} \alpha_1 = diag\{70,\ 70\} \quad \alpha_2 = diag\{25,\ 25\} \\ \beta_1 = diag\{10,\ 0.1\} \quad k_s = diag\{100,\ 20\}. \end{aligned} \tag{4–74}$$

4.10.1 Modular Adaptive Update Law

The desired trajectories for this experiment were chosen as

$$q_{d_1} = -q_{d_2} = 60\sin(2.0t)\left(1 - \exp\left(-0.01t^3\right)\right). \tag{4–75}$$

To test the modularity of the controller, two separate adaptive update laws were tested including a standard gradient update law defined as

$$\dot{\hat{\theta}} = proj\left(\Gamma Y_d^T r\right),$$

where $\Gamma \in \mathbb{R}^{6\times 6}$ is a diagonal positive-definite gain matrix, and a least squares update law defined as

$$\dot{\hat{\theta}} = proj\left(PY_d^T r\right), \qquad \dot{P} = -PY_d^T Y_d P$$

where $P(t) \in \mathbb{R}^{6\times 6}$ is a time-varying symmetric matrix. The parameter estimates were all initialized to zero. In practice, the adaptive estimates would be initialized to a best-guess estimate of the values. Initializing the estimates to zero was done to test a scenario of no parameter knowledge. For the gradient and least squares update laws the adaptation gains and the initial value of $P(t)$ were selected as

$$\Gamma = P(0) = diag\left([0.15, 0.01, 0.01, 0.01, 0.01, 0.2]\right). \tag{4–76}$$

Table 4-1. LP case: Average RMS values for 10 trials

	Gradient	Least Squares
Average RMS Error (deg) - Link 1	0.0203	0.0218
Average RMS Error (deg) - Link 2	0.0120	0.0131
Average RMS Torque (Nm) - Link 1	10.3068	10.4125
Average RMS Torque (Nm) - Link 2	1.5770	1.5959
Error Standard Deviation (deg) - Link 1	0.0016	0.0011
Error Standard Deviation (deg) - Link 2	0.0021	0.0014
Torque Standard Deviation (Nm) - Link 1	0.1545	0.1029
Torque Standard Deviation (Nm) - Link 2	0.0797	0.0677

The adaptation gain in (4–76) is gradually increased by trial and error tuning procedure based on our previous experience to achieve faster adaptation until a point when no significant performance improvement is noticed without causing unnecessary oscillations in the parameter estimates. Each experiment was performed ten times and following statistical data is provided in Table 4-1.

Figure 4-2 depicts the tracking errors for one experimental trial with a gradient update law. The control torques and adaptive estimates for the same experimental trial are shown in Figs. 4-3 and 4-4, respectively. The tracking errors for a representative experimental trial with a least squares update law is depicted in Figure 4-5. The torques for the least squares update law are shown in Figure 4-6. The adaptive estimates for the least squares update law are shown in Figure 4-6.

4.10.2 Modular Neural Network Update Law

The desired trajectories for this experiment were chosen as

$$q_{d_1} = -q_{d_2} = 60 \sin(2.5t) \left(1 - \exp\left(-0.01t^3\right)\right). \tag{4–77}$$

To test the modularity of the controller, two separate neural network tuning laws were simulated including a standard gradient tuning law based on backpropagated errors [76]

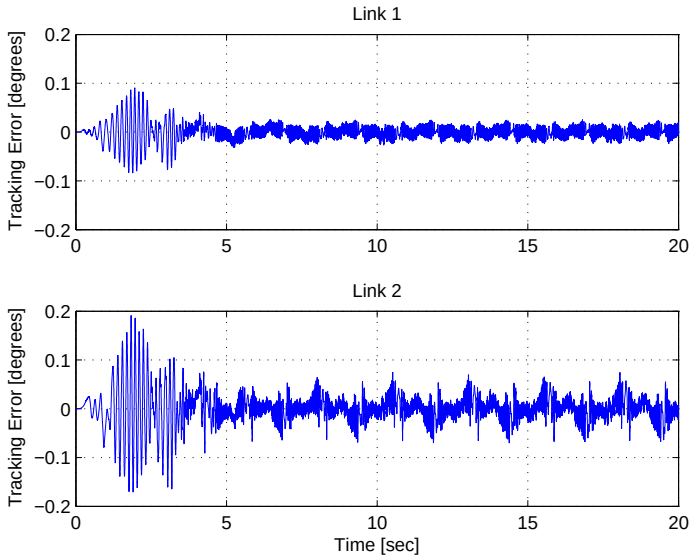

Figure 4-2. Link position tracking error with a gradient-based adaptive update law.

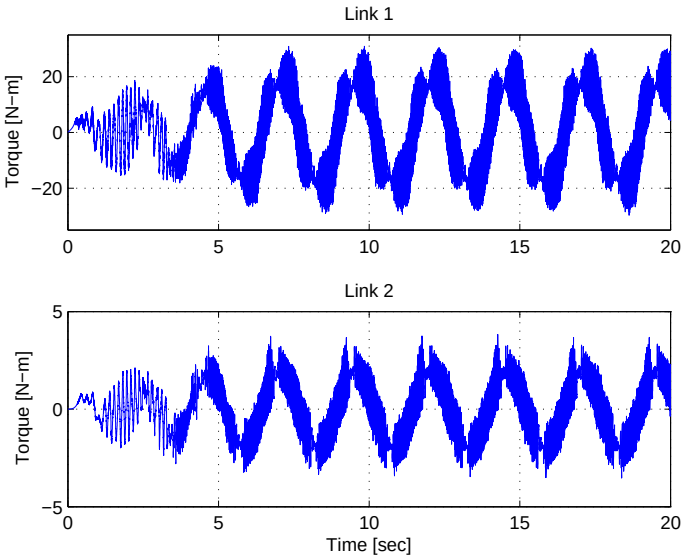

Figure 4-3. Torque input for the modular adaptive controller with a gradient-based adaptive update law.

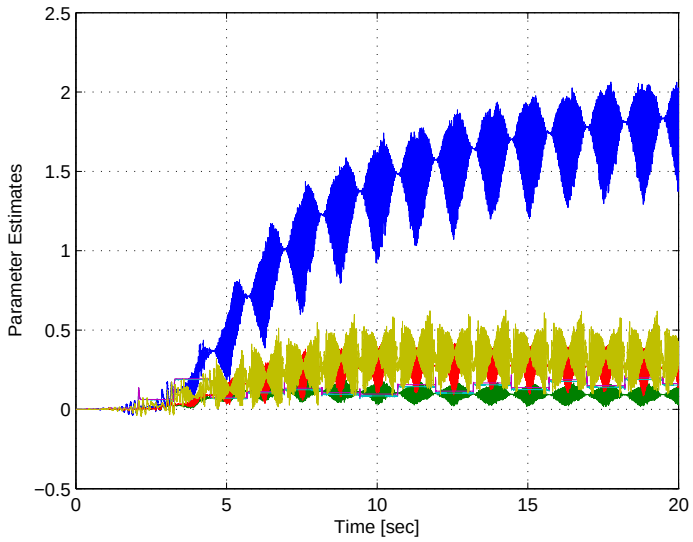

Figure 4-4. Adaptive estimates for the gradient update law.

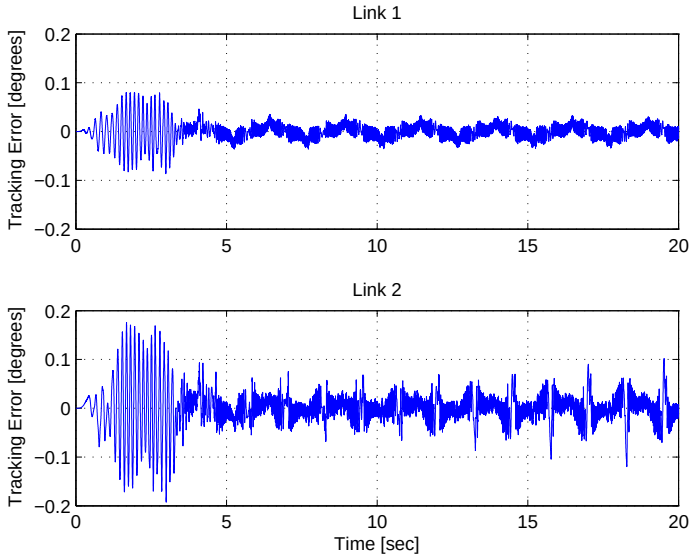

Figure 4-5. Link position tracking error with a least-squares adaptive update law.

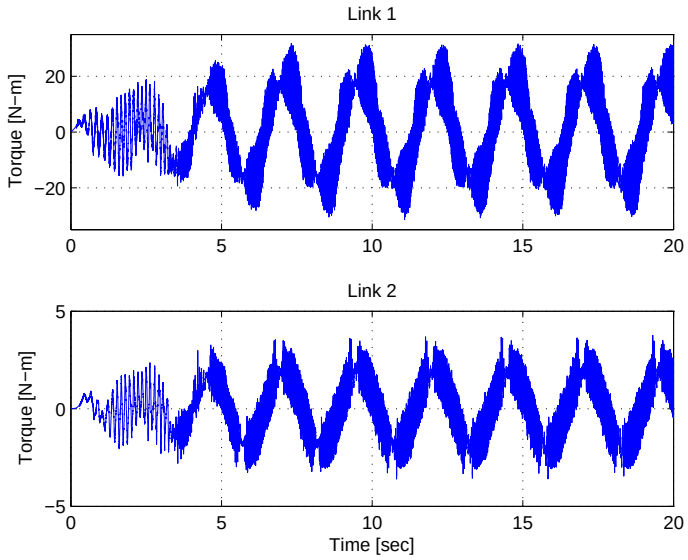

Figure 4-6. Torque input for the modular adaptive controller with a least-squares adaptive update law.

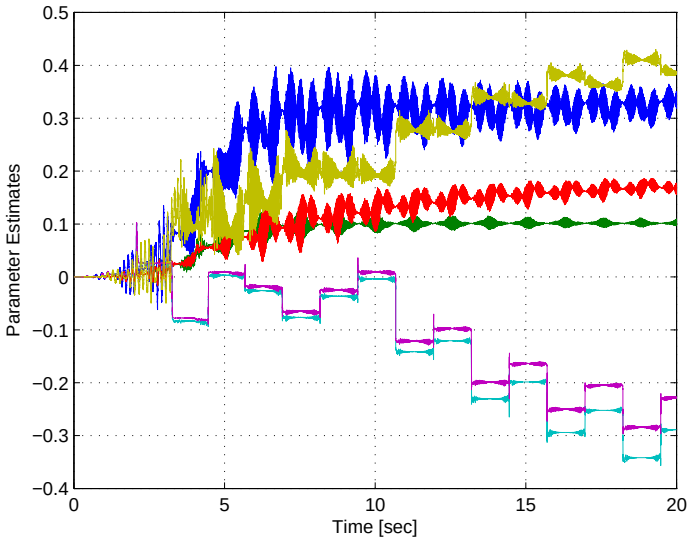

Figure 4-7. Adaptive estimates for the least squares update law.

Table 4-2. Non-LP case: Average RMS values for 10 trials

	Gradient	Hebbian
Average RMS Error (deg) - Link 1	0.0221	0.0216
Average RMS Error (deg) - Link 2	0.0173	0.0153
Average RMS Torque (Nm) - Link 1	12.5369	12.5223
Average RMS Torque (Nm) - Link 2	2.2129	2.1272
Error Standard Deviation (deg) - Link 1	0.0006	0.0011
Error Standard Deviation (deg)- Link 2	0.0009	0.0009
Torque Standard Deviation (Nm) - Link 1	0.0512	0.0429
Torque Standard Deviation (Nm) - Link 2	0.1129	0.0945

and a Hebbian tuning law [77]. The gradient update law is defined as

$$\dot{\hat{W}} = proj\left(F\hat{\sigma}'\hat{V}^T\dot{\bar{x}}_d e_2^T\right)$$
$$\dot{\hat{V}} = proj\left(G\dot{\bar{x}}_d\left(\hat{\sigma}'^T\hat{W}e_2\right)^T\right),$$

where $F \in \mathbb{R}^{11\times 11}$ and $G \in \mathbb{R}^{7\times 7}$ are gain matrixes and $\sigma(\cdot) \in \mathbb{R}^{11}$ is a sigmoidal activation function, and the input vector $\dot{\bar{x}}_d(t) \in \mathbb{R}^7$ is defined as

$$\dot{\bar{x}}_d = [1 \quad q_{d_1} \quad q_{d_2} \quad \dot{q}_{d_1} \quad \dot{q}_{d_2} \quad \ddot{q}_{d_1} \quad \ddot{q}_{d_2}]^T.$$

The Hebbian update law is defined as

$$\dot{\hat{W}} = proj\left(F\hat{\sigma}e_2^T\right)$$
$$\dot{\hat{V}} = proj\left(G\dot{\bar{x}}_d\hat{\sigma}^T\right).$$

The adaptation gains for both estimates were selected as

$$F = 20I_{11} \qquad G = 0.5I_7,$$

where $I_{11} \in \mathbb{R}^{11\times 11}$ and $I_7 \in \mathbb{R}^{7\times 7}$ are identity matrixes. As with the LP case, the initial values of $\hat{W}(0)$ were chosen to to be a zero matrix; however, the initial values of $\hat{V}(0)$ were selected randomly between -1.0 and 1.0 to provide a basis [71]. A different transient response could be obtained if the NN weights are initialized differently.

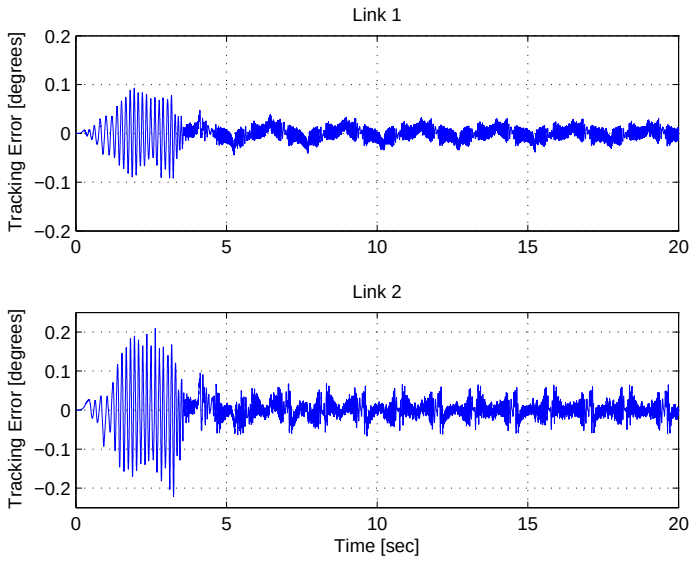

Figure 4-8. Link position tracking error for the modular NN controller with a gradient-based tuning law.

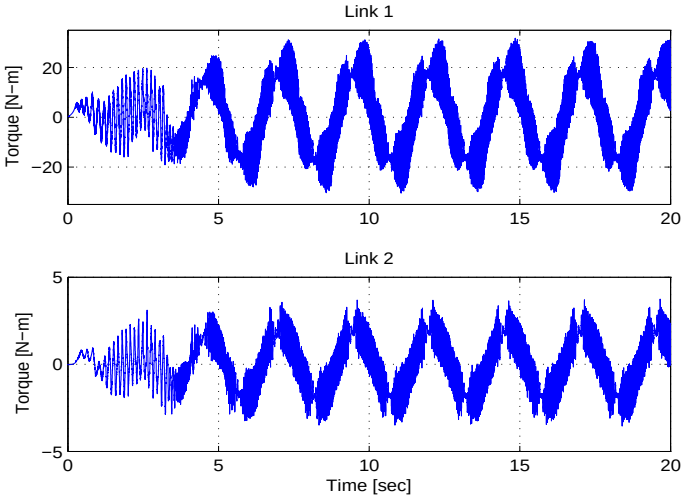

Figure 4-9. Torque input for the modular NN controller with a gradient-based tuning law.

Figure 4-8 depicts the tracking errors for one experimental trial with a gradient update law. The control torques for the same experimental trial are shown in Figure 4-9. The tracking errors for a representative experimental trial with a Hebbian update law is depicted in Figure 4-10. The torques for the Hebbian update law are shown in Figure 4-11.

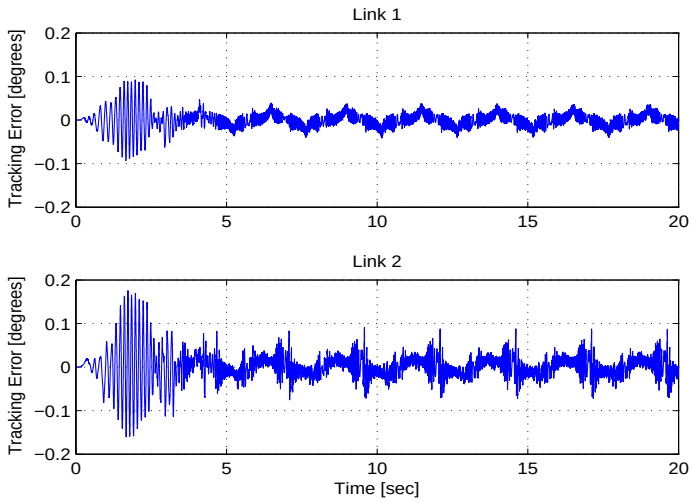

Figure 4-10. Link position tracking error for the modular NN controller with a Hebbian tuning law.

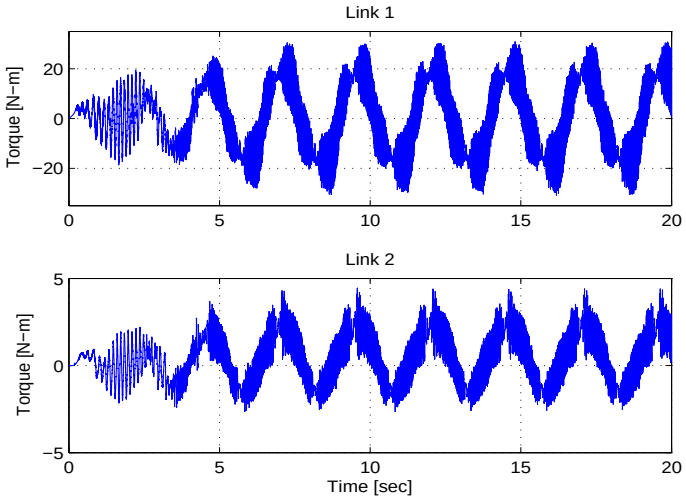

Figure 4-11. Torque input for the modular NN controller with a Hebbian tuning law.

4.10.3 Discussion

Data from the two sets of experiments illustrate that different adaptive update laws (which are specific parts of the more general update laws considered in the control development) can be used for the proposed modular adaptive controller both for the LP and non-LP case. The different update laws can be used with no change required in the overall structure of the controller and the stability is guaranteed through the Lyapunov analysis. The stability results for previous continuous modular adaptive controllers would

not have been valid for the dynamic model developed for this robot. Specifically, the advanced friction model derived from [26] contains non-LP disturbances that can not be considered in previous results.

In Experiment 1, the system dynamics are assumed to be partially LP. The model-based adaptive controller in (4–11) is implemented with two different update laws - the standard gradient-based and the least-squares update law. Our experimental results confirm the widely acknowledged fact that least-squares update laws yield faster convergence of parameter estimates compared to the gradient-based update laws. The parameter estimates converge much faster when using the least-squares law as compared to the gradient-based law (cf. Figure 4-4 and Figure 4-7). But this faster convergence of parameter estimates does not seem to be beneficial, as the overall tracking performance and control efforts required are similar for both cases (see Table 4-1).

In Experiment 2, the system dynamics are not assumed to be LP. The NN-based controller in (4–52) is implemented with two different update laws, specifically the gradient-based and the Hebbian law. One outcome of the experimental results is the fact that the Hebbian update laws give a tracking performance that is on par compared to that of the gradient-based laws (see Table 4-2). This result is significant because in general it is difficult to prove stability and guarantee performance using the Hebbian laws [15]. On the contrary, the gradient-based laws are designed to cancel some cross terms in the Lyapunov stability analysis [32, 75], thus facilitating the analysis and guaranteeing stability. But the gradient-based laws have a complicated form and require the computation of the Jacobian of the activation function. Hebbian laws, on the other hand, have a simple structure and do not require the computation of the Jacobian of the activation function. The fact that a simpler update law yields better performance in our experiments is interesting and may lead to a greater use of the Hebbian (or other simpler) update laws in NN-based control.

4.11 Conclusion

A RISE-based approach was presented to achieve modularity in the controller/update law for a general class of multi-input systems. Specifically, for systems with structured and unstructured uncertainties, a controller was employed that uses a model-based feedforward adaptive term in conjunction with the RISE feedback term (see [19]). The adaptive feedforward term was made modular by considering a generic form of the adaptive update law and its corresponding parameter estimate. This generic form of the update law was used to develop a new closed-loop error system, and the typical RISE stability analysis was modified. New sufficient gain conditions were derived to show asymptotic tracking of the desired link position. The class of RISE-based modular adaptive controllers is then extended to include uncertain dynamic systems that do not satisfy the LP assumption. Specifically, the result allows the NN weight tuning laws to be determined from a developed generic update law (rather than being restricted to a gradient update law). The modular adaptive control development is then applied to Euler-Lagrange dynamic systems. An experimental section is included that illustrates the concept.

CHAPTER 5
COMPOSITE ADAPTIVE CONTROL FOR SYSTEMS WITH ADDITIVE DISTURBANCES

5.1 Introduction

Applying the swapping approach to dynamics with additive disturbances is problematic because the unknown disturbance terms also get filtered and included in the filtered control input. This problem motivates the question of how can a prediction error-based adaptive update law be developed for systems with additive disturbances.

To address this motivating question, a general Euler-Lagrange-like MIMO system is considered with structured and unstructured uncertainties, and a gradient-based composite adaptive update law is developed that is driven by both the tracking error and the prediction error. The control development is based on the recent continuous Robust Integral of the Sign of the Error (RISE) [19] technique that was originally developed in [21] and [22]. The RISE architecture is adopted since this method can accommodate for C^2 disturbances and yield asymptotic stability. For example, the RISE technique was used in [23] to develop a tracking controller for nonlinear systems in the presence of additive disturbances and parametric uncertainties. Based on the well accepted heuristic notion that the addition of system knowledge in the control structure yields better performance and reduces control effort, model-based adaptive and neural network feedforward elements were added to the RISE controller in [19] and [75], respectively. In comparison to these approaches that used the RISE method in the feedback component of the controller, the RISE structure is used in both the feedback and feedforward elements of the control structure to enable, for the first time, the construction of a prediction error in the presence of additive disturbances. Specifically, since the swapping method will result in disturbances in the prediction error (the main obstacle that has previously limited this development), an innovative use of the RISE structure is also employed in the prediction error update (i.e., the filtered control input estimate). A block diagram indicating the unique use of the RISE method in the control and the prediction error formulation is

provided in Figure 5-1. Sufficient gain conditions are developed under which this unique double RISE controller guarantees semi-global asymptotic tracking. Experimental results are presented to illustrate the performance of the proposed approach.

The asymptotic stability for the proposed RISE-based composite adaptive controller comes at the expense of achieving semi-global stability which requires the initial condition to be within a specified region of attraction that can be made larger by increasing certain gains as subsequently discussed in Section 5.5. Development is also provided that proves the prediction error is square integrable; yet, no conclusion can be drawn about the convergence of the parameter estimation error due to the presence of filtered additive disturbances in the prediction error. The proposed method uses a gradient-based composite adaptive law with a fixed adaptation gain. Future efforts could also focus on designing a composite law with least-squares estimation with time-varying adaptation gain for the considered class of systems.

5.2 Dynamic System

Consider a class of MIMO nonlinear Euler-Lagrange systems of the following form:

$$x^{(m)} = f(x, \dot{x}, ..., x^{(m-1)}) + G(x, \dot{x}, ..., x^{(m-2)})u + h(t) \tag{5–1}$$

where $(\cdot)^{(i)}(t)$ denotes the i^{th} derivative with respect to time, $x^{(i)}(t) \in \mathbb{R}^n$, $i = 0, ..., m-1$ are the system states, $u(t) \in \mathbb{R}^n$ is the control input, $f\left(x, \dot{x}, ..., x^{(m-1)}\right) \in \mathbb{R}^n$ and $G\left(x, \dot{x}, ..., x^{(m-2)}\right) \in \mathbb{R}^{n \times n}$ are unknown nonlinear $\mathcal{C}^2$ functions, and $h(t) \in \mathbb{R}^n$ denotes a general nonlinear disturbance (e.g., unmodeled effects). Throughout the chapter, $|\cdot|$ denotes the absolute value of the scalar argument, $\|\cdot\|$ denotes the standard Euclidean norm for a vector or the induced infinity norm for a matrix.

The subsequent development is based on the assumption that all the system states are measurable outputs. Moreover, the following assumptions will be exploited in the subsequent development.

Assumption 5-1: $G(\cdot)$ is symmetric positive definite, and satisfies the following inequality $\forall y(t) \in \mathbb{R}^n$:

$$\underline{g} \|y\|^2 \leq y^T G^{-1} y \leq \bar{g}(x, \dot{x}, ..., x^{(m-2)}) \|y\|^2 \tag{5–2}$$

where $\underline{g} \in \mathbb{R}$ is a known positive constant, and $\bar{g}(x, \dot{x}, ..., x^{(m-2)}) \in \mathbb{R}$ is a known positive function.

Assumption 5-2: The functions $G^{-1}(\cdot)$ and $f(\cdot)$ are second order differentiable such that G^{-1}, $\dot{G}^{-1}$, $\ddot{G}^{-1}$, f, $\dot{f}$, $\ddot{f} \in \mathcal{L}_\infty$ if $x^{(i)}(t) \in \mathcal{L}_\infty$, $i = 0, 1, ..., m+1$.

Assumption 5-3: The nonlinear disturbance term and its first two time derivatives (i.e., h, $\dot{h}$, $\ddot{h}$) are bounded by known constants.

Assumption 5-4: The unknown nonlinearities $G^{-1}(\cdot)$ and $f(\cdot)$ are linear in terms of unknown constant system parameters (i.e., LP).

Assumption 5-5: The desired trajectory $x_d(t) \in \mathbb{R}^n$ is assumed to be designed such that $x_d^{(i)}(t) \in \mathcal{L}_\infty$, $i = 0, 1, ..., m+2$. The desired trajectory $x_d(t)$ need not be persistently exciting and can be set to a constant value for the regulation problem.

5.3 Control Objective

The objective is to design a continuous composite adaptive controller which ensures that the system state $x(t)$ tracks a desired time-varying trajectory $x_d(t)$ despite uncertainties and bounded disturbances in the dynamic model. To quantify this objective, a tracking error, denoted by $e_1(t) \in \mathbb{R}^n$, is defined as

$$e_1 \triangleq x_d - x. \tag{5–3}$$

To facilitate a compact presentation of the subsequent control development and stability analysis, auxiliary error signals denoted by $e_i(t) \in \mathbb{R}^n$, $i = 2, 3, ..., m$ are defined as

$$\begin{aligned} e_2 &\triangleq \dot{e}_1 + \alpha_1 e_1 \\ e_3 &\triangleq \dot{e}_2 + \alpha_2 e_2 + e_1 \\ e_4 &\triangleq \dot{e}_3 + \alpha_3 e_3 + e_2 \\ &\vdots \\ e_i &\triangleq \dot{e}_{i-1} + \alpha_{i-1} e_{i-1} + e_{i-2} \\ &\vdots \\ e_m &\triangleq \dot{e}_{m-1} + \alpha_{m-1} e_{m-1} + e_{m-2} \end{aligned} \tag{5–4}$$

where $\alpha_i \in \mathbb{R}$, $i = 1, 2, ..., m-1$ denote constant positive control gains. The error signals $e_i(t)$, $i = 2, 3, ..., m$ can be expressed in terms of $e_1(t)$ and its time derivatives as

$$e_i = \sum_{j=0}^{i-1} b_{i,j} e_1^{(j)}, \qquad b_{i,i-1} = 1 \tag{5–5}$$

where the constant coefficients $b_{i,j} \in \mathbb{R}$ can be evaluated by substituting (5–5) in (5–4), and comparing coefficients. A filtered tracking error [57], denoted by $r(t) \in \mathbb{R}^n$, is also defined as

$$r \triangleq \dot{e}_m + \alpha_m e_m \tag{5–6}$$

where $\alpha_m \in \mathbb{R}$ is a positive, constant control gain. The filtered tracking error $r(t)$ is not measurable since the expression in (5–6) depends on $x^{(m)}$.

5.4 Control Development

To develop the open-loop tracking error system, the filtered tracking error in (5–6) is premultiplied by $G^{-1}(\cdot)$ to yield

$$G^{-1} r = G^{-1} \dot{e}_m + G^{-1} \alpha_m e_m. \tag{5–7}$$

Substituting (5–5) in to (5–7) for $\dot{e}_m(t)$ yields

$$G^{-1}r = G^{-1}\sum_{j=0}^{m-1} b_{m,j} e_1^{(j+1)} + G^{-1}\alpha_m e_m. \tag{5–8}$$

By separating the last term from the summation, (5–8) can also be expressed as

$$G^{-1}r = G^{-1}b_{m,m-1}e_1^{(m)} + G^{-1}\sum_{j=0}^{m-2} b_{m,j} e_1^{(j+1)} + G^{-1}\alpha_m e_m. \tag{5–9}$$

Using the fact that $b_{m,m-1} = 1$ and making substitutions from (5–1) and (5–3), the expression in (5–9) is rewritten as

$$G^{-1}r = G^{-1}x_d^{(m)} - G^{-1}f - G^{-1}h - u + G^{-1}\sum_{j=0}^{m-2} b_{m,j} e_1^{(j+1)} + G^{-1}\alpha_m e_m$$

which can be rearranged as

$$G^{-1}r = Y_d\theta + S_1 - G_d^{-1}h - u. \tag{5–10}$$

In (5–10), the auxiliary function $S_1\left(x, \dot{x}, ..., x^{(m-1)}, t\right) \in \mathbb{R}^n$ is defined as

$$S_1 \triangleq G^{-1}\left(\sum_{j=0}^{m-2} b_{m,j} e_1^{(j+1)} + \alpha_m e_m\right) + G^{-1}x_d^{(m)} - G_d^{-1}x_d^{(m)} - G^{-1}f + G_d^{-1}f_d - G^{-1}h + G_d^{-1}h. \tag{5–11}$$

Also in (5–10), $Y_d\theta \in \mathbb{R}^n$ is defined as

$$Y_d\theta \triangleq G_d^{-1}x_d^{(m)} - G_d^{-1}f_d \tag{5–12}$$

where $Y_d(x_d, \dot{x}_d, ..., x_d^{(m)}) \in \mathbb{R}^{n\times p}$ is a desired regression matrix, and $\theta \in \mathbb{R}^p$ contains the constant unknown system parameters. In (5–12), the functions $G_d^{-1}(x_d, \dot{x}_d, ..., x_d^{(m-2)}) \in \mathbb{R}^{n\times n}$ and $f_d(x_d, \dot{x}_d, ..., x_d^{(m-1)}) \in \mathbb{R}^n$ are defined as

$$\begin{aligned} G_d^{-1} &\triangleq G^{-1}(x_d, \dot{x}_d, ..., x_d^{(m-2)}) \\ f_d &\triangleq f(x_d, \dot{x}_d, ..., x_d^{(m-1)}). \end{aligned} \tag{5–13}$$

The open-loop error system in (5–10) is typically written in a form similar to

$$G^{-1}\dot{e}_m = Y_d\theta + S_1 - G^{-1}\alpha_m e_m - G_d^{-1}h - u \tag{5–14}$$

which can be obtained by substituting (5–6) into (5–10) for the filtered tracking error. Although (5–10) and (5–14) are equivalent, the atypical form in (5–10) is used to facilitate the subsequent closed-loop error system development and stability analysis. Specifically, the subsequent RISE control method is designed based on the time derivative of the control input. The design of the filtered tracking error in (5–6) is not necessary, but it simplifies the subsequent development by allowing the closed-loop error system to be expressed in terms of $\dot{r}(t)$ rather than $\ddot{e}_m(t)$.

5.4.1 RISE-based Swapping

A measurable form of the prediction error $\varepsilon(t) \in \mathbb{R}^n$ is defined as the difference between the filtered control input $u_f(t) \in \mathbb{R}^n$ and the estimated filtered control input $\hat{u}_f(t) \in \mathbb{R}^n$ as

$$\varepsilon \triangleq u_f - \hat{u}_f \tag{5–15}$$

where the filtered control input $u_f(t) \in \mathbb{R}^n$ is generated by [3]

$$\dot{u}_f + \omega u_f = \omega u \ , \qquad u_f(0) = 0 \tag{5–16}$$

where $\omega \in \mathbb{R}$ is a known positive constant, and $\hat{u}_f(t) \in \mathbb{R}^n$ is subsequently designed. The differential equation in (5–16) can be directly solved to yield

$$u_f = v * u \tag{5–17}$$

where $*$ is used to denote the standard convolution operation, and the scalar function $v(t)$ is defined as

$$v \triangleq \omega e^{-\omega t}. \tag{5–18}$$

Using (5–1), the expression in (5–17) can be rewritten as

$$u_f = v * \left(G^{-1} x^{(m)} - G^{-1} f - G^{-1} h \right). \tag{5–19}$$

Since the system dynamics in (5–1) include non-LP bounded disturbances $h(t)$, they also get filtered and included in the filtered control input in (5–19). To compensate for the effects of these disturbances, the typical prediction error formulation is modified to include a RISE-like structure in the design of the estimated filtered control input. With this motivation, the structure of the open-loop prediction error system is engineered to facilitate the RISE-based design of the estimated filtered control input.

Adding and subtracting the term $G_d^{-1} x_d^{(m)} + G_d^{-1} f_d + G_d^{-1} h$ to the expression in (5–19) yields

$$u_f = v*(G_d^{-1} x_d^{(m)} + G_d^{-1} f_d + G^{-1} x^{(m)} - G_d^{-1} x_d^{(m)} - G^{-1} f - G_d^{-1} f_d - G^{-1} h + G_d^{-1} h - G_d^{-1} h). \tag{5–20}$$

Using (5–12), the expression in (5–20) is simplified as

$$u_f = v * \left(Y_d \theta + S - S_d - G_d^{-1} h \right) \tag{5–21}$$

where $S(x, \dot{x}, ..., x^{(m)})$, $S_d(x_d, \dot{x}_d, ..., x_d^{(m)}) \in \mathbb{R}^n$ are defined as

$$S \triangleq G^{-1} x^{(m)} - G^{-1} f - G^{-1} h \tag{5–22}$$

$$S_d \triangleq G_d^{-1} x_d^{(m)} - G_d^{-1} f_d - G_d^{-1} h. \tag{5–23}$$

The expression in (5–21) is further simplified as

$$u_f = Y_{df} \theta + v * S - v * S_d + h_f \tag{5–24}$$

where the filtered regressor matrix $Y_{df}(x_d, \dot{x}_d, ..., x_d^{(m)}) \in \mathbb{R}^{n \times p}$ is defined as

$$Y_{df} \triangleq v * Y_d \tag{5–25}$$

and the disturbance $h_f(t) \in \mathbb{R}^n$ is defined as

$$h_f \triangleq -v * G_d^{-1} h.$$

The term $v * S(x, \dot{x}, ..., x^{(m)}) \in \mathbb{R}^n$ in (5–24) depends on $x^{(m)}$. Using the following property of convolution [57]:

$$g_1 * \dot{g}_2 = \dot{g}_1 * g_2 + g_1(0) g_2 - g_1 g_2(0) \tag{5–26}$$

an expression independent of $x^{(m)}$ can be obtained. Consider

$$v * S = v * \left(G^{-1} x^{(m)} - G^{-1} f - G^{-1} h\right)$$

which can be rewritten as

$$v * S = v * (\frac{d}{dt}(G^{-1} x^{(m-1)}) - \dot{G}^{-1} x^{(m-1)} - G^{-1} f - G^{-1} h). \tag{5–27}$$

Applying the property in (5–26) to the first term of (5–27) yields

$$v * S = S_f + W \tag{5–28}$$

where the state-dependent terms are included in the auxiliary function $S_f(x, \dot{x}, ..., x^{(m-1)}) \in \mathbb{R}^n$, defined as

$$S_f \triangleq \dot{v} * \left(G^{-1} x^{(m-1)}\right) + v(0) G^{-1} x^{(m-1)} - v * \dot{G}^{-1} x^{(m-1)} - v * G^{-1} f - v * G^{-1} h \tag{5–29}$$

and the terms that depend on the initial states are included in $W(t) \in \mathbb{R}^n$, defined as

$$W \triangleq -v G^{-1} \left(x(0), \dot{x}(0), ..., x^{(m-2)}(0)\right) x^{(m-1)}(0). \tag{5–30}$$

Similarly, following the procedure in (5–27)-(5–30), the expression $v * S_d$ in (5–24) is evaluated as

$$v * S_d = S_{df} + W_d \tag{5–31}$$

where $S_{df}(x_d, \dot{x}_d, ..., x_d^{(m-1)}) \in \mathbb{R}^n$ is defined as

$$S_{df} \triangleq \dot{v} * (G_d^{-1} x_d^{(m-1)}) + v(0) G_d^{-1} x_d^{(m-1)} - v * \dot{G}_d^{-1} x_d^{(m-1)} - v * G_d^{-1} f_d - v * G_d^{-1} h \quad (5\text{–}32)$$

and $W_d(t) \in \mathbb{R}^n$ is defined as

$$W_d \triangleq -vG_d^{-1}(x_d(0), \dot{x}_d(0), ..., x_d^{(m-2)}(0)) x_d^{(m-1)}(0). \quad (5\text{–}33)$$

Substituting (5–28)-(5–33) into (5–24), and then substituting the resulting expression into (5–15) yields

$$\varepsilon = Y_{df}\theta + S_f - S_{df} + W - W_d + h_f - \hat{u}_f. \quad (5\text{–}34)$$

5.4.2 Composite Adaptation

The composite adaptation for the adaptive estimates $\hat{\theta}(t) \in \mathbb{R}^p$ in (5–47) is given by

$$\dot{\hat{\theta}} = \Gamma \dot{Y}_d^T r + \Gamma \dot{Y}_{df}^T \varepsilon \quad (5\text{–}35)$$

where $\Gamma \in \mathbb{R}^{p \times p}$ is a positive definite, symmetric, constant gain matrix and the filtered regressor matrix $Y_{df}(x_d, \dot{x}_d, ..., x_d^{(m)}) \in \mathbb{R}^{n \times p}$ is defined in (5–25).

Remark 5.1. *The parameter estimate update law in (5–35) depends on the unmeasurable signal $r(t)$, but the parameter estimates are independent of $r(t)$ as can be shown by directly solving (5–35) as*

$$\hat{\theta}(t) = \hat{\theta}(0) + \Gamma \dot{Y}_d^T(\sigma) e_m(\sigma)\Big|_0^t + \int_0^t \Gamma \dot{Y}_{df}^T(\sigma)\varepsilon(\sigma)\, d\sigma$$
$$- \int_0^t \left\{ \Gamma \ddot{Y}_d^T(\sigma) e_m(\sigma) - \alpha_m \Gamma \dot{Y}_d^T(\sigma) e_m(\sigma) \right\} d\sigma.$$

5.4.3 Closed-Loop Prediction Error System

Based on (5–36) and the subsequent analysis, the filtered control input estimate is designed as

$$\hat{u}_f = Y_{df}\hat{\theta} + \mu_2, \quad (5\text{–}36)$$

where $\mu_2(t) \in \mathbb{R}^n$ is a RISE-like term defined as

$$\mu_2(t) \triangleq \int_0^t [k_2\varepsilon(\sigma) + \beta_2 sgn(\varepsilon(\sigma))]d\sigma, \tag{5–37}$$

where k_2, $\beta_2 \in \mathbb{R}$ denote constant positive control gains. In a typical prediction error formulation, the estimated filtered control input is designed to include just the first term $Y_{df}\hat{\theta}$ in (5–36). But as previously discussed, the presence of non-LP disturbances in the system model results in filtered disturbances in the unmeasurable form of the prediction error in (5–34). Hence, the estimated filtered control input is augmented with an additional RISE-like term $\mu_2(t)$ to cancel the effects of disturbances in the prediction error as illustrated in Figure 5-1 and the subsequent design and stability analysis. Substituting (5–36) into (5–34) yields the following closed-loop prediction error system:

$$\varepsilon = Y_{df}\tilde{\theta} + S_f - S_{df} + W - W_d + h_f - \mu_2 \tag{5–38}$$

where $\tilde{\theta}(t) \in \mathbb{R}^p$ denotes the parameter estimate mismatch defined as

$$\tilde{\theta} \triangleq \theta - \hat{\theta}. \tag{5–39}$$

To facilitate the subsequent composite adaptive control development and stability analysis, the time derivative of (5–38) is expressed as

$$\dot{\varepsilon} = \dot{Y}_{df}\tilde{\theta} - Y_{df}\Gamma\dot{Y}_{df}^T\varepsilon + \tilde{N}_2 + N_{2B} - k_2\varepsilon - \beta_2 sgn(\varepsilon), \tag{5–40}$$

where (5–35) and the fact that

$$\dot{\mu}_2 = k_2\varepsilon + \beta_2 sgn(\varepsilon) \tag{5–41}$$

were utilized. In (5–40), the unmeasurable/unknown auxiliary term $\tilde{N}_2(e_1, e_2, ..., e_m, r, t) \in \mathbb{R}^n$ is defined as

$$\tilde{N}_2 \triangleq \dot{S}_f - \dot{S}_{df} - Y_{df}\Gamma\dot{Y}_d^T r, \tag{5–42}$$

where the update law in (5–35) was utilized, and the term $N_{2B}(t) \in \mathbb{R}^n$ is defined as

$$N_{2B} \triangleq \dot{W} - \dot{W}_d + \dot{h}_f. \tag{5–43}$$

In a similar manner as in Lemma 1 of the Appendix, by applying the Mean Value Theorem can be used to develop the following upper bound for the expression in (5–42):

$$\left\| \tilde{N}_2(t) \right\| \leq \rho_2 \left(\|z\| \right) \|z\|, \tag{5–44}$$

where the bounding function $\rho_2(\cdot) \in \mathbb{R}$ is a positive, globally invertible, nondecreasing function, and $z(t) \in \mathbb{R}^{n(m+1)}$ is defined as

$$z(t) \triangleq \begin{bmatrix} e_1^T & e_2^T & \cdots & e_m^T & r^T \end{bmatrix}^T. \tag{5–45}$$

Using Assumption 5-3, and the fact that $v(t)$ is a linear, strictly proper, exponentially stable transfer function, the following inequality can be developed based on the expression in (5–43) with a similar approach as in Lemma 2 of [42]:

$$\|N_{2B}(t)\| \leq \xi, \tag{5–46}$$

where $\xi \in \mathbb{R}$ is a known positive constant.

5.4.4 Closed-Loop Tracking Error System

Based on the open-loop error system in (5–10), the control input is composed of an adaptive feedforward term plus the RISE feedback term as

$$u \triangleq Y_d \hat{\theta} + \mu_1 \tag{5–47}$$

where $\mu_1(t) \in \mathbb{R}^n$ denotes the RISE feedback term defined as

$$\mu_1(t) \triangleq (k_1+1)e_m(t) - (k_1+1)e_m(0) + \int_0^t \{(k_1+1)\alpha_m e_m(\sigma) + \beta_1 sgn(e_m(\sigma))\} d\sigma \tag{5–48}$$

where k_1, $\beta_1 \in \mathbb{R}$ are positive constant control gains, and $\alpha_m \in \mathbb{R}$ was introduced in (5–6). In (5–47), $\hat{\theta}(t) \in \mathbb{R}^p$ denotes a parameter estimate vector for unknown system parameters

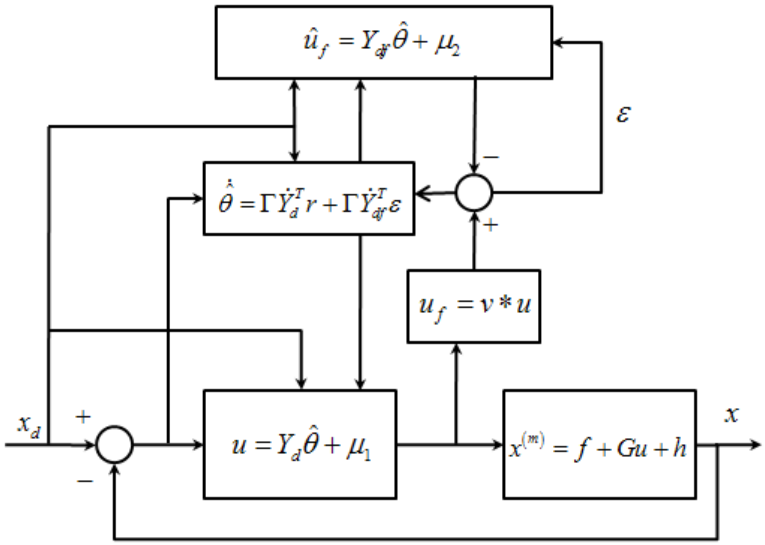

Figure 5-1. Block diagram of the proposed RISE-based composite adaptive controller

$\theta \in \mathbb{R}^p$, generated by a subsequently designed gradient-based composite adaptive update law [38, 39, 82].

The closed-loop tracking error system can be developed by substituting (5–47) into (5–10) as

$$G^{-1}r = Y_d\tilde{\theta} + S_1 - G_d^{-1}h - \mu_1. \tag{5–49}$$

To facilitate the subsequent composite adaptive control development and stability analysis, the time derivative of (5–49) is expressed as

$$G^{-1}\dot{r} = -\frac{1}{2}\dot{G}^{-1}r + \dot{Y}_d\tilde{\theta} - Y_d\Gamma\dot{Y}_{df}^T\varepsilon + \tilde{N}_1 + N_{1B} - (k_1+1)r - \beta_1 sgn(e_m) - e_m \tag{5–50}$$

where (5–35) and the fact that the time derivative of (5–48) is given as

$$\dot{\mu}_1 = (k_1+1)r + \beta_1 sgn(e_m) \tag{5–51}$$

was utilized. In (5–50), the unmeasurable/unknown auxiliary terms $\tilde{N}_1(e_1, e_2, ..., e_m, r, t)$ and $N_{1B}(t) \in \mathbb{R}^n$ are defined as

$$\tilde{N}_1 \triangleq -\frac{1}{2}\dot{G}^{-1}r + \dot{S}_1 + e_m - Y_d\Gamma\dot{Y}_d^T r \tag{5–52}$$

where (5–35) was used, and

$$N_{1B} \triangleq -\dot{G}_d^{-1} h - G_d^{-1} \dot{h}. \tag{5–53}$$

The structure of (5–50) and the introduction of the auxiliary terms in (5–52) and (5–53) is motivated by the desire to segregate terms that can be upper bounded by state-dependent terms and terms that can be upper bounded by constants. In a similar fashion as in (5–44), the following upper bound can be developed for the expression in (5–52):

$$\left\| \tilde{N}_1(t) \right\| \leq \rho_1 \left(\|z\| \right) \|z\| \tag{5–54}$$

where the bounding function $\rho_1(\cdot) \in \mathbb{R}$ is a positive, globally invertible, nondecreasing function, and $z(t) \in \mathbb{R}^{n(m+1)}$ was defined in (5–45). Using Assumptions 5-2 and 5-3, the following inequalities can be developed based on the expression in (5–53) and its time derivative:

$$\|N_{1B}(t)\| \leq \zeta_1 \ , \qquad \left\| \dot{N}_{1B}(t) \right\| \leq \zeta_2 \tag{5–55}$$

where $\zeta_i \in \mathbb{R}$, $i = 1, 2$ are known positive constants.

The RISE controller in (5–47) and (5–48), and sliding mode controllers (SMCs) (e.g., see the classic results in [3, 12]) are the only methods that have been proven to yield an asymptotic tracking result for an open-loop error system such as (5–10) where additive bounded disturbances are present that are upper bounded by a constant. Other approaches lack a mechanism to cancel the disturbance terms (these terms are typically eliminated through nonlinear damping and yield a uniformly ultimately bounded (UUB) result). SMC is a discontinuous control method that requires infinite control bandwidth and a known upper bound on the disturbance term. Continuous modifications of SMC reduce the stability result to UUB. The RISE control method in (5–47) and (5–48) is continuous/differentiable (i.e., finite bandwidth) and requires a known upper bound on the disturbance and the time derivative of the disturbance. Despite which feedback control method is selected, the control challenge is that the disturbance term $h(t)$ in (5–1) will be included in the swapping (or torque filtering) method in the prediction error formulation

as shown in (5–34). This technical obstacle has prevented the development of any previous composite adaptive controller for a dynamic system with added disturbances such as $h(t)$. The contribution of the current result is the development of the RISE-based swapping method to enable the development of composite adaptive controllers for systems such as (5–1). Specifically, the RISE-based swapping technique provides a means to cancel the filtered disturbance terms in (5–34).

5.5 Stability Analysis

Theorem 5-1: The controller given in (5–47) and (5–48) in conjunction with the composite adaptive update law in (5–35), where the prediction error is generated from (5–15), (5–16), (5–36), and (5–37), ensures that all system signals are bounded under closed-loop operation and that the position tracking error and the prediction error are regulated in the sense that

$$\|e_1(t)\| \to 0 \text{ and } \|\varepsilon(t)\| \to 0 \qquad \text{as} \qquad t \to \infty$$

provided the control gains k_1 and k_2 introduced in (5–48) and (5–37) are selected sufficiently large based on the initial conditions of the system (see the subsequent proof), and the following conditions are satisfied:

$$\alpha_{m-1} > \frac{1}{2}, \qquad \alpha_m > \frac{1}{2}, \tag{5–56}$$

$$\beta_1 > \zeta_1 + \frac{1}{\alpha_m}\zeta_2, \qquad \beta_2 > \xi, \tag{5–57}$$

where the gains α_{m-1} and α_m were introduced in (5–4), β_1 was introduced in (5–48), β_2 was introduced in (5–37), ζ_1 and ζ_2 were introduced in (5–55), and ξ was introduced in (5–46).

Proof: Let $\mathcal{D} \subset \mathbb{R}^{n(m+2)+p+2}$ be a domain containing $y(t) = 0$, where $y(t) \in \mathbb{R}^{n(m+2)+p+2}$ is defined as

$$y \triangleq [z^T \quad \varepsilon^T \quad \sqrt{P_1} \quad \sqrt{P_2} \quad \tilde{\theta}^T]^T. \tag{5–58}$$

In (5–58), the auxiliary function $P_1(t) \in \mathbb{R}$ is defined as

$$P_1(t) \triangleq \beta_1 \sum_{i=1}^{n} |e_{mi}(0)| - e_m(0)^T N_{1B}(0) - \int_0^t L_1(\tau) d\tau, \tag{5–59}$$

where $e_{mi}(0) \in \mathbb{R}$ denotes the ith element of the vector $e_m(0)$, and the auxiliary function $L_1(t) \in \mathbb{R}$ is defined as

$$L_1 \triangleq r^T (N_{1B} - \beta_1 sgn(e_m)), \tag{5–60}$$

where $\beta_1 \in \mathbb{R}$ is a positive constant chosen according to the sufficient condition in (5–57). Provided the sufficient condition introduced in (5–57) is satisfied, the following inequality is obtained [22]:

$$\int_0^t L_1(\tau) d\tau \leq \beta_1 \sum_{i=1}^{n} |e_{mi}(0)| - e_m(0)^T N_{1B}(0). \tag{5–61}$$

Hence, (5–61) can be used to conclude that $P_1(t) \geq 0$. Also in (5–58), the auxiliary function $P_2(t) \in \mathbb{R}$ is defined as

$$P_2(t) \triangleq - \int_0^t L_2(\tau) d\tau, \tag{5–62}$$

where the auxiliary function $L_2(t) \in \mathbb{R}$ is defined as

$$L_2 \triangleq \varepsilon^T (N_{2B} - \beta_2 sgn(\varepsilon)), \tag{5–63}$$

where $\beta_2 \in \mathbb{R}$ is a positive constant chosen according to the sufficient condition in (5–57). Provided the sufficient condition introduced in (5–57) is satisfied, then $P_2(t) \geq 0$.

Let $V_L(y,t) : \mathcal{D} \times [0,\infty) \to \mathbb{R}$ be a continuously differentiable, positive definite function defined as

$$V_L(y,t) \triangleq \frac{1}{2} \sum_{i=1}^{m} e_i^T e_i + \frac{1}{2} r^T G^{-1} r + \frac{1}{2} \varepsilon^T \varepsilon + P_1 + P_2 + \frac{1}{2} \tilde{\theta}^T \Gamma^{-1} \tilde{\theta} \tag{5–64}$$

which satisfies the inequalities

$$U_1(y) \leq V_L(y,t) \leq U_2(y) \tag{5–65}$$

provided the sufficient conditions introduced in (5–57) are satisfied. In (5–65), the continuous positive definite functions $U_1(y)$, $U_2(y) \in \mathbb{R}$ are defined as $U_1(y) \triangleq \lambda_1 \|y\|^2$ and $U_2(y) \triangleq \lambda_2(x, \dot{x}, ..., x^{(m-2)}) \|y\|^2$, where λ_1, $\lambda_2(x, \dot{x}, ..., x^{(m-2)}) \in \mathbb{R}$ are defined as

$$\begin{aligned} \lambda_1 &\triangleq \frac{1}{2} \min \left\{1, \underline{g}, \lambda_{\min} \left\{\Gamma^{-1}\right\}\right\} \\ \lambda_2 &\triangleq \max\{\frac{1}{2}\bar{g}(x, \dot{x}, ..., x^{(m-2)}), \frac{1}{2}\lambda_{\max} \left\{\Gamma^{-1}\right\}, 1\} \end{aligned} \tag{5–66}$$

where $\underline{g}$, $\bar{g}(x, \dot{x}, ..., x^{(m-2)})$ are introduced in (5–2), and $\lambda_{\min}\{\cdot\}$ and $\lambda_{\max}\{\cdot\}$ denote the minimum and maximum eigenvalue of the arguments, respectively.

After using (5–4), (5–6), (5–35), (5–40), (5–50), (5–59), (5–60), (5–62) and (5–63), the time derivative of (5–64) can be expressed as

$$\begin{aligned} \dot{V}_L(y,t) = &-\sum_{i=1}^{m} \alpha_i e_i^T e_i + e_{m-1}^T e_m - r^T r - k_1 r^T r + r^T \dot{Y}_d \tilde{\theta} + r^T \tilde{N}_1 \\ &+ r^T N_{1B} - r^T Y_d \Gamma \dot{Y}_{df}^T \varepsilon - \beta_1 r^T sgn(e_m) + \varepsilon^T \dot{Y}_{df} \tilde{\theta} \\ &+ \varepsilon^T \tilde{N}_2 + \varepsilon^T N_{2B} - k_2 \varepsilon^T \varepsilon - \varepsilon^T Y_{df} \Gamma \dot{Y}_{df}^T \varepsilon - \beta_2 \varepsilon^T sgn(\varepsilon) \\ &- r^T (N_{1B} - \beta_1 sgn(e_m)) - \varepsilon^T N_{2B} + \varepsilon^T \beta_2 sgn(\varepsilon) - \tilde{\theta}^T \Gamma^{-1} (\Gamma \dot{Y}_d^T r + \Gamma \dot{Y}_{df}^T \varepsilon). \end{aligned} \tag{5–67}$$

After canceling the similar terms and using the fact that $a^T b \leq \frac{1}{2}(\|a\|^2 + \|b\|^2)$ for some $a, b \in \mathbb{R}^n$, the expression in (5–67) is upper bounded as

$$\begin{aligned} \dot{V}_L(y,t) \leq &-\sum_{i=1}^{m} \alpha_i e_i^T e_i + \frac{1}{2} \|e_{m-1}\|^2 + \frac{1}{2} \|e_m\|^2 - \|r\|^2 \\ &- k_1 \|r\|^2 + r^T \tilde{N}_1 - r^T Y_d \Gamma \dot{Y}_{df}^T \varepsilon + \varepsilon^T \tilde{N}_2 - k_2 \varepsilon^T \varepsilon - \varepsilon^T Y_{df} \Gamma \dot{Y}_{df}^T \varepsilon. \end{aligned}$$

Using the following upper bounds:

$$\left\| Y_d \Gamma \dot{Y}_{df}^T \right\| \leq c_1, \qquad \left\| Y_{df} \Gamma \dot{Y}_{df}^T \right\| \leq c_2,$$

where $c_1, c_2 \in \mathbb{R}$ are positive constants, $\dot{V}_L(y,t)$ is upper bounded using the squares of the components of $z(t)$ as

$$\dot{V}_L(y,t) \leq -\lambda_3 \|z\|^2 - k_1 \|r\|^2 + \|r\| \left\|\tilde{N}_1\right\| + c_1 \|\varepsilon\| \|r\| + \|\varepsilon\| \left\|\tilde{N}_2\right\| - (k_2 - c_2) \|\varepsilon\|^2, \quad (5\text{–}68)$$

where

$$\lambda_3 \triangleq \min\{\alpha_1, \alpha_2, ..., \alpha_{m-2}, \alpha_{m-1} - \frac{1}{2}, \alpha_m - \frac{1}{2}, 1\}.$$

Letting

$$k_2 = k_{2a} + k_{2b}$$

where $k_{2a}, k_{2b} \in \mathbb{R}$ are positive constants, and using the inequalities in (5–54) and (5–44), the expression in (5–68) is upper bounded as

$$\begin{aligned} \dot{V}_L(y,t) \leq & -\lambda_3 \|z\|^2 - k_{2b} \|\varepsilon\|^2 - \left[k_1 \|r\|^2 - \rho_1(\|z\|) \|r\| \|z\|\right] \\ & - \left[(k_{2a} - c_2) \|\varepsilon\|^2 - (\rho_2(\|z\|) + c_1) \|\varepsilon\| \|z\|\right]. \end{aligned} \quad (5\text{–}69)$$

Completing the squares for the terms inside the brackets in (5–69) yields

$$\begin{aligned} \dot{V}_L(y,t) &\leq -\lambda_3 \|z\|^2 - k_{2b} \|\varepsilon\|^2 + \frac{\rho_1^2(\|z\|) \|z\|^2}{4k_1} + \frac{(\rho_2(\|z\|) + c_1)^2 \|z\|^2}{4(k_{2a} - c_2)} \\ &\leq -\lambda_3 \|z\|^2 + \frac{\rho^2(\|z\|) \|z\|^2}{4k} - k_{2b} \|\varepsilon\|^2, \end{aligned} \quad (5\text{–}70)$$

where $k \in \mathbb{R}$ is defined as

$$k \triangleq \frac{k_1 (k_{2a} - c_2)}{\max\{k_1, (k_{2a} - c_2)\}}, \qquad k_{2a} > c_2 \quad (5\text{–}71)$$

and $\rho(\cdot) \in \mathbb{R}$ is a positive, globally invertible, nondecreasing function defined as

$$\rho^2(\|z\|) \triangleq \rho_1^2(\|z\|) + (\rho_2(\|z\|) + c_1)^2.$$

The expression in (5–70) can be further upper bounded by a continuous, positive semi-definite function

$$\dot{V}_L(y,t) \leq -U(y) = -c \left\| \begin{bmatrix} z^T & \varepsilon^T \end{bmatrix}^T \right\|^2 \qquad \forall y \in \mathcal{D} \tag{5–72}$$

for some positive constant c, where

$$\mathcal{D} \triangleq \left\{ y(t) \in \mathbb{R}^{n(m+2)+p+2} \mid \|y\| \leq \rho^{-1}\left(2\sqrt{\lambda_3 k}\right) \right\}.$$

Larger values of k will expand the size of the domain $\mathcal{D}$. The inequalities in (5–65) and (5–70) can be used to show that $V_L(y,t) \in \mathcal{L}_\infty$ in $\mathcal{D}$; hence, $e_i(t) \in \mathcal{L}_\infty$ and $\varepsilon(t), r(t), \tilde{\theta}(t) \in \mathcal{L}_\infty$ in $\mathcal{D}$. Given that $e_i(t) \in \mathcal{L}_\infty$ and $r(t) \in \mathcal{L}_\infty$ in $\mathcal{D}$, standard linear analysis methods can be used to prove that $\dot{e}_i(t) \in \mathcal{L}_\infty$ in $\mathcal{D}$ from (5–4) and (5–6). Since $e_i(t) \in \mathcal{L}_\infty$, and $r(t) \in \mathcal{L}_\infty$ in $\mathcal{D}$, Assumption 5-5 can be used along with (5–3)-(5–6) to conclude that $x^{(i)}(t) \in \mathcal{L}_\infty$, $i = 0, 1, ..., m$ in $\mathcal{D}$. Since $\tilde{\theta}(t) \in \mathcal{L}_\infty$ in $\mathcal{D}$, (5–39) can be used to prove that $\hat{\theta}(t) \in \mathcal{L}_\infty$ in $\mathcal{D}$. Since $x^{(i)}(t) \in \mathcal{L}_\infty$, $i = 0, 1, ..., m$ in $\mathcal{D}$, Assumption 5-2 can be used to conclude that $G^{-1}(\cdot)$ and $f(\cdot) \in \mathcal{L}_\infty$ in $\mathcal{D}$. Thus, from (5–1) and Assumption 5-3, we can show that $u(t) \in \mathcal{L}_\infty$ in $\mathcal{D}$. Therefore, $u_f(t) \in \mathcal{L}_\infty$ in $\mathcal{D}$, and hence, from (5–15), $\hat{u}_f(t) \in \mathcal{L}_\infty$ in $\mathcal{D}$. Given that $r(t) \in \mathcal{L}_\infty$ in $\mathcal{D}$, (5–51) can be used to show that $\dot{\mu}_1(t) \in \mathcal{L}_\infty$ in $\mathcal{D}$, and since $\dot{G}^{-1}(\cdot)$ and $\dot{f}(\cdot) \in \mathcal{L}_\infty$ in $\mathcal{D}$, (5–50) can be used to show that $\dot{r}(t) \in \mathcal{L}_\infty$ in $\mathcal{D}$, and (5–40) can be used to show that $\dot{\varepsilon}(t) \in \mathcal{L}_\infty$ in $\mathcal{D}$. Since $\dot{e}_i(t) \in \mathcal{L}_\infty$, $\dot{r}(t)$, and $\dot{\varepsilon}(t) \in \mathcal{L}_\infty$ in $\mathcal{D}$, the definitions for $U(y)$ and $z(t)$ can be used to prove that $U(y)$ is uniformly continuous in $\mathcal{D}$.

Let $\mathcal{S} \subset \mathcal{D}$ denote a set defined as

$$\mathcal{S} \triangleq \left\{ y(t) \in \mathcal{D} \mid U_2(y(t)) < \lambda_1 \left(\rho^{-1}\left(2\sqrt{\lambda_3 k}\right) \right)^2 \right\}. \tag{5–73}$$

The region of attraction in (5–73) can be made arbitrarily large to include any initial conditions by increasing the control gain k (i.e., a semi-global stability result). Theorem

8.4 of [63] can now be invoked to state that

$$c \left\| \begin{bmatrix} z^T & \varepsilon^T \end{bmatrix}^T \right\|^2 \to 0 \qquad \text{as} \qquad t \to \infty \qquad \forall y(0) \in \mathcal{S}. \tag{5–74}$$

Based on the definition of $z(t)$, (5–74) can be used to show that

$$\begin{aligned} \|e_1(t)\| &\to 0 \qquad \text{as} \qquad t \to \infty \qquad \forall y(0) \in \mathcal{S} \\ \|\varepsilon(t)\| &\to 0 \qquad \text{as} \qquad t \to \infty \qquad \forall y(0) \in \mathcal{S}. \end{aligned} \tag{5–75}$$

5.6 Experiment

As in Chapter 2, the testbed depicted in Figure 2-1 was used to implement the developed controller. The desired link trajectory is selected as follows (in degrees):

$$q_d(t) = 60.0 \sin(1.2t)(1 - \exp(-0.01t^3)). \tag{5–76}$$

For all experiments, the rotor velocity signal is obtained by applying a standard backwards difference algorithm to the position signal. The integral structure for the RISE term in (5–48) was computed on-line via a standard trapezoidal algorithm. The parameter estimates were all initialized to zero. In practice, the adaptive estimates would be initialized to a best-guess estimate of the values. Initializing the estimates to zero was done to test a scenario of no parameter knowledge. In addition, all the states were initialized to zero. The following control gains and best guess estimates were used to implement the controller in (5–47) and (5–48) in conjunction with the composite adaptive update law in (5–35), where the prediction error is generated from (5–15), (5–16), (5–36), and (5–37):

$$\begin{aligned} &k_1 = 70, \quad \beta_1 = 50, \quad \alpha_1 = 20, \quad \alpha_2 = 10, \quad \Gamma = diag\,\{4,\, 0.9,\, 0.9,\, 2\} \\ &k_2 = 400, \quad \beta_2 = 1, \quad \omega = 10, \quad \bar{\gamma}_2 = 50, \quad \bar{\gamma}_3 = 1, \quad \bar{\gamma}_5 = 50. \end{aligned} \tag{5–77}$$

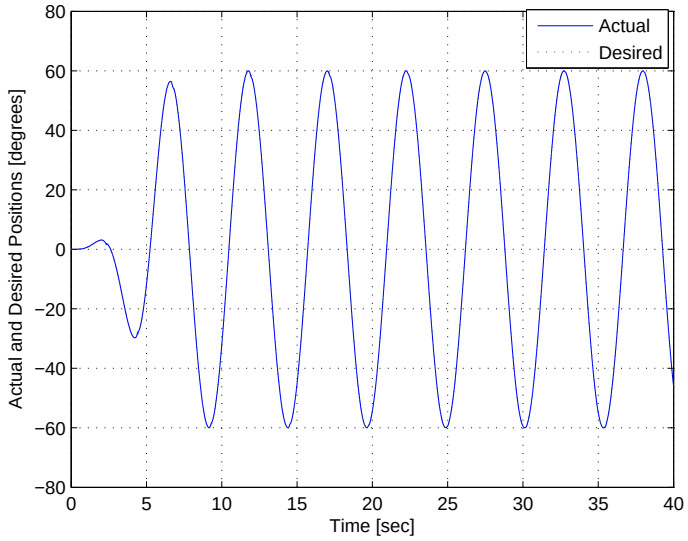

Figure 5-2. Actual and desired trajectories for the proposed composite adaptive control law (RISE+CFF).

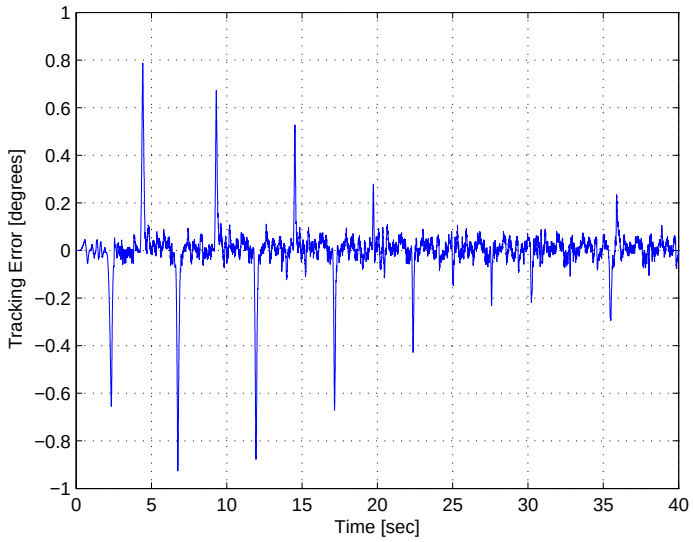

Figure 5-3. Tracking error for the proposed composite adaptive control law (RISE+CFF).

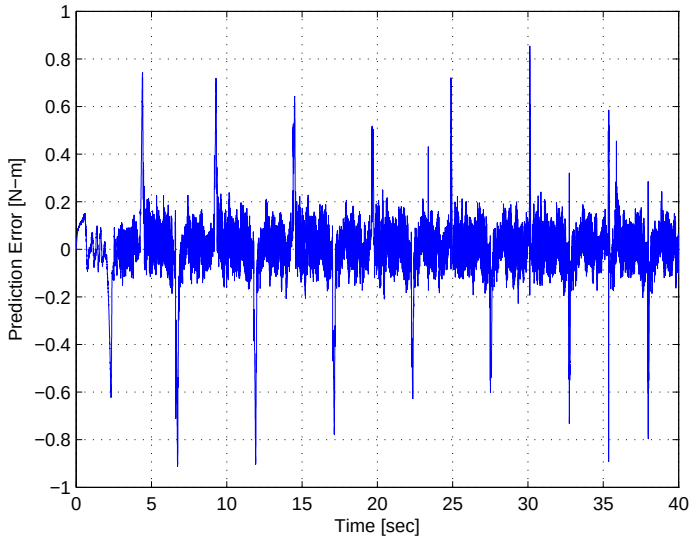

Figure 5-4. Prediction error for the proposed composite adaptive control law (RISE+CFF).

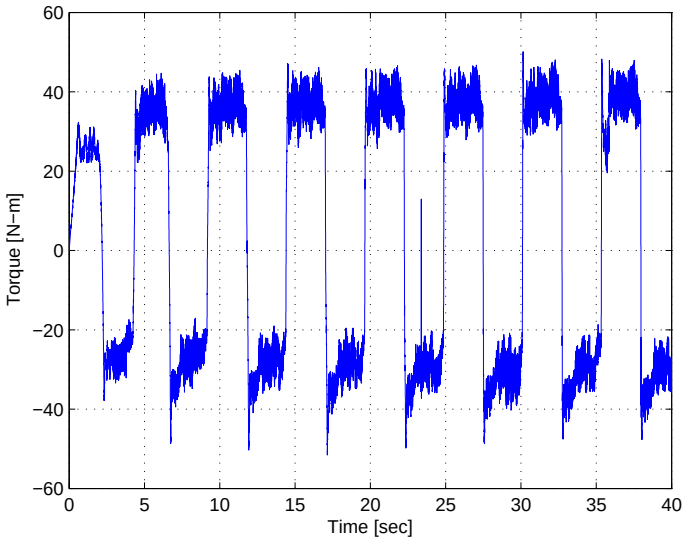

Figure 5-5. Control torque for the proposed composite adaptive control law (RISE+CFF).

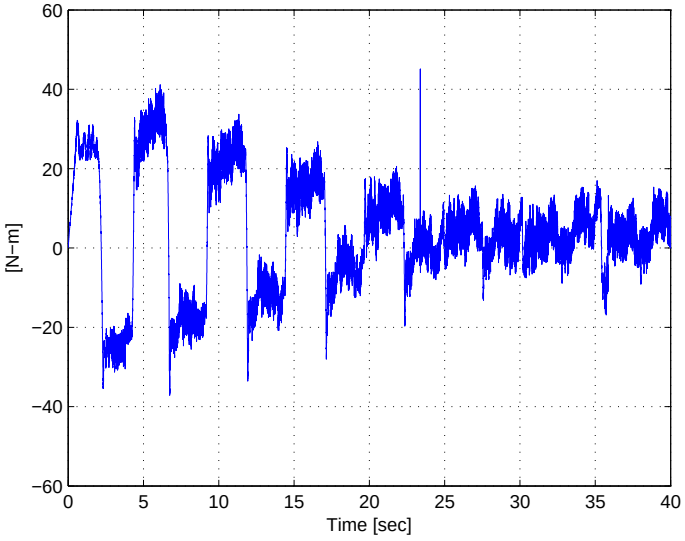

Figure 5-6. Contribution of the RISE term in the proposed composite adaptive control law (RISE+CFF).

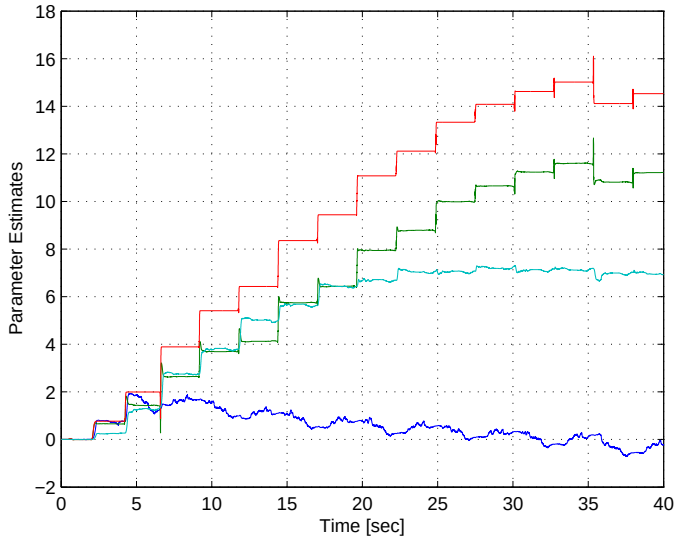

Figure 5-7. Adaptive estimates for the proposed composite adaptive control law (RISE+CFF).

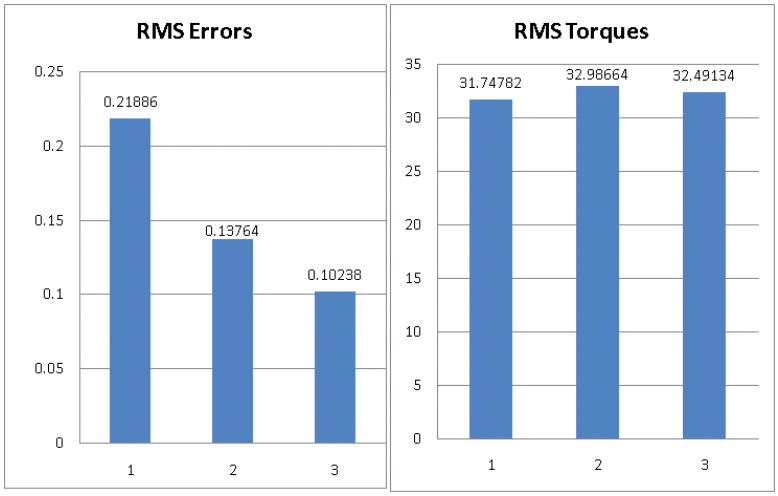

Figure 5-8. Average RMS errors (degrees) and torques (N-m). 1- RISE, 2- RISE+FF, 3- RISE+CFF (proposed).

5.6.1 Discussion

Three different experiments were conducted to demonstrate the efficacy of the proposed controller. For each controller, the gains were not retuned (i.e., the common control gains remain the same for all controllers). First, no adaptation was used and the controller with only the RISE feedback was implemented. For the second experiment, the prediction error component of the update law in (5–35) was removed, resulting in a standard gradient-based update law (hereinafter denoted as RISE+FF). For the third experiment, the proposed composite adaptive controller in (5–47)-(5–48) (hereinafter denoted as RISE+CFF) was implemented. Figure 5-2 depicts the actual position compared with the desired trajectory for the RISE+CFF controller, while the tracking error and the prediction error are shown in Figure 5-3 and Figure 5-4, respectively. The control torque is shown in Figure 5-5, and the contribution of the RISE term in the overall torque is depicted in Figure 5-6. The contribution of the feedback RISE term decreases as the adaptive estimates converge as shown in Figure 5-7. Each experiment was performed five times and the average RMS error and torque values are shown in Figure 5-8, which indicate that the proposed RISE+CFF controller yields the lowest RMS error with a similar control effort.

5.7 Conclusion

A novel approach for the design of a gradient-based composite adaptive controller was proposed for generic MIMO systems subjected to bounded disturbances. A model-based feedforward adaptive component was used in conjunction with the RISE feedback, where the adaptive estimates were generated using a composite update law driven by both the tracking and prediction error with the motivation of using more information in the adaptive update law. To account for the effects of non-LP disturbances, the typical prediction error formulation was modified to include a second RISE-like term in the estimated filtered control input design. Using a Lyapunov stability analysis, sufficient gain conditions were derived under which the proposed controller yields semi-global asymptotic stability. The current development, as well as all previous RISE controllers, require full-state feedback. The development of an output feedback result remains an open problem. Experiments on a rotating disk with externally applied friction indicate that the proposed method yields better tracking performance with a similar control effort.

CHAPTER 6
COMPOSITE ADAPTATION FOR NN-BASED CONTROLLERS

6.1 Introduction

This chapter presents the first ever attempt to develop a prediction error-based composite adaptive NN controller for an Euler-Lagrange second-order dynamic system using the recent continuous Robust Integral of the Sign of the Error (RISE) [19] technique that was originally developed in [21] and [22]. The RISE architecture is adopted since this method can accommodate for C^2 disturbances and yield asymptotic stability. The RISE technique was used in [75] to prove the first ever asymptotic result for a NN-based controller using a continuous feedback. In this chapter, the RISE feedback is used in conjunction with a NN feedfoward element similar to [75], however, unlike the typical tracking error-based gradient update law used in [75], the result in this chapter uses a composite update law driven by both the tracking and the prediction error. In order to compensate for the effect of NN reconstruction error, an innovative use of the RISE structure is also employed in the prediction error update (i.e., the filtered control input estimate). A block diagram indicating the unique use of the RISE method in the control and the prediction error formulation is provided in Figure 6-1. Sufficient gain conditions are derived using a Lyapunov-based stability analysis under which this unique double-RISE control strategy yields a semi-global asymptotic stability for the system tracking errors and the prediction error, while all other signals and the control input are shown to be bounded. Since a multi-layer NN includes the first layer weight estimate inside of a nonlinear activation function, proving that the NN weight estimates are bounded is a challenging task. A projection algorithm is used to guarantee the boundedness of the weight estimates. However, if instead a single-layer NN is used, projection is not required and the weight estimates can be shown bounded via the stability analysis. The control development in this chapter can be easily simplified for a single-layer NN by choosing fixed first layer weights.

A usual concern about the RISE feedback is the presence of high-gain and high-frequency components in the control structure. However, in contrast to a typical widely used discontinuous high-gain sliding mode controller, the RISE feedback offers a continuous alternative. Moreover, the proposed controller is not purely high gain as a multi-layer NN is used as a feedforward component that learns and incorporates the knowledge of system dynamics in the control structure.

6.2 Dynamic System

Consider a class of second order nonlinear systems of the following form:

$$\ddot{x} = f(x, \dot{x}) + G(x)u \tag{6–1}$$

where $x(t), \dot{x}(t) \in \mathbb{R}^n$ are the system states, $u(t) \in \mathbb{R}^n$ is the control input, $f(x, \dot{x}) \in \mathbb{R}^n$ and $G(x) \in \mathbb{R}^{n \times n}$ are unknown nonlinear $\mathcal{C}^2$ functions. The control development for the dynamic system in (6–1) can be easily extended to a second-order Euler-Lagrange system of the following form:

$$M(q)\ddot{q} + V_m(q, \dot{q})\dot{q} + G(q) + F(\dot{q}) = \tau(t)$$

where $M(q) \in \mathbb{R}^{n \times n}$ denotes the inertia matrix, $V_m(q, \dot{q}) \in \mathbb{R}^{n \times n}$ denotes the centripetal-Coriolis matrix, $G(q) \in \mathbb{R}^n$ denotes the gravity vector, $F(\dot{q}) \in \mathbb{R}^n$ denotes friction, $\tau(t) \in \mathbb{R}^n$ represents the torque input control vector, and $q(t)$, $\dot{q}(t)$, $\ddot{q}(t) \in \mathbb{R}^n$ denote the link position, velocity, and acceleration vectors, respectively. Throughout the chapter, $|\cdot|$ denotes the absolute value of the scalar argument, $\|\cdot\|$ denotes the standard Euclidean norm for a vector or the induced infinity norm for a matrix, and $\|\cdot\|_F$ denotes the Frobenius norm of a matrix.

The following properties and assumptions will be exploited in the subsequent development.

Assumption 6-1: $G(\cdot)$ is symmetric positive definite, and satisfies the following inequality $\forall \xi(t) \in \mathbb{R}^n$:

$$\underline{g} \|\xi\|^2 \leq \xi^T G^{-1} \xi \leq \bar{g}(x) \|\xi\|^2 \tag{6–2}$$

where $\underline{g} \in \mathbb{R}$ is a known positive constant, and $\bar{g}(x) \in \mathbb{R}$ is a known positive function.

Assumption 6-2: The functions $G^{-1}(\cdot)$ and $f(\cdot)$ are second order differentiable such that $G^{-1}(\cdot)$, $\dot{G}^{-1}(\cdot)$, $\ddot{G}^{-1}(\cdot)$, $f(\cdot)$, $\dot{f}(\cdot)$, $\ddot{f}(\cdot) \in \mathcal{L}_\infty$ if $x^{(i)}(t) \in \mathcal{L}_\infty$, $i = 0, 1, 2, 3$, where $(\cdot)^{(i)}(t)$ denotes the i^{th} derivative with respect to time.

Assumption 6-3: The desired trajectory $x_d(t) \in \mathbb{R}^n$ is designed such that $x_d^{(i)}(t) \in \mathcal{L}_\infty$, $i = 0, 1, ..., 4$ with known bounds.

6.3 Control Objective

The objective is to design a continuous *composite* adaptive NN controller which ensures that the system state $x(t)$ tracks a desired time-varying trajectory $x_d(t)$ despite uncertainties in the dynamic model. To quantify this objective, a tracking error, denoted by $e_1(t) \in \mathbb{R}^n$, is defined as

$$e_1 \triangleq x_d - x. \tag{6–3}$$

To facilitate the subsequent analysis, filtered tracking errors, denoted by $e_2(t)$, $r(t) \in \mathbb{R}^n$, are also defined as

$$e_2 \triangleq \dot{e}_1 + \alpha_1 e_1 \tag{6–4}$$

$$r \triangleq \dot{e}_2 + \alpha_2 e_2 \tag{6–5}$$

where α_1, $\alpha_2 \in \mathbb{R}$ denote positive constants. The subsequent development is based on the assumption that the system states $x(t), \dot{x}(t)$ are measurable. Hence, the filtered tracking error $r(t)$ is not measurable since the expression in (6–5) depends on $\ddot{x}(t)$.

6.4 Control Development

The open-loop tracking error system is developed by premultiplying (6–5) by $G^{-1}(\cdot)$ and utilizing the expressions in (6–1), (6–3), (6–4) as

$$G^{-1}r = \psi + S_1 - u. \tag{6–6}$$

In (6–6), $\psi(x_d, \dot{x}_d, \ddot{x}_d) \in \mathbb{R}^n$ is defined as

$$\psi \triangleq G_d^{-1}\ddot{x}_d - G_d^{-1}f_d \tag{6–7}$$

where the functions $G_d^{-1}(x_d) \in \mathbb{R}^{n\times n}$ and $f_d(x_d, \dot{x}_d) \in \mathbb{R}^n$ are defined as

$$G_d^{-1} \triangleq G^{-1}(x_d), \qquad f_d \triangleq f(x_d, \dot{x}_d). \tag{6–8}$$

Also in (6–6), the auxiliary function $S_1(x, \dot{x}, t) \in \mathbb{R}^n$ is defined as

$$S_1 \triangleq G^{-1}\alpha_2 e_2 + G^{-1}\ddot{x}_d - G_d^{-1}\ddot{x}_d - G^{-1}f + G_d^{-1}f_d + G^{-1}\alpha_1\dot{e}_1. \tag{6–9}$$

The unknown dynamics in (6–7) can be represented by a three-layer NN [15, 32] using the universal approximation property as described in Section 3.4 of Chapter 3.

$$\psi = W^T\sigma(V^T\bar{x}_d) + \varepsilon(\bar{x}_d). \tag{6–10}$$

Based on (6–10), the typical three-layer NN approximation for $\psi(\bar{x}_d)$ is given as [15, 32]

$$\hat{\psi} \triangleq \hat{W}^T\sigma\left(\hat{V}^T\bar{x}_d\right) \tag{6–11}$$

where $\hat{V}(t) \in \mathbb{R}^{(N_1+1)\times N_2}$ and $\hat{W}(t) \in \mathbb{R}^{(N_2+1)\times n}$ are subsequently designed estimates of the ideal weight matrices. The estimate mismatch for the ideal weight matrices, denoted by $\tilde{V}(t) \in \mathbb{R}^{(N_1+1)\times N_2}$ and $\tilde{W}(t) \in \mathbb{R}^{(N_2+1)\times n}$, are defined as

$$\tilde{V} \triangleq V - \hat{V}, \qquad \tilde{W} \triangleq W - \hat{W}$$

and the mismatch for the hidden-layer output error for a given $\bar{x}_d(t)$, denoted by $\tilde{\sigma}(\bar{x}_d) \in \mathbb{R}^{N_2+1}$, is defined as

$$\tilde{\sigma} \triangleq \sigma - \hat{\sigma} = \sigma\left(V^T \bar{x}_d\right) - \sigma\left(\hat{V}^T \bar{x}_d\right). \tag{6–12}$$

Property 6-1: (*Taylor Series Approximation*) The Taylor series expansion for $\sigma\left(V^T \bar{x}_d\right)$ for a given $\bar{x}_d(t)$ may be written as [15, 32]

$$\sigma\left(V^T \bar{x}_d\right) = \sigma\left(\hat{V}^T \bar{x}_d\right) + \sigma'\left(\hat{V}^T \bar{x}_d\right) \tilde{V}^T \bar{x}_d + O\left(\tilde{V}^T \bar{x}_d\right)^2 \tag{6–13}$$

where $\sigma'\left(\hat{V}^T \bar{x}_d\right) \equiv d\sigma\left(V^T \bar{x}_d\right)/d\left(V^T \bar{x}_d\right)|_{V^T \bar{x}_d = \hat{V}^T \bar{x}_d}$, and $O\left(\hat{V}^T \bar{x}_d\right)^2$ denotes the higher order terms. After substituting (6–13) into (6–12), the following expression can be obtained

$$\tilde{\sigma} = \hat{\sigma}' \tilde{V}^T \bar{x}_d + O\left(\tilde{V}^T \bar{x}_d\right)^2 \tag{6–14}$$

where $\hat{\sigma}' \triangleq \sigma'\left(\hat{V}^T \bar{x}_d\right)$.

Based on the open-loop error system in (6–6), the control input is composed of a NN estimate term plus the RISE feedback term as [75]

$$u \triangleq \hat{\psi} + \mu_1 \tag{6–15}$$

where $\hat{\psi}(t) \in \mathbb{R}^n$ denotes a first ever, subsequently designed, prediction-error based NN feedfoward term. In (6–15), $\mu_1(t) \in \mathbb{R}^n$ denotes the RISE feedback term defined as [21, 22, 75]

$$\mu_1(t) \triangleq (k_1+1)e_2(t) - (k_1+1)e_2(0) + \int_0^t \{(k_1+1)\alpha_2 e_2(\sigma) + \beta_1 sgn(e_2(\sigma))\} d\sigma \tag{6–16}$$

where k_1, $\beta_1 \in \mathbb{R}$ are positive constant control gains, $\alpha_2 \in \mathbb{R}$ was introduced in (6–5), and $sgn(\cdot)$ denotes the signum function defined as

$$sgn(e_2) \triangleq [sgn(e_{2_1}) \;\; sgn(e_{2_2}) \; ... \; sgn(e_{2_i}) \; ... \; sgn(e_{2_n})]^T.$$

The closed-loop tracking error system can be developed by substituting (6–15) into (6–6) as

$$G^{-1}r = \psi - \hat{\psi} + S_1 - \mu_1. \tag{6–17}$$

To facilitate the subsequent composite adaptive control development and stability analysis, (6–10) and (6–11) are used to express the time derivative of (6–17) as

$$\begin{aligned} G^{-1}\dot{r} = &-\dot{G}^{-1}r + W^T\sigma'\left(V^T\bar{x}_d\right)V^T\dot{\bar{x}}_d - \dot{\hat{W}}^T\sigma(\hat{V}^T\bar{x}_d) - \hat{W}^T\sigma'(\hat{V}^T\bar{x}_d)\dot{\hat{V}}^T\bar{x}_d \\ &- \hat{W}^T\sigma'(\hat{V}^T\bar{x}_d)\hat{V}^T\dot{\bar{x}}_d + \dot{\varepsilon} + \dot{S}_1 - \dot{\mu}_1. \end{aligned} \tag{6–18}$$

After adding and subtracting the terms $W^T\hat{\sigma}'\hat{V}^T\dot{\bar{x}}_d + \hat{W}^T\hat{\sigma}'\tilde{V}^T\dot{\bar{x}}_d$ to (6–18), the following expression can be obtained:

$$\begin{aligned} G^{-1}\dot{r} = &-\dot{G}^{-1}r + \hat{W}^T\hat{\sigma}'\tilde{V}^T\dot{\bar{x}}_d + \tilde{W}^T\hat{\sigma}'\hat{V}^T\dot{\bar{x}}_d + W^T\sigma'V^T\dot{\bar{x}}_d - W^T\hat{\sigma}'\hat{V}^T\dot{\bar{x}}_d \\ &- \hat{W}^T\hat{\sigma}'\tilde{V}^T\dot{\bar{x}}_d + \dot{S}_1 - \dot{\hat{W}}^T\hat{\sigma} - \hat{W}^T\hat{\sigma}'\dot{\hat{V}}^T\bar{x}_d + \dot{\varepsilon} - \dot{\mu}_1 \end{aligned} \tag{6–19}$$

where the notations $\hat{\sigma}\left(\hat{V}^T\bar{x}_d\right)$ and $\hat{\sigma}'\left(\hat{V}^T\bar{x}_d\right)$ are introduced in (6–12) and (6–14), respectively.

6.4.1 Swapping

In this section, the swapping procedure is used to generate a measurable form of a prediction error that relates to the function mismatch error (i.e., $\psi(t) - \hat{\psi}(t)$). A measurable form of the prediction error $\eta(t) \in \mathbb{R}^n$ is defined as the difference between a filtered control input $u_f(t) \in \mathbb{R}^n$ and an estimated filtered control input $\hat{u}_f(t) \in \mathbb{R}^n$ as

$$\eta \triangleq u_f - \hat{u}_f \tag{6–20}$$

where the filtered control input is generated from the stable first order differential equation

$$\dot{u}_f + \omega u_f = \omega u\ , \qquad u_f(0) = 0 \tag{6–21}$$

where $\omega \in \mathbb{R}$ is a known positive constant. The differential equation in (6–21) can be expressed as a convolution as

$$u_f = v * u \tag{6–22}$$

where $*$ is used to denote the standard convolution operation, and the scalar function $v(t)$ is defined as

$$v \triangleq \omega e^{-\omega t}. \tag{6–23}$$

Using (6–1), the expression in (6–22) can be rewritten as

$$u_f = v * \left(G^{-1}\ddot{x} - G^{-1}f\right). \tag{6–24}$$

The construction of a NN-based controller to approximate the unknown system dynamics in (6–24) will inherently result in a residual function reconstruction error $\varepsilon(\bar{x}_d)$. The presence of the reconstruction error has been the technical obstacle that has prevented the development of composite adaptation laws for NNs. To compensate for the effects of the reconstruction error, the typical prediction error formulation is modified to include a RISE-like structure in the design of the estimated filtered control input. With this motivation, the open-loop prediction error system is engineered to facilitate the RISE-based design of the estimated filtered control input.

Adding and subtracting the term $v * \left(G_d^{-1}\ddot{x}_d + G_d^{-1}f_d\right)$ to the expression in (6–24), and using (6–7) yields

$$u_f = v * (\psi + S - S_d) \tag{6–25}$$

where $S(x, \dot{x}, \ddot{x})$, $S_d(x_d, \dot{x}_d, \ddot{x}_d) \in \mathbb{R}^n$ are defined as

$$S \triangleq G^{-1}\ddot{x} - G^{-1}f \tag{6–26}$$

$$S_d \triangleq G_d^{-1}\ddot{x}_d - G_d^{-1}f_d. \tag{6–27}$$

The expression in (6–25) is further simplified as

$$u_f = v * \psi + v * S - v * S_d. \tag{6–28}$$

The term $v * S(x, \dot{x}, \ddot{x}) \in \mathbb{R}^n$ in (6–28) depends on $\ddot{x}(t)$. Using the following property of convolution [57]:

$$g_1 * \dot{g}_2 = \dot{g}_1 * g_2 + g_1(0) g_2 - g_1 g_2(0) \tag{6–29}$$

an expression independent of $\ddot{x}(t)$ can be obtained as

$$v * S = S_f + D \tag{6–30}$$

where the state-dependent terms are included in the auxiliary function $S_f(x, \dot{x}) \in \mathbb{R}^n$, defined as

$$S_f \triangleq \dot{v} * \left(G^{-1}\dot{x}\right) + v(0) G^{-1}\dot{x} - v * \dot{G}^{-1}\dot{x} - v * G^{-1} f \tag{6–31}$$

and the terms that depend on the initial states are included in $D(t) \in \mathbb{R}^n$, defined as

$$D \triangleq -vG^{-1}(x(0))\dot{x}(0). \tag{6–32}$$

Similarly, the expression $v * S_d(x_d, \dot{x}_d, \ddot{x}_d)$ in (6–28) is evaluated as

$$v * S_d = S_{df} + D_d \tag{6–33}$$

where $S_{df}(x_d, \dot{x}_d) \in \mathbb{R}^n$ is defined as

$$S_{df} \triangleq \dot{v} * (G_d^{-1}\dot{x}_d) + v(0) G_d^{-1}\dot{x}_d - v * \dot{G}_d^{-1}\dot{x}_d - v * G_d^{-1} f_d \tag{6–34}$$

and $D_d(t) \in \mathbb{R}^n$ is defined as

$$D_d \triangleq -vG_d^{-1}(x_d(0))\dot{x}_d(0). \tag{6–35}$$

Substituting (6–30)-(6–35) into (6–28), and then substituting the resulting expression into (6–20) yields

$$\eta = v * \psi + S_f - S_{df} + D - D_d - \hat{u}_f. \tag{6–36}$$

Based on (6–36) and the subsequent analysis, the filtered control input estimate is designed as

$$\hat{u}_f = \hat{\psi}_f + \mu_2 \tag{6–37}$$

where the filtered NN estimate $\hat{\psi}_f(t) \in \mathbb{R}^n$ is generated by from the stable first order differential equation

$$\dot{\hat{\psi}}_f + \omega \hat{\psi}_f = \omega \hat{\psi}, \qquad \hat{\psi}_f(0) = 0$$

which can be expressed as a convolution

$$\hat{\psi}_f = v * \hat{\psi}.$$

In (6–37), $\mu_2(t) \in \mathbb{R}^n$ is a RISE-like term defined as

$$\mu_2(t) \triangleq \int_0^t [k_2 \eta(\sigma) + \beta_2 sgn(\eta(\sigma))] d\sigma \tag{6–38}$$

where k_2, $\beta_2 \in \mathbb{R}$ denote constant positive control gains. In a typical prediction error formulation, the estimated filtered control input is designed to include just the first term $\hat{\psi}_f(t)$ in (6–37). But as discussed earlier, due to the presence of the NN reconstruction error, the unmeasurable form of the prediction error in (6–36) also includes the filtered reconstruction error. Hence, the estimated filtered control input is augmented with an additional RISE-like term $\mu_2(t)$ to cancel the effects of reconstruction error in the prediction error measurement as illustrated in Figure 6-1 and the subsequent design and stability analysis.

Substituting (6–37) into (6–36) yields the following closed-loop prediction error system:

$$\eta = v * \left(\psi - \hat{\psi}\right) + S_f - S_{df} + D - D_d - \mu_2. \tag{6–39}$$

To facilitate the subsequent composite adaptive control development and stability analysis, the time derivative of (6–39) is expressed as

$$\dot{\eta} = \dot{v} * \left(\psi - \hat{\psi}\right) + \omega \left(\psi - \hat{\psi}\right) + \dot{S}_f - \dot{S}_{df} + \dot{D} - \dot{D}_d - \dot{\mu}_2 \tag{6–40}$$

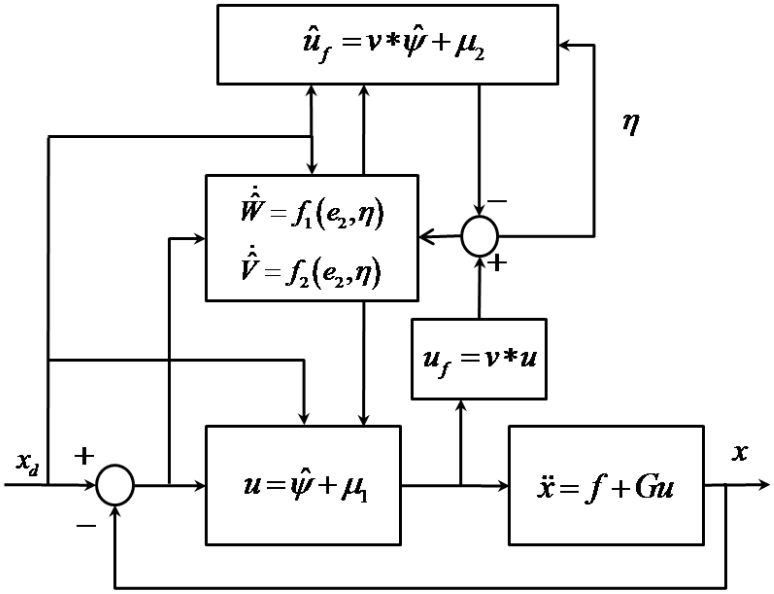

Figure 6-1. Block diagram of the proposed RISE-based composite NN controller.

where the property $\frac{d}{dt}(f * g) = (\dot{f} * g)(t) + f(0)\, g(t)$ was used. Substituting (6–10) and (6–11) into (6–40) yields

$$\dot{\eta} = \dot{v} * \left(W^T \sigma(V^T \bar{x}_d) + \varepsilon - \hat{W}^T \sigma(\hat{V}^T \bar{x}_d) \right) + \omega \left(W^T \sigma(V^T \bar{x}_d) + \varepsilon - \hat{W}^T \sigma(\hat{V}^T \bar{x}_d) \right) \quad (6\text{–}41)$$
$$+ \dot{S}_f - \dot{S}_{df} + \dot{D} - \dot{D}_d - \dot{\mu}_2.$$

Adding and subtracting $\dot{v}(t) * (\hat{W}^T \sigma + \tilde{W}^T \hat{\sigma}) + \omega(\hat{W}^T \sigma + \tilde{W}^T \hat{\sigma})$ to (6–41) and rearranging the terms yields

$$\dot{\eta} = \dot{v} * \left(\hat{W}^T \tilde{\sigma} + \tilde{W}^T \hat{\sigma} + \tilde{W}^T \tilde{\sigma} + \varepsilon \right) + \omega \left(\hat{W}^T \tilde{\sigma} + \tilde{W}^T \hat{\sigma} + \tilde{W}^T \tilde{\sigma} + \varepsilon \right) \quad (6\text{–}42)$$
$$+ \dot{S}_f - \dot{S}_{df} + \dot{D} - \dot{D}_d - \dot{\mu}_2.$$

By using the Taylor series expansion in (6–13), (6–42) can be expressed as

$$\dot{\eta} = \dot{v} * \left(\tilde{W}^T \hat{\sigma} + \hat{W}^T \hat{\sigma}' \tilde{V}^T \bar{x}_d \right) + \dot{v} * \left(\hat{W}^T O \left(\tilde{V}^T \bar{x}_d \right)^2 + \tilde{W}^T \tilde{\sigma} + \varepsilon \right) \quad (6\text{–}43)$$
$$+ \omega \left(\tilde{W}^T \hat{\sigma} + \hat{W}^T \hat{\sigma}' \tilde{V}^T \bar{x}_d \right) + \omega \left(\hat{W}^T O \left(\tilde{V}^T \bar{x}_d \right)^2 + \tilde{W}^T \tilde{\sigma} + \varepsilon \right) + \dot{S}_f - \dot{S}_{df} + \dot{D} - \dot{D}_d - \dot{\mu}_2.$$

Using the commutativity and distributivity property of the convolution, and rearranging the terms in (6–43) yields

$$\dot{\eta} = \tilde{W}^T \left(\hat{\sigma} * \dot{v} + \omega \hat{\sigma} \right) + \hat{W}^T \hat{\sigma}' \tilde{V}^T \left(\bar{x}_d * \dot{v} + \omega \bar{x}_d \right) + \tilde{N}_2 + N_{2B} - k_2 \eta - \beta_2 sgn(\eta) \tag{6–44}$$

where the fact that

$$\dot{\mu}_2 = k_2 \eta + \beta_2 sgn(\eta) \tag{6–45}$$

was utilized. In (6–44), the unmeasurable/unknown auxiliary term $\tilde{N}_2(e_1, e_2, r, t) \in \mathbb{R}^n$ is defined as

$$\tilde{N}_2 \triangleq \dot{S}_f - \dot{S}_{df} \tag{6–46}$$

and the term $N_{2B}(t) \in \mathbb{R}^n$ is defined as

$$N_{2B} \triangleq \dot{D} - \dot{D}_d + \dot{v} * \left(\hat{W}^T O \left(\tilde{V}^T \bar{x}_d \right)^2 + \tilde{W}^T \tilde{\sigma} + \varepsilon \right) + \omega \left(\hat{W}^T O \left(\tilde{V}^T \bar{x}_d \right)^2 + \tilde{W}^T \tilde{\sigma} + \varepsilon \right). \tag{6–47}$$

In a similar manner as in Lemma 1 of the Appendix, by applying the Mean Value Theorem can be used to develop the following upper bound for the expression in (6–46):

$$\left\| \tilde{N}_2(t) \right\| \leq \rho_2 \left(\|z\| \right) \|z\| \tag{6–48}$$

where the bounding function $\rho_2(\cdot) \in \mathbb{R}$ is a positive, globally invertible, nondecreasing function, and $z(t) \in \mathbb{R}^{3n}$ is defined as

$$z(t) \triangleq \begin{bmatrix} e_1^T & e_2^T & r^T \end{bmatrix}^T. \tag{6–49}$$

Using Assumption 6-3, and the fact that $v(t)$ is a linear, strictly proper, exponentially stable transfer function, the following inequality can be developed based on the expression in (6–47) with a similar approach as in Lemma 2 of [42]:

$$\|N_{2B}(t)\| \leq \xi \tag{6–50}$$

where $\xi \in \mathbb{R}$ is a known positive constant.

6.4.2 Composite Adaptation

The composite adaptation for the NN weight estimates is given by

$$\dot{\hat{W}} \triangleq \Gamma_1 proj(\alpha_2 \hat{\sigma}' \hat{V}^T \dot{\bar{x}}_d e_2^T + \dot{\hat{\sigma}}_f \eta^T) \tag{6–51}$$

$$\dot{\hat{V}} \triangleq \Gamma_2 proj(\alpha_2 \dot{\bar{x}}_d e_2^T \hat{W}^T \hat{\sigma}' + \dot{\bar{x}}_{df} \eta^T \hat{W}^T \hat{\sigma}') \tag{6–52}$$

where $\Gamma_1 \in \mathbb{R}^{(N_2+1)\times(N_2+1)}$, $\Gamma_2 \in \mathbb{R}^{(N_1+1)\times(N_1+1)}$ are constant, positive definite, symmetric control gain matrices, $proj(\cdot)$ denotes a smooth projection operator (see [70, 75]) that is used to ensure that $\hat{W}(t)$ and $\hat{V}(t)$ remain inside the bounded convex region. Also, $\eta(t) \in \mathbb{R}^n$ denotes the measurable prediction error defined in (6–20), and the scalar function $v(t)$ was defined in (6–23). The filtered activation function $\hat{\sigma}_f(t) \in \mathbb{R}^{N_2+1}$ is generated from the stable first order differential equation

$$\dot{\hat{\sigma}}_f + \omega \hat{\sigma}_f = \omega \hat{\sigma}, \qquad \hat{\sigma}_f(0) = 0 \tag{6–53}$$

while the filtered NN input vector $\bar{x}_{df}(t) \in \mathbb{R}^{3n+1}$ is generated by

$$\dot{\bar{x}}_{df} + \omega \bar{x}_{df} = \omega \bar{x}_d, \qquad \bar{x}_{df}(0) = 0. \tag{6–54}$$

In a typical NN weight adaptation law, only the system tracking errors are used to update the weights and no information about the actual estimate mismatch (i.e., $\psi(t) - \hat{\psi}(t)$) is utilized as it is unmeasurable, and hence cannot be used in control implementation. The proposed method uses the swapping procedure in Section 6.4.1 to generate a measurable prediction error $\eta(t)$ that contains information related to the estimate mismatch error.

The projection used in the NN weight adaptation laws in (6–51) and (6–52) can be decomposed into two terms as[1]

$$\dot{\hat{W}} = \chi_\eta^W + \chi_{e_2}^W, \qquad \dot{\hat{V}} = \chi_\eta^V + \chi_{e_2}^V \tag{6–55}$$

such that the auxiliary functions $\chi_\eta^W\left(\hat{\sigma}_f, \eta\right)$, $\chi_{e_2}^W\left(\hat{V}, \bar{x}_d, \dot{\bar{x}}_d, e_2\right) \in \mathbb{R}^{(N_2+1)\times n}$ and $\chi_\eta^V\left(\bar{x}_{df}, \hat{W}, \hat{V}, \eta\right)$, $\chi_{e_2}^V\left(\hat{W}, \hat{V}, \bar{x}_d, \dot{\bar{x}}_d, e_2\right) \in \mathbb{R}^{(N_1+1)\times N_2}$ satisfy the following bounds

$$\begin{aligned} \left\|\chi_\eta^W\right\| &\leq b_1 \|\eta\|, \qquad \left\|\chi_{e_2}^W\right\| \leq b_2 \|e_2\| \\ \left\|\chi_\eta^V\right\| &\leq b_1' \|\eta\|, \qquad \left\|\chi_{e_2}^V\right\| \leq b_2' \|e_2\| \end{aligned} \tag{6–56}$$

where b_1, b_2, b_1', and $b_2' \in \mathbb{R}$ are known positive constants. To facilitate the subsequent stability analysis, the following inequality is developed based on (6–56) and the fact that the NN weight estimates are bounded by the smooth projection algorithm:

$$\left\|\chi_\eta^W \hat{\sigma} + \hat{W}^T \hat{\sigma}' \chi_\eta^V \bar{x}_d\right\| \leq c_1 \|\eta\| \tag{6–57}$$

where $c_1 \in \mathbb{R}$ is a positive constant.

6.4.3 Closed-Loop Error System

Substituting for $\dot{\hat{W}}(t)$ and $\dot{\hat{V}}(t)$ from (6–55), the expression in (6–19) can be rewritten as

$$G^{-1}\dot{r} = -\frac{1}{2}\dot{G}^{-1}r - \chi_\eta^W \hat{\sigma} - \hat{W}^T \hat{\sigma}' \chi_\eta^V \bar{x}_d + \tilde{N}_1 + N_1 - (k_1+1)r - \beta_1 sgn(e_2) - e_2 \tag{6–58}$$

where the fact that the time derivative of (6–16) is given as

$$\dot{\mu}_1 = (k_1+1)r + \beta_1 sgn(e_2) \tag{6–59}$$

[1] See Lemma 5 of the Appendix for the proof of the decomposition in (6–55) and the inequalities in (6–56).

was utilized. In (6–58), the unmeasurable/unknown auxiliary terms $\tilde{N}_1(e_1, e_2, r, t)$ and $N_1(t) \in \mathbb{R}^n$ are defined as

$$\tilde{N}_1 \triangleq -\frac{1}{2}\dot{G}^{-1}r + \dot{S}_1 + e_2 - \chi_{e_2}^W \hat{\sigma} - \hat{W}^T \hat{\sigma}' \chi_{e_2}^V \bar{x}_d \tag{6–60}$$

$$N_1 \triangleq N_d + N_{1B}. \tag{6–61}$$

In (6–61), $N_d(\bar{x}_d, \dot{\bar{x}}_d, t) \in \mathbb{R}^n$ is defined as

$$N_d \triangleq W^T \sigma' V^T \dot{\bar{x}}_d + \dot{\varepsilon} \tag{6–62}$$

while $N_{1B}(\hat{W}, \hat{V}, \bar{x}_d, \dot{\bar{x}}_d, t) \in \mathbb{R}^n$ is further segregated as

$$N_{1B} \triangleq N_{1B_a} + N_{1B_b} \tag{6–63}$$

where $N_{1B_a}(\hat{W}, \hat{V}, \bar{x}_d, \dot{\bar{x}}_d, t) \in \mathbb{R}^n$ is defined as

$$N_{1B_a} \triangleq -W^T \hat{\sigma}' \hat{V}^T \dot{\bar{x}}_d - \hat{W}^T \hat{\sigma}' \tilde{V}^T \dot{\bar{x}}_d \tag{6–64}$$

and the term $N_{1B_b}(\hat{W}, \hat{V}, \bar{x}_d, \dot{\bar{x}}_d, t) \in \mathbb{R}^n$ is defined as

$$N_{1B_b} \triangleq \hat{W}^T \hat{\sigma}' \tilde{V}^T \dot{\bar{x}}_d + \tilde{W}^T \hat{\sigma}' \hat{V}^T \dot{\bar{x}}_d. \tag{6–65}$$

Motivation for segregating the terms in (6–61) is derived from the fact that the different components in (6–61) have different bounds. Segregating the terms as in (6–61)-(6–65) facilitates the development of the NN weight update laws and the subsequent stability analysis. For example, the terms in (6–62) are grouped together because the terms and their time derivatives can be upper bounded by a constant and rejected by the RISE feedback, whereas the terms grouped in (6–63) can be upper bounded by a constant but their derivatives are state dependent. The state dependency of the time derivatives of the terms in (6–63) violates the assumptions given in previous RISE-based controllers (e.g., [19, 20, 22, 23, 25–27]), and requires additional consideration in the adaptation law design and stability analysis. The terms in (6–63) are further segregated because

$N_{1B_a}(\hat{W}, \hat{V}, \bar{x}_d, \dot{\bar{x}}_d)$ will be rejected by the RISE feedback, whereas $N_{1B_b}(\hat{W}, \hat{V}, \bar{x}_d, \dot{\bar{x}}_d)$ will be partially rejected by the RISE feedback and partially canceled by the adaptive update law for the NN weight estimates. In a similar manner as in (6–48), the following upper bound is developed for the expression in (6–60):

$$\left\| \tilde{N}_1(t) \right\| \leq \rho_1 \left(\|z\| \right) \|z\| \tag{6–66}$$

where the bounding function $\rho_1(\cdot) \in \mathbb{R}$ is a positive, globally invertible, nondecreasing function, and $z(t) \in \mathbb{R}^{3n}$ was defined in (6–49). The following inequalities can be developed based on Assumption 6-3, (3–7), (3–8), (3–16), (6–63)-(6–65):

$$\|N_d\| \leq \zeta_1, \qquad \|N_{1B_a}\| \leq \zeta_2, \qquad \|N_{1B_b}\| \leq \zeta_3, \qquad \left\| \dot{N}_d \right\| \leq \zeta_4. \tag{6–67}$$

From (6–61), (6–63) and (6–67), the following bound can be developed

$$\|N_1\| \leq \|N_d\| + \|N_{1B}\| \leq \|N_d\| + \|N_{1B_a}\| + \|N_{1B_b}\| \leq \zeta_1 + \zeta_2 + \zeta_3. \tag{6–68}$$

By using (6–51) and (6–52), the time derivative of $N_{1B}(\hat{W}, \hat{V}, x_d)$ can be bounded as

$$\left\| \dot{N}_{1B} \right\| \leq \zeta_5 + \zeta_6 \|e_2\| + \zeta_7 \|\eta\| . \tag{6–69}$$

In (6–67) and (6–69), $\zeta_i \in \mathbb{R}$, $(i = 1, 2, ..., 7)$ are known positive constants.

For the subsequent stability analysis, let $\mathcal{D} \subset \mathbb{R}^{4n+3}$ be a domain containing $y(t) = 0$, where $y(t) \in \mathbb{R}^{4n+3}$ is defined as

$$y \triangleq [z^T \quad \eta^T \quad \sqrt{P_1} \quad \sqrt{P_2} \quad \sqrt{Q}]^T. \tag{6–70}$$

In (6–70), the auxiliary function $P_1(t) \in \mathbb{R}$ is defined as

$$P_1(t) \triangleq \beta_1 \sum_{i=1}^{n} |e_{2i}(0)| - e_2(0)^T N_1(0) - \int_0^t L_1(\tau) d\tau \tag{6–71}$$

where $e_{2i}(0) \in \mathbb{R}$ denotes the ith element of the vector $e_2(0)$, and the auxiliary function $L_1(t) \in \mathbb{R}$ is defined as

$$L_1 \triangleq r^T(N_{1B_a} + N_d - \beta_1 sgn(e_2)) + \dot{e}_2^T N_{1B_b} - \beta_3 \|e_2\|^2 - \beta_4 \|\eta\|^2 \tag{6–72}$$

where β_1, β_3, $\beta_4 \in \mathbb{R}$ are positive constants chosen according to the sufficient conditions

$$\beta_1 > \max\left\{\zeta_1 + \zeta_2 + \zeta_3,\ \zeta_1 + \zeta_2 + \frac{\zeta_4}{\alpha_2} + \frac{\zeta_5}{\alpha_2}\right\},\quad \beta_3 > \zeta_6 + \frac{\zeta_7}{2},\quad \beta_4 > \frac{\zeta_7}{2} \tag{6–73}$$

where $\zeta_1 - \zeta_7$ were introduced in (6–67) and (6–69). Provided the sufficient conditions introduced in (6–73) are satisfied, the following inequality is obtained [22], [20]:

$$\int_0^t L_1(\tau)d\tau \leq \beta_1 \sum_{i=1}^{n} |e_{2i}(0)| - e_2(0)^T N_1(0). \tag{6–74}$$

Hence, (6–74) can be used to conclude that $P_1(t) \geq 0$. Also in (6–70), the auxiliary function $P_2(t) \in \mathbb{R}$ is defined as

$$P_2(t) \triangleq -\int_0^t L_2(\tau)d\tau \tag{6–75}$$

where the auxiliary function $L_2(t) \in \mathbb{R}$ is defined as

$$L_2 \triangleq \eta^T(N_{2B} - \beta_2 sgn(\eta)) \tag{6–76}$$

where $\beta_2 \in \mathbb{R}$ is a positive constant chosen according to the sufficient condition

$$\beta_2 > \xi \tag{6–77}$$

where ξ was introduced in (6–50). Provided the sufficient condition introduced in (6–77) is satisfied, then $P_2(t) \geq 0$. The auxiliary function $Q(t) \in \mathbb{R}$ in (6–70) is defined as

$$Q(t) \triangleq \frac{1}{2} tr\left(\tilde{W}^T \Gamma_1^{-1} \tilde{W}\right) + \frac{1}{2} tr\left(\tilde{V}^T \Gamma_2^{-1} \tilde{V}\right). \tag{6–78}$$

Since Γ_1 and Γ_2 are constant, symmetric, and positive definite matrices, it is straightforward that $Q(t) \geq 0$.

6.5 Stability Analysis

Theorem 6-1: The controller given in (6–15) and (6–16) in conjunction with the composite NN adaptation laws in (6–51) and (6–52), where the prediction error is generated from (6–20), (6–21), (6–37), and (6–38), ensures that all system signals are bounded under closed-loop operation and that the position tracking error and the prediction error are regulated in the sense that

$$\|e_1(t)\| \to 0 \text{ and } \|\eta(t)\| \to 0 \qquad \text{as} \qquad t \to \infty$$

provided the control gains k_1 and k_2 introduced in (6–16) and (6–38) are selected sufficiently large based on the initial conditions of the systems states (see the subsequent semi-global stability proof), the sufficient conditions in (6–73) and (6–77) are satisfied, and the following conditions are satisfied:

$$\alpha_1 > \frac{1}{2}, \qquad \alpha_2 > \beta_3 + \frac{1}{2} \tag{6–79}$$

where the gains α_1 and α_2 were introduced in (6–4) and (6–5).

Proof: Let $V_L(y,t) : \mathcal{D} \times [0,\infty) \to \mathbb{R}$ be a continuously differentiable, positive definite function defined as

$$V_L \triangleq \frac{1}{2}e_1^T e_1 + \frac{1}{2}e_2^T e_2 + \frac{1}{2}r^T G^{-1} r + \frac{1}{2}\eta^T \eta + P_1 + P_2 + Q \tag{6–80}$$

which satisfies the inequalities

$$U_1(y) \leq V_L(y,t) \leq U_2(y) \tag{6–81}$$

provided the sufficient conditions introduced in (6–73) and (6–77) are satisfied. In (6–81), the continuous positive definite functions $U_1(y), U_2(y) \in \mathbb{R}$ are defined as $U_1(y) \triangleq \lambda_1 \|y\|^2$

and $U_2(y) \triangleq \lambda_2(x) \|y\|^2$, where λ_1, $\lambda_2(x) \in \mathbb{R}$ are defined as

$$\lambda_1 \triangleq \frac{1}{2} \min\{1, \underline{g}\} \qquad \lambda_2 \triangleq \max\{\frac{1}{2}\bar{g}(x), 1\} \tag{6–82}$$

where $\underline{g}$, $\bar{g}(x)$ are introduced in (6–2). Using (6–4), (6–5), (6–44), (6–58), (6–71), (6–72), (6–75) and (6–76), the time derivative of (6–80) can be expressed as

$$\begin{aligned}\dot{V}_L = {} & e_1^T (e_2 - \alpha_1 e_1) + e_2^T (r - \alpha_2 e_2) + r^T(-\frac{1}{2}\dot{G}^{-1} r - \chi_\eta^W \hat{\sigma} - \hat{W}^T \hat{\sigma}' \chi_\eta^V \bar{x}_d + \tilde{N}_1 \\ & + N_1 - (k_1+1)r - \beta_1 sgn(e_2) - e_2) + \frac{1}{2} r^T \dot{G}^{-1} r + \eta^T (\tilde{W}^T \dot{\hat{\sigma}}_f + \hat{W}^T \hat{\sigma}' \tilde{V}^T \dot{\bar{x}}_{df} \\ & + \tilde{N}_2 + N_{2B} - k_2 \eta - \beta_2 sgn(\eta)) - r^T (N_{1B_a} + N_d - \beta_1 sgn(e_2)) - \dot{e}_2^T N_{1B_b} \\ & + \beta_3 \|e_2\|^2 + \beta_4 \|\eta\|^2 - \eta^T (N_{2B} - \beta_2 sgn(\eta)) - tr(\tilde{W}^T \Gamma_1^{-1} \dot{\hat{W}}) - tr(\tilde{V}^T \Gamma_2^{-1} \dot{\hat{V}}).\end{aligned} \tag{6–83}$$

Expanding the terms in (6–83) and using (6–61) and (6–63) yields

$$\begin{aligned}\dot{V}_L = {} & e_1^T e_2 - \alpha_1 e_1^T e_1 + e_2^T r - \alpha_2 e_2^T e_2 + r^T \tilde{N}_1 - \frac{1}{2} r^T \dot{G}^{-1} r - r^T \chi_\eta^W \hat{\sigma} - r^T \hat{W}^T \hat{\sigma}' \chi_\eta^V \bar{x}_d \\ & + r^T (N_d + N_{1B_a}) + (\dot{e}_2 + \alpha_2 e_2)^T N_{1B_b} - (k_1+1) r^T r - \beta_1 r^T sgn(e_2) - r^T e_2 \\ & + \eta^T \tilde{W}^T \dot{\hat{\sigma}}_f + \eta^T \hat{W}^T \hat{\sigma}' \tilde{V}^T \dot{\bar{x}}_{df} - \eta^T N_{2B} + \eta^T \tilde{N}_2 + \eta^T N_{2B} - k_2 \eta^T \eta - \beta_2 \eta^T sgn(\eta) \\ & - r^T (N_{1B_a} + N_d - \beta_1 sgn(e_2)) - \dot{e}_2(t)^T N_{1B_b} + \beta_3 \|e_2\|^2 + \beta_4 \|\eta\|^2 + \beta_2 \eta^T sgn(\eta)) \\ & + \frac{1}{2} r^T \dot{G}^{-1} r - tr(\tilde{W}^T \Gamma_1^{-1} \dot{\hat{W}}) - tr(\tilde{V}^T \Gamma_2^{-1} \dot{\hat{V}}).\end{aligned} \tag{6–84}$$

Canceling the common terms in (6–84), and substituting for N_{1B_b} from (6–65), and using the fact that $a^T b = tr\left(b a^T\right)$, $\dot{V}_L(y,t)$ is expressed as

$$\begin{aligned}\dot{V}_L = {} & e_1^T e_2 - \alpha_1 e_1^T e_1 - \alpha_2 e_2^T e_2 - k_2 \eta^T \eta - r^T \chi_\eta^W \hat{\sigma} - r^T \hat{W}^T \hat{\sigma}' \chi_\eta^V \bar{x}_d + r^T \tilde{N}_1 \\ & - (k_1+1) r^T r + \beta_3 \|e_2\|^2 + \beta_4 \|\eta\|^2 + \eta^T \tilde{N}_2 + tr\left(\alpha_2 \tilde{W}^T \hat{\sigma}' \hat{V}^T \dot{\bar{x}}_d e_2^T\right) + tr\left(\tilde{W}^T \dot{\hat{\sigma}}_f \eta^T\right) \\ & + tr\left(\alpha_2 \tilde{V}^T \dot{\bar{x}}_d (\hat{\sigma}'^T \hat{W} e_2)^T\right) + tr\left(\tilde{V}^T \dot{\bar{x}}_{df} \left(\hat{\sigma}'^T \hat{W} \eta\right)^T\right) - tr(\tilde{W}^T \Gamma_1^{-1} \dot{\hat{W}}) - tr(\tilde{V}^T \Gamma_2^{-1} \dot{\hat{V}}).\end{aligned} \tag{6–85}$$

Substituting the update laws from (6–51) and (6–52) in (6–85), canceling the similar terms, and using the fact that $e_1^T e_2 \leq \frac{1}{2}(\|e_1\|^2 + \|e_2\|^2)$, the expression in (6–85) is upper bounded as

$$\dot{V}_L \leq -\left(\alpha_1 - \frac{1}{2}\right)\|e_1\|^2 - \left(\alpha_2 - \frac{1}{2} - \beta_3\right)\|e_2\|^2 - \|r\|^2 + c_1\|\eta\|\|r\| + \|r\|\left\|\tilde{N}_1\right\| - k_1\|r\|^2 + \|\eta\|\left\|\tilde{N}_2\right\| - (k_2 - \beta_4)\|\eta\|^2$$

where (6–57) was used. Using the squares of the components of $z(t)$, $\dot{V}_L(y,t)$ is upper bounded as

$$\dot{V}_L \leq -\lambda_3\|z\|^2 - k_1\|r\|^2 + \|r\|\left\|\tilde{N}_1\right\| + c_1\|\eta\|\|z\| + \|\eta\|\left\|\tilde{N}_2\right\| - k_2\|\eta\|^2 \tag{6–86}$$

where

$$\lambda_3 \triangleq \min\{\alpha_1 - \frac{1}{2}, \alpha_2 - \frac{1}{2} - \beta_3, 1\}.$$

Letting

$$k_2 = k_{2a} + k_{2b}$$

where k_{2a}, $k_{2b} \in \mathbb{R}$ are positive constants, and using the inequalities in (6–48) and (6–66), the expression in (6–86) is upper bounded as

$$\dot{V}_L \leq -\lambda_3\|z\|^2 - (k_{2b} - \beta_4)\|\eta\|^2 - \left[k_1\|r\|^2 - \rho_1(\|z\|)\|r\|\|z\|\right] - \left[k_{2a}\|\eta\|^2 - (\rho_2(\|z\|) + c_1)\|\eta\|\|z\|\right]. \tag{6–87}$$

Completing the squares for the terms inside the brackets in (6–87) yields

$$\begin{aligned}\dot{V}_L &\leq -\lambda_3\|z\|^2 - (k_{2b} - \beta_4)\|\eta\|^2 + \frac{\rho_1^2(\|z\|)\|z\|^2}{4k_1} + \frac{(\rho_2(\|z\|) + c_1)^2\|z\|^2}{4k_{2a}} \\ &\leq -\lambda_3\|z\|^2 + \frac{\rho^2(\|z\|)\|z\|^2}{4k} - (k_{2b} - \beta_4)\|\eta\|^2 \end{aligned} \tag{6–88}$$

where $k \in \mathbb{R}$ is defined as

$$k \triangleq \min\{k_1, k_{2a}\} \tag{6–89}$$

and $\rho(\cdot) \in \mathbb{R}$ is a positive, globally invertible, nondecreasing function defined as

$$\rho^2(\|z\|) \triangleq \rho_1^2(\|z\|) + (\rho_2(\|z\|) + c_1)^2 .$$

The expression in (6–88) can be further upper bounded by a continuous, positive semi-definite function

$$\dot{V}_L(y,t) \leq -U(y) = -c \left\| \begin{bmatrix} z^T & \eta^T \end{bmatrix}^T \right\|^2 \qquad \forall y \in \mathcal{D} \tag{6–90}$$

for some positive constant $c \in \mathbb{R}$, where

$$\mathcal{D} \triangleq \left\{ y(t) \in \mathbb{R}^{4n+3} \mid \|y\| \leq \rho^{-1}\left(2\sqrt{\lambda_3 k}\right) \right\}.$$

Larger values of k will expand the size of the domain $\mathcal{D}$. The inequalities in (6–81) and (6–90) can be used to show that $V_L(y,t) \in \mathcal{L}_\infty$ in $\mathcal{D}$; hence, $e_1(t)$, $e_2(t)$, $r(t)$, and $\eta(t) \in \mathcal{L}_\infty$ in $\mathcal{D}$. Given that $e_1(t)$, $e_2(t)$, and $r(t) \in \mathcal{L}_\infty$ in $\mathcal{D}$, standard linear analysis methods can be used to prove that $\dot{e}_1(t)$, and $\dot{e}_2(t) \in \mathcal{L}_\infty$ in $\mathcal{D}$ from (6–4) and (6–5). Since $\dot{e}_1(t)$, $\dot{e}_2(t)$, and $r(t) \in \mathcal{L}_\infty$ in $\mathcal{D}$, Assumption 6-3 can be used along with (6–3)-(6–5) to conclude that $x^{(i)}(t) \in \mathcal{L}_\infty$, in $\mathcal{D}$. Since $x^{(i)}(t) \in \mathcal{L}_\infty$, in $\mathcal{D}$, Assumption 6-2 can be used to conclude that $G^{-1}(\cdot)$ and $f(\cdot) \in \mathcal{L}_\infty$ in $\mathcal{D}$. Thus, from (6–1) we can show that $u(t) \in \mathcal{L}_\infty$ in $\mathcal{D}$. Therefore, $u_f(t) \in \mathcal{L}_\infty$ in $\mathcal{D}$, and hence, from (6–20), $\hat{u}_f(t) \in \mathcal{L}_\infty$ in $\mathcal{D}$. Given that $r(t) \in \mathcal{L}_\infty$ in $\mathcal{D}$, (6–59) can be used to show that $\dot{\mu}_1(t) \in \mathcal{L}_\infty$ in $\mathcal{D}$, and since $\dot{G}^{-1}(\cdot)$ and $\dot{f}(\cdot) \in \mathcal{L}_\infty$ in $\mathcal{D}$, (6–58) can be used to show that $\dot{r}(t) \in \mathcal{L}_\infty$ in $\mathcal{D}$, and (6–44) can be used to show that $\dot{\eta}(t) \in \mathcal{L}_\infty$ in $\mathcal{D}$. Since $\dot{e}_1(t)$, $\dot{e}_2(t)$, $\dot{r}(t)$, and $\dot{\eta}(t) \in \mathcal{L}_\infty$ in $\mathcal{D}$, the definitions for $U(y)$ and $z(t)$ can be used to prove that $U(y)$ is uniformly continuous in $\mathcal{D}$.

Let $\mathcal{S} \subset \mathcal{D}$ denote a set defined as

$$\mathcal{S} \triangleq \left\{ y(t) \in \mathcal{D} \mid U_2(y(t)) < \lambda_1 \left(\rho^{-1}\left(2\sqrt{\lambda_3 k}\right) \right)^2 \right\}. \tag{6–91}$$

The region of attraction in (6–91) can be made arbitrarily large to include any initial conditions by increasing the control gain k (i.e., a semi-global stability result). Theorem

8.4 of [63] can now be invoked to state that

$$c \left\| \begin{bmatrix} z^T & \eta^T \end{bmatrix}^T \right\|^2 \to 0 \qquad \text{as} \qquad t \to \infty \qquad \forall y(0) \in \mathcal{S}. \tag{6–92}$$

Based on the definition of $z(t)$, (6–92) can be used to show that

$$\|e_1(t)\| \to 0 \qquad \text{as} \qquad t \to \infty \qquad \forall y(0) \in \mathcal{S}$$
$$\|\eta(t)\| \to 0 \qquad \text{as} \qquad t \to \infty \qquad \forall y(0) \in \mathcal{S}.$$

□

6.6 Experiment

As in Chapter 2, the testbed depicted in Figure 2-1 was used to implement the developed controller. No external friction is applied to the circular disk. The desired link trajectory is selected as follows (in degrees):

$$q_d(t) = 60.0 \sin(3.0t)(1 - \exp(-0.01t^3)). \tag{6–93}$$

For all experiments, the rotor velocity signal is obtained by applying a standard backwards difference algorithm to the position signal. The integral structure for the RISE term in (6–16) was computed on-line via a standard trapezoidal algorithm. The NN input vector $\bar{x}_d(t) \in \mathbb{R}^4$ is defined as

$$\bar{x}_d = \begin{bmatrix} 1 & q_d & \dot{q}_d & \ddot{q}_d \end{bmatrix}^T.$$

The initial values of $\hat{W}(0)$ were chosen to be a zero matrix; however, the initial values of $\hat{V}(0)$ were selected randomly between -1.0 and 1.0 to provide a basis [71]. A different transient response could be obtained if the NN weights are initialized differently. Ten hidden layer neurons were chosen based on trial and error. In addition, all the states were initialized to zero. The following control gains were used to implement the controller in (6–15) in conjunction with the composite adaptive update laws in (6–51) and (6–52), where the prediction error is generated from (6–20), (6–21), (6–37), and (6–38):

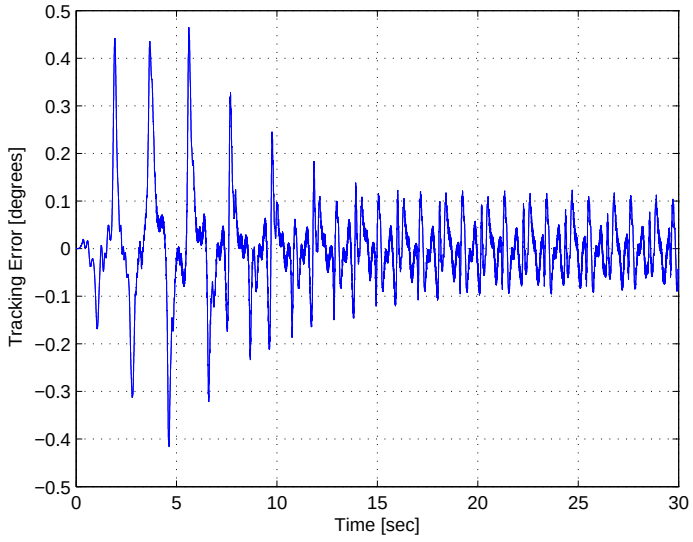

Figure 6-2. Tracking error for the proposed composite adaptive control law (RISE+CNN).

$$k_1 = 30, \quad \beta_1 = 10, \quad \alpha_1 = 10, \quad \alpha_2 = 10, \quad \Gamma_1 = 5I_{11}, \quad \Gamma_2 = 0.05I_4$$
$$k_2 = 30, \quad \beta_2 = 10, \quad \omega = 2. \tag{6–94}$$

6.6.1 Discussion

Three different experiments were conducted to demonstrate the efficacy of the proposed controller. The control gains were chosen to obtain an arbitrary tracking error accuracy (not necessarily the best performance), and for each controller, the gains were not retuned (i.e., the common control gains remain the same for all controllers). First, no adaptation was used and the controller with only the RISE feedback was implemented. For the second experiment, the prediction error component of the update laws in (6–51) and (6–52) was removed, resulting in a standard gradient-based NN update law (hereinafter denoted as RISE+NN). For the third experiment, the proposed composite adaptive controller in (6–15) (hereinafter denoted as RISE+CNN) was implemented. The tracking error and the prediction error are shown in Figure 6-2 and Figure 6-3,

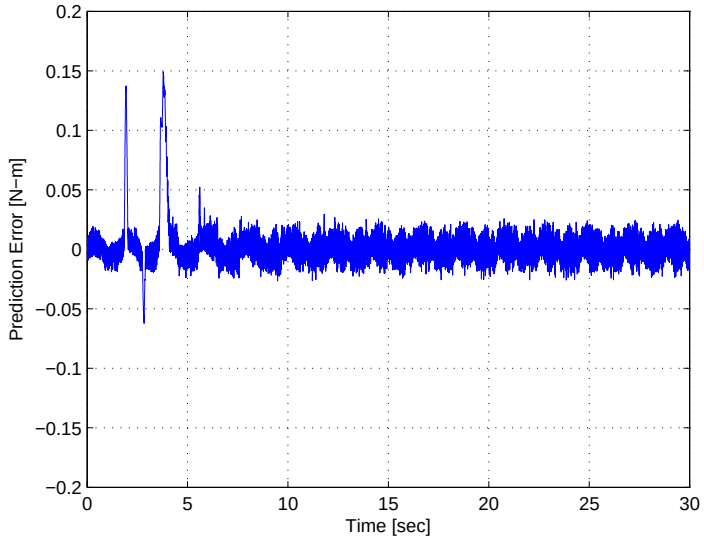

Figure 6-3. Prediction error for the proposed composite adaptive control law (RISE+CNN).

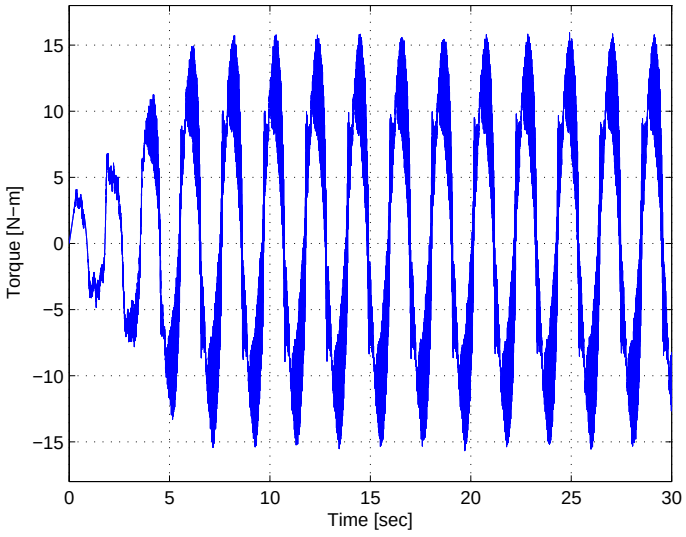

Figure 6-4. Control torque for the proposed composite adaptive control law (RISE+CNN).

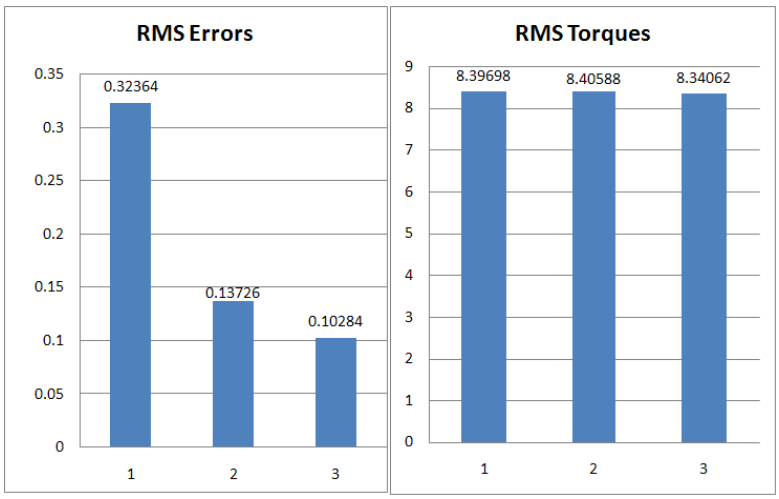

Figure 6-5. Average RMS errors (degrees) and torques (N-m). 1- RISE, 2- RISE+NN, 3- RISE+CNN (proposed).

respectively. The control torque is shown in Figure 6-4. Each experiment was performed five times and the average RMS error and torque values are shown in Figure 6-5, which indicate that the proposed RISE+CNN controller yields the lowest RMS error with a similar control effort.

6.7 Conclusion

A first ever gradient-based composite NN controller is developed for nonlinear uncertain systems. A NN feedforward component is used in conjunction with the RISE feedback, where the NN weight estimates are generated using a composite update law driven by both the tracking and the prediction error with the motivation of using more information in the NN update law. The construction of a NN-based controller to approximate the unknown system dynamics inherently results in a residual function reconstruction error. The presence of the reconstruction error has been the technical obstacle that has prevented the development of composite adaptation laws for NNs. To compensate for the effects of the reconstruction error, the typical prediction error formulation is modified to include a RISE-like structure in the design of the estimated filtered control input. Using a Lyapunov stability analysis, sufficient gain conditions are derived under which the proposed controller yields semi-global asymptotic stability.

Experiments on a rotating disk indicate that the proposed method yields better tracking performance with a similar control effort.

CHAPTER 7
CONCLUSIONS AND FUTURE WORK

7.1 Conclusions

A new class of asymptotic controllers is developed that contains an adaptive feedforward term to account for linear parameterizable uncertainty and a high gain RISE feedback term which accounts for unstructured disturbances. In comparison with previous results that used a similar high gain feedback control structure, new control development was required to include the additional adaptive feedforward term. The motivation for injecting the adaptive feedforward term is that improved tracking performance and reduced control effort result from including more knowledge of the system dynamics in the control structure. This heuristic idea was verified by our experimental results that indicate reduced control effort and reduced RMS tracking errors.

The research further illustrates how a multilayer NN feedforward term can be fused with a RISE feedback term in a continuous controller to achieve semi-global asymptotic tracking. Improved weight tuning laws are presented which guarantee boundedness of NN weights. To blend the NN and RISE methods, several technical challenges were addressed through Lyapunov-based techniques. These challenges include developing adaptive update laws for the NN weight estimates that do not depend on acceleration, and developing new RISE stability analysis methods and sufficient gain conditions to accommodate the incorporation of the NN adaptive updates in the RISE structure. Experimental results are presented that indicate reduced RMS tracking errors.

Further, a RISE-based approach was presented to achieve modularity in the controller/update law for a general class of multi-input systems. Specifically, for systems with structured and unstructured uncertainties, a controller was employed that uses a model-based feedforward adaptive term in conjunction with the RISE feedback term. The adaptive feedforward term was made modular by considering a generic form of the adaptive update law and its corresponding parameter estimate. This generic form

of the update law was used to develop a new closed-loop error system, and the typical RISE stability analysis was modified. New sufficient gain conditions were derived to show asymptotic tracking of the desired link position. The class of RISE-based modular adaptive controllers is then extended to include uncertain dynamic systems that do not satisfy the LP assumption. Specifically, the result allows the NN weight tuning laws to be determined from a developed generic update law (rather than being restricted to a gradient update law). The modular adaptive control development is then applied to Euler-Lagrange dynamic systems. An experimental section is included that illustrates the concept.

In addition, a novel approach for the design of a gradient-based composite adaptive controller was proposed for generic MIMO systems subjected to bounded disturbances. A model-based feedforward adaptive component was used in conjunction with the RISE feedback, where the adaptive estimates were generated using a composite update law driven by both the tracking and prediction error with the motivation of using more information in the adaptive update law. To account for the effects of non-LP disturbances, the typical prediction error formulation was modified to include a second RISE-like term in the estimated filtered control input design. Using a Lyapunov stability analysis, sufficient gain conditions were derived under which the proposed controller yields semi-global asymptotic stability. Experiments on a rotating disk with externally applied friction indicate that the proposed method yields better tracking performance with a similar control effort.

This technique is then extended to develop a first ever gradient-based composite NN controller for nonlinear uncertain systems. A NN feedforward component is used in conjunction with the RISE feedback, where the NN weight estimates are generated using a composite update law driven by both the tracking and the prediction error with the motivation of using more information in the NN update law. The construction of a NN-based controller to approximate the unknown system dynamics inherently results

in a residual function reconstruction error. The presence of the reconstruction error has been the technical obstacle that has prevented the development of composite adaptation laws for NNs. To compensate for the effects of the reconstruction error, the typical prediction error formulation is modified to include a RISE-like structure in the design of the estimated filtered control input. Using a Lyapunov stability analysis, sufficient gain conditions are derived under which the proposed controller yields semi-global asymptotic stability.

7.2 Future Work

- The results in this dissertation, as well as all previous RISE controllers, require full-state feedback. The development of an output feedback result remains an open problem.
- Also, one of the shortcomings of current work is that only a semi-global asymptotic stability is achieved, and further investigation is needed to achieve a global stability result. Inroads to solve the global tracking problem are provided in [78] under a set of assumptions.
- While the modular adaptive result in Chapter 4 encompasses a large variety of adaptive update laws, an update law design based on the prediction error is not possible because the formulation of a prediction error requires the system dynamics to be completely LP. Future efforts can focus on developing a adaptive controller that could also use a prediction error in the modular adaptive update law.
- The composite adaptation presented in Chapters 5 and 6 utilize the gradient-based update laws. Future efforts could focus on developing composite adaptation that use least-squares estimation.

APPENDIX

Lemma 1. *The Mean Value Theorem can be used to develop the upper bound in (2–21)*

$$\left\|\tilde{N}(t)\right\| \leq \rho\left(\|z\|\right)\|z\|$$

where $z(t) \in \mathbb{R}^{3n}$ *is defined as*

$$z(t) \triangleq \left[e_1^T \quad e_2^T \quad r^T\right]^T. \tag{A–1}$$

Proof: The auxiliary error $\tilde{N}(t)$ in (2–18) can be written as the sum of errors pertaining to each of its arguments as follows:

$$\begin{aligned}
\tilde{N}(t) &= N\left(q, \dot{q}, \ddot{q}_d, \dddot{q}_d, e_1, e_2, r\right) - N\left(q_d, \dot{q}_d, \ddot{q}_d, \dddot{q}_d, 0, 0, 0\right) \\
&= N\left(q, \dot{q}_d, \ddot{q}_d, \dddot{q}_d, 0, 0, 0\right) - N\left(q_d, \dot{q}_d, \ddot{q}_d, \dddot{q}_d, 0, 0, 0\right) \\
&+ N\left(q, \dot{q}, \ddot{q}_d, \dddot{q}_d, 0, 0, 0\right) - N\left(q, \dot{q}_d, \ddot{q}_d, \dddot{q}_d, 0, 0, 0\right) \\
&+ N\left(q, \dot{q}, \ddot{q}_d, \dddot{q}_d, 0, 0, 0\right) - N\left(q, \dot{q}, \ddot{q}_d, \dddot{q}_d, 0, 0, 0\right) \\
&+ N\left(q, \dot{q}, \ddot{q}_d, \dddot{q}_d, 0, 0, 0\right) - N\left(q, \dot{q}, \ddot{q}_d, \dddot{q}_d, 0, 0, 0\right) \\
&+ N\left(q, \dot{q}, \ddot{q}_d, \dddot{q}_d, e_1, 0, 0\right) - N\left(q, \dot{q}, \ddot{q}_d, \dddot{q}_d, 0, 0, 0\right) \\
&+ N\left(q, \dot{q}, \ddot{q}_d, \dddot{q}_d, e_1, e_2, 0\right) - N\left(q, \dot{q}, \ddot{q}_d, \dddot{q}_d, e_1, 0, 0\right) \\
&+ N\left(q, \dot{q}, \ddot{q}_d, \dddot{q}_d, e_1, e_2, r\right) - N\left(q, \dot{q}, \ddot{q}_d, \dddot{q}_d, e_1, e_2, 0\right).
\end{aligned}$$

Applying the Mean Value Theorem to further describe $\tilde{N}(t)$,

$$\begin{aligned}
\tilde{N}(t) = &\frac{\partial N(\sigma_1, \dot{q}_d, \ddot{q}_d, \dddot{q}_d, 0, 0, 0)}{\partial \sigma_1}\Big|_{\sigma_1 = v_1}(q - q_d) + \frac{\partial N(q, \sigma_2, \ddot{q}_d, \dddot{q}_d, 0, 0, 0)}{\partial \sigma_2}\Big|_{\sigma_2 = v_2}(\dot{q} - \dot{q}_d) \\
&+ \frac{\partial N(q, \dot{q}, \sigma_3, \dddot{q}_d, 0, 0, 0)}{\partial \sigma_3}\Big|_{\sigma_3 = v_3}(\ddot{q}_d - \ddot{q}_d) + \frac{\partial N(q, \dot{q}, \ddot{q}_d, \sigma_4, 0, 0, 0)}{\partial \sigma_4}\Big|_{\sigma_4 = v_4}(\dddot{q}_d - \dddot{q}_d) \\
&+ \frac{\partial N(q, \dot{q}, \ddot{q}_d, \dddot{q}_d, \sigma_5, 0, 0)}{\partial \sigma_5}\Big|_{\sigma_5 = v_5}(e_1 - 0) + \frac{\partial N(q, \dot{q}, \ddot{q}_d, \dddot{q}_d, e_1, \sigma_6, 0)}{\partial \sigma_6}\Big|_{\sigma_6 = v_6}(e_2 - 0) \\
&+ \frac{\partial N(q, \dot{q}, \ddot{q}_d, \dddot{q}_d, e_1, e_2, \sigma_7)}{\partial \sigma_7}\Big|_{\sigma_7 = v_7}(r - 0)
\end{aligned} \tag{A–2}$$

where

$$v_1 \in (q_d, q)\,, \quad v_2 \in (\dot{q}_d, \dot{q})\,, \; v_3 \in (\ddot{q}_d, \ddot{q}_d)\,, \quad v_4 \in (\dddot{q}_d, \dddot{q}_d)\,, \quad v_5 \in (0, e_1)\,,$$
$$v_6 \in (0, e_2)\,, \quad v_7 \in (0, r)\,.$$

From equation (A–2), $\tilde{N}(t)$ can be upper bounded as follows:

$$\begin{aligned}\left\|\tilde{N}(t)\right\| \leq & \left\|\frac{\partial N(\sigma_1, \dot{q}_d, \ddot{q}_d, \dddot{q}_d, 0, 0, 0)}{\partial \sigma_1}|_{\sigma_1 = v_1}\right\| \|e_1\| \\ & + \left\|\frac{\partial N(q, \sigma_2, \ddot{q}_d, \dddot{q}_d, 0, 0, 0)}{\partial \sigma_2}|_{\sigma_2 = v_2}\right\| \|e_2 - a_1 e_1\| \\ & + \left\|\frac{\partial N(q, \dot{q}, \ddot{q}_d, \dddot{q}_d, \sigma_5, 0, 0)}{\partial \sigma_5}|_{\sigma_5 = v_5}\right\| \|e_1\| \\ & + \left\|\frac{\partial N(q, \dot{q}, \ddot{q}_d, \dddot{q}_d, e_1, \sigma_6, 0)}{\partial \sigma_6}|_{\sigma_6 = v_6}\right\| \|e_2\| \\ & + \left\|\frac{\partial N(q, \dot{q}, \ddot{q}_d, \dddot{q}_d, e_1, e_2, \sigma_7)}{\partial \sigma_7}|_{\sigma_7 = v_7}\right\| \|r\|\,.\end{aligned} \tag{A–3}$$

By noting that

$$v_1 = q - c_1\,(q - q_d)\,, \quad v_2 = \dot{q} - c_2\,(\dot{q} - \dot{q}_d)\,, \quad v_5 = e_1\,(1 - c_5)\,, \quad v_6 = e_2\,(1 - c_6)\,,$$
$$v_7 = r\,(1 - c_7)$$

where $c_i \in (0, 1) \in \mathbb{R}$, $i = 1, 2, 5, 6, 7$ are unknown constants, we can upper bound the partial derivatives as follows:

$$\begin{aligned}\left\|\frac{\partial N(\sigma_1, \dot{q}_d, \ddot{q}_d, \dddot{q}_d, 0, 0, 0)}{\partial \sigma_1}|_{\sigma_1 = v_1}\right\| &\leq \rho_1(e_1) \\ \left\|\frac{\partial N(q, \sigma_2, \ddot{q}_d, \dddot{q}_d, 0, 0, 0)}{\partial \sigma_2}|_{\sigma_2 = v_2}\right\| &\leq \rho_2(e_1, e_2) \\ \left\|\frac{\partial N(q, \dot{q}, \ddot{q}_d, \dddot{q}_d, \sigma_5, 0, 0)}{\partial \sigma_5}|_{\sigma_5 = v_5}\right\| &\leq \rho_5(e_1, e_2) \\ \left\|\frac{\partial N(q, \dot{q}, \ddot{q}_d, \dddot{q}_d, e_1, \sigma_6, 0)}{\partial \sigma_6}|_{\sigma_6 = v_6}\right\| &\leq \rho_6(e_1, e_2) \\ \left\|\frac{\partial N(q, \dot{q}, \ddot{q}_d, \dddot{q}_d, e_1, e_2, \sigma_7)}{\partial \sigma_7}|_{\sigma_7 = v_7}\right\| &\leq \rho_7(e_1, e_2, r).\end{aligned}$$

The bound on $\tilde{N}(t)$ can be further simplified:

$$\left\|\tilde{N}(t)\right\| \leq \rho_1(e_1)\|e_1\| + \rho_2(e_1,e_2)\|e_2 - \alpha_1 e_1\| + \rho_5(e_1,e_2)\|e_1\| + \rho_6(e_1,e_2)\|e_2\| + \rho_7(e_1,e_2,r)\|r\|.$$

Using the upper bound

$$\|e_2 - \alpha_1 e_1\| \leq \|e_2\| + \alpha_1\|e_1\|.$$

$\tilde{N}(t)$ can be further upper bounded as follows:

$$\left\|\tilde{N}(t)\right\| \leq (\rho_1(e_1) + \alpha_1\rho_2(e_1,e_2) + \rho_5(e_1,e_2))\|e_1\| + (\rho_2(e_1,e_2) + \rho_6(e_1,e_2))\|e_2\| + \rho_7(e_1,e_2,r)\|r\|.$$

Using the definition of $z(t) \in \mathbb{R}^{3n}$ in (A–1), $\tilde{N}(t)$ can be expressed in terms of $z(t)$ as follows:

$$\begin{aligned}\left\|\tilde{N}(t)\right\| &\leq (\rho_1(e_1) + \alpha_1\rho_2(e_1,e_2) + \rho_5(e_1,e_2))\|z(t)\| + (\rho_2(e_1,e_2) + \rho_6(e_1,e_2))\|z(t)\| \\ &\quad + \rho_7(e_1,e_2,r)\|z(t)\| \\ &\leq (\rho_1(e_1) + \alpha_1\rho_2(e_1,e_2) + \rho_5(e_1,e_2) + \rho_2(e_1,e_2) + \rho_6(e_1,e_2) + \rho_7(e_1,e_2,r))\|z(t)\|.\end{aligned}$$

Therefore,

$$\left\|\tilde{N}(t)\right\| \leq \rho(\|z\|)\|z\|$$

where $\rho(\|z\|)$ is some positive globally invertible nondecreasing function. □

Lemma 2. *Let the function $L(t) \in \mathbb{R}$ be defined as*

$$L(t) \triangleq r^T(N_B(t) - \beta_1 sgn(e_m)) - \sum_{i=1}^{m}\beta_{i+1}\|e_i(t)\|\|e_m(t)\| - \beta_{m+2}\|e_m(t)\|\|r(t)\|. \quad \text{(A–4)}$$

If the following sufficient conditions are satisfied:

$$\beta_1 > \zeta_1 + \frac{1}{\alpha_m}\zeta_2 + \frac{1}{\alpha_m}\zeta_3 \quad \text{(A–5)}$$

$$\beta_{i+1} > \zeta_{i+3},\ i = 1,2,...,m+1,$$

then

$$\int_0^t L(\tau)d\tau \leq \beta_1 \sum_{i=1}^{n} |e_{mi}(0)| - e_m(0)^T N_B(0). \tag{A–6}$$

Proof: Integrating both sides of the equation in (A–6)

$$\int_0^t L(\tau)d\tau = \int_0^t (r(\tau)^T (N_B(\tau) - \beta_1 sgn(e_m(\tau)) - \sum_{i=1}^{m} \beta_{i+1} \|e_i(\tau)\| \|e_m(\tau)\| \tag{A–7}$$
$$- \beta_{m+2} \|e_m(\tau)\| \|r(\tau)\|)d\tau.$$

Substituting (4–6) into (A–7),

$$\begin{aligned}\int_0^t L(\tau)d\tau = &\int_0^t \frac{de_m(\tau)}{d\tau}^T N_B(\tau)d\tau + \int_0^t \alpha_m e_m(\tau)^T (N_B(\tau) - \beta_1 sgn(e_m(\tau)))d\tau \\ &- \int_0^t \frac{de_m(\tau)}{d\tau}^T \beta_1 sgn(e_m(\tau))d\tau - \int_0^t \sum_{i=1}^{m} \beta_{i+1} \|e_i(\tau)\| \|e_m(\tau)\| \, d\tau \\ &- \int_0^t \beta_{m+2} \|e_m(\tau)\| \|r(\tau)\| \, d\tau.\end{aligned} \tag{A–8}$$

Integrating the first integral in (A–8) by parts yields

$$\begin{aligned}\int_0^t L(\tau)d\tau = &\, e_m(\tau)^T N_B(\tau)\Big|_0^t - \int_0^t e_m(\tau)^T \frac{dN_B(\tau)}{d\tau} d\tau \\ &+ \int_0^t \alpha_m e_m(\tau)^T (N_B(\tau) - \beta_1 sgn(e_m(\tau)))d\tau \\ &- \int_0^t \frac{de_m(\tau)}{d\tau}^T \beta_1 sgn(e_m(\tau))d\tau - \int_0^t \sum_{i=1}^{m} \beta_{i+1} \|e_i(\tau)\| \|e_m(\tau)\| \, d\tau \\ &- \int_0^t \beta_{m+2} \|e_m(\tau)\| \|r(\tau)\| \, d\tau.\end{aligned} \tag{A–9}$$

By using the fact that

$$\frac{dN_B(\tau)}{d\tau} = \frac{d\left(N_{B_1}(\tau) + N_{B_2}(\tau)\right)}{d\tau} = \frac{dN_{B_1}(\tau)}{d\tau} + \frac{dN_{B_2}(\tau)}{d\tau},$$

the expression in (A–9) is rewritten as

$$\int_0^t L(\tau)d\tau = \int_0^t \alpha_m e_m(\tau)^T (N_B(\tau) - \frac{1}{\alpha_m}\frac{dN_{B_1}(\tau)}{d\tau} - \beta_1 sgn(e_m(\tau)))d\tau \tag{A–10}$$
$$- \int_0^t e_m(\tau)^T \frac{dN_{B_2}(\tau)}{d\tau}d\tau - \int_0^t \sum_{i=1}^{m} \beta_{i+1} \|e_i(\tau)\| \|e_m(\tau)\| d\tau$$
$$- \int_0^t \beta_{m+2} \|e_m(\tau)\| \|r(\tau)\| d\tau - \beta_1 \sum_{i=1}^{n} |e_{mi}(t)| + \beta_1 \sum_{i=1}^{n} |e_{mi}(0)|$$
$$+ e_m(t)^T N_B(t) - e_m(0)^T N_B(0).$$

Rearranging terms in (A–10), yields

$$\int_0^t L(\tau)d\tau \leq \int_0^t \alpha_m \|e_m(\tau)\| (\|N_B(\tau)\| + \frac{1}{\alpha_m}\left\|\frac{dN_{B_1}(\tau)}{d\tau}\right\| - \beta_1)d\tau$$
$$+ \int_0^t \|e_m(\tau)\| \left\|\frac{dN_{B_2}(\tau)}{d\tau}\right\| d\tau - \int_0^t \sum_{i=1}^{m} \beta_{i+1} \|e_i(\tau)\| \|e_m(\tau)\| d\tau - \int_0^t \beta_{m+2} \|e_m(\tau)\| \|r(\tau)\| d\tau \tag{A–11}$$
$$- \beta_1 \|e_m(t)\| + \beta_1 \sum_{i=1}^{n} |e_{mi}(0)| + \|e_m(t)\| \|N_B(t)\| - e_m(0)^T N_B(0)$$

where the fact that

$$\sum_{i=1}^{n} |e_{mi}(t)| \geq \|e_m(t)\|$$

was used. Using the inequalities (4–31) in (A–11) yields

$$\int_0^t L(\tau)d\tau \leq \int_0^t \alpha_m \|e_m(\tau)\| (\zeta_1 + \frac{1}{\alpha_m}\zeta_2 + \frac{1}{\alpha_m}\zeta_3 - \beta_1)d\tau \tag{A–12}$$
$$+ \int_0^t \|e_m(\tau)\| (\sum_{i=1}^{m} \|e_i(\tau)\| (\zeta_{i+3} - \beta_{i+1}))d\tau + \int_0^t \|e_m(\tau)\| \|r(\tau)\| (\zeta_{m+4} - \beta_{m+2})d\tau$$
$$+ \|e_m(t)\| (\zeta_1 - \beta_1) + \beta_1 \sum_{i=1}^{n} |e_{mi}(0)| - e_m(0)^T N_B(0).$$

From (A–12), if the sufficient conditions in (A–5) are satisfied, then (A–6) holds. □

Lemma 3. *The regions Λ_V and Λ_W defined in (3–9) and (3–11), respectively, are convex [83].*

Proof: Let $vec\,(V_1)$ and $vec\,(V_2) \in \Lambda_V$, therefore $vec\,(V_1)^T\, vec\,(V_1) \leq \bar{V}_B$ and $vec\,(V_2)^T\, vec\,(V_2) \leq \bar{V}_B$.

Consider

$$vec\,(V) = \lambda vec\,(V_1) + (1-\lambda)\, vec\,(V_2)\,, \quad \lambda \in [0,1]\,. \tag{A–13}$$

Taking the transpose of (A–13) and multiplying by itself yields

$$\begin{aligned} vec\,(V)^T\, vec\,(V) = \lambda^2 vec\,(V_1)^T\, vec\,(V_1) + (1-\lambda)^2\, vec\,(V_2)^T\, vec\,(V_2) \\ + 2\lambda\,(1-\lambda)\, vec\,(V_1)^T\, vec\,(V_2)\,. \end{aligned}$$

Using (3–7), the following inequality can be developed:

$$\begin{aligned} vec\,(V)^T\, vec\,(V) &\leq \lambda^2 \bar{V}_B + (1-\lambda)^2\, \bar{V}_B + 2\lambda\,(1-\lambda)\, \bar{V}_B \\ &\leq \bar{V}_B. \end{aligned}$$

Therefore, Λ_V is convex. The convexity of Λ_W follows the same development. □

Lemma 4. *Given the composite NN and RISE controller in (3–17)-(3–21), if* $vec(\hat{W}\,(0)) \in int\,(\Lambda_W)$ *and* $vec(\hat{V}\,(0)) \in int\,(\Lambda_V)$*, then* $\hat{W}\,(t)$ *and* $\hat{V}\,(t)$ *never leave the regions* Λ_W *and* Λ_V *described in Assumption 3-2, respectively, and an upper bound for the expression given in (3–51) can be formulated as follows*

$$\begin{aligned} \dot{V}_L(y,t) \leq r^T \tilde{N}(t) - (k_s+1)\, \|r\|^2 \\ - (2\alpha_1 - 1)\, \|e_1\|^2 - (\alpha_2 - \beta_2 - 1)\, \|e_2\|^2\,. \end{aligned} \tag{A–14}$$

Proof: The following nine cases must be considered (see Appendix B.3.2 of [70]).

Case 1: $vec(\hat{W}\,(t)) \in int\,(\Lambda_W)$, $vec(\hat{V}\,(t)) \in int\,(\Lambda_V)$

In this case, (3–51) can be expressed as

$$\begin{aligned} \dot{V}_L(y,t) = -2\alpha_1\, \|e_1\|^2 + 2e_2^T e_1 + r^T \tilde{N}(t) - (k_s+1)\, \|r\|^2 - \alpha_2\, \|e_2\|^2 + \beta_2\, \|e_2\|^2 \\ + \alpha_2 e_2^T \left[\tilde{W}^T\,(\hat{\sigma}) + \hat{W}^T \hat{\sigma}'\, \tilde{V}^T x_d\right] - tr(\alpha_2 \tilde{W}^T \hat{\sigma} e_2^T) - tr(\alpha_2 \tilde{V}^T x_d (\hat{\sigma}'^T \hat{W} e_2)^T), \end{aligned} \tag{A–15}$$

Based on the fact that

$$a^T b = tr\left(ba^T\right) \qquad \forall\ a, b \in \mathbb{R}^n$$

(A–15) can be reduced to (A–14). In addition, the direction in which the estimates $vec(\hat{W})$ and $vec(\hat{V})$ are updated for Case 1 is irrelevant, since the worst case scenario is that $vec(\hat{W})$ and $vec(\hat{V})$ will move towards the boundaries of the convex regions denoted by $\partial(\Lambda_W)$ and $\partial(\Lambda_V)$, respectively, which is addressed subsequently.

Case 2: $vec(\hat{W}(t)) \in int(\Lambda_W)$,

$vec(\hat{V}) \in \partial(\Lambda_V)$ and $vec(\mu_2)^T vec(\hat{V})^{\perp} \leq 0$

In this case, (3–51) can be expressed as (A–15), which can be reduced to (A–14). In addition, the vector $vec(\mu_2)$ has a zero or nonzero component perpendicular to the boundary $\partial(\Lambda_V)$ at $vec(\hat{V})$ that points in the direction towards the $int(\Lambda_V)$. Geometrically, this means that $vec(\hat{V})$ is updated such that it either moves towards the $int(\Lambda_V)$ or remains on the boundary. Hence, $vec(\hat{V})$ never leaves Λ_V.

Case 3: $vec(\hat{W}(t)) \in int(\Lambda_W)$,

$vec(\hat{V}) \in \partial(\Lambda_V)$ and $vec(\mu_2)^T vec(\hat{V})^{\perp} > 0$

$$\begin{aligned}\dot{V}_L(y,t) = &-2\alpha_1 \|e_1\|^2 + 2e_2^T e_1 + r^T \tilde{N}(t) - (k_s+1)\|r\|^2 - \alpha_2 \|e_2\|^2 + \beta_2 \|e_2\|^2 \\ &+ \alpha_2 e_2^T \left[\tilde{W}^T(\hat{\sigma}) + \hat{W}^T \hat{\sigma}' \tilde{V}^T x_d\right] - tr\left(\alpha_2 \tilde{W}^T \hat{\sigma} e_2^T\right) \\ &- tr\left(\alpha_2 \tilde{V}^T \Gamma_2^{-1} devec\left(P_r^t(vec(\mu_2))\right)\right),\end{aligned}$$

$$\begin{aligned}\dot{V}_L(y,t) = &-2\alpha_1 \|e_1\|^2 + 2e_2^T e_1 + r^T \tilde{N}(t) - (k_s+1)\|r\|^2 - \alpha_2 \|e_2\|^2 + \beta_2 \|e_2\|^2 \\ &+ tr\left(\alpha_2 \tilde{V}^T \Gamma_2^{-1} \mu_2\right) - tr\left(\alpha_2 \tilde{V}^T \Gamma_2^{-1} devec\left(P_r^t(vec(\mu_2))\right)\right),\end{aligned}$$

$$\begin{aligned}\dot{V}_L(y,t) = &-2\alpha_1 \|e_1\|^2 + 2e_2^T e_1 + r^T \tilde{N}(t) - (k_s+1)\|r\|^2 - \alpha_2 \|e_2\|^2 + \beta_2 \|e_2\|^2 \\ &+ tr\left(\alpha_2 \tilde{V}^T \Gamma_2^{-1}\left(\mu_2 - devec\left(P_r^t(vec(\mu_2))\right)\right)\right),\end{aligned}$$

Using (3–10), we get

$$\dot{V}_L(y,t) = -2\alpha_1 \|e_1\|^2 + 2e_2^T e_1 + r^T \tilde{N}(t) - (k_s+1)\|r\|^2 - \alpha_2 \|e_2\|^2 + \beta_2 \|e_2\|^2 + tr\left(\alpha_2 \tilde{V}^T \Gamma_2^{-1}\left(devec\left(P_r^{\perp}\left(vec\left(\mu_2\right)\right)\right)\right)\right),$$

$$\begin{aligned}\dot{V}_L(y,t) = &-2\alpha_1 \|e_1\|^2 + 2e_2^T e_1 + r^T \tilde{N}(t) \\ &- (k_s+1)\|r\|^2 - \alpha_2 \|e_2\|^2 + \beta_2 \|e_2\|^2 \\ &+ \alpha_2 vec(\tilde{V})^T diag\left\{\Gamma_2^{-1}, \Gamma_2^{-1}, ...N_2 \text{ times}\right\} \\ &\times P_r^{\perp}\left(vec\left(\mu_2\right)\right),\end{aligned} \tag{A–16}$$

where N_2 was described in (3–4). Because $vec(\hat{V}) \in \partial\left(\Lambda_V\right)$, and $vec\left(V\right)$ must lie either on the boundary or in the interior of Λ_V, then the convexity of Λ_V implies that $vec(\tilde{V})$ will either point tangent to $\partial\left(\Lambda_V\right)$ or towards $int\left(\Lambda_V\right)$. That is, $vec(\tilde{V})$ will have a component in the direction of $vec(\hat{V})^{\perp}$ that is either zero or negative. In addition, since $P_r^{\perp}\left(vec\left(\mu_2\right)\right)$ points away from $int\left(\Lambda_V\right)$, the following inequality can be determined

$$\alpha_2 vec(\tilde{V})^T diag\left\{\Gamma_2^{-1}, \Gamma_2^{-1}, ...N_2 \text{ times}\right\} \times P_r^{\perp}\left(vec\left(\mu_2\right)\right) \leq 0 \tag{A–17}$$

The inequality given in (A–17) can now be used to simplify the expression given in (A–16) as (A–14). Furthermore, since $\dot{\hat{V}} = devec\left(P_r^t\left(vec\left(\mu_2\right)\right)\right)$, the parameter estimate $vec(\hat{V})$ is ensured to be updated such that it moves tangent to $\partial\left(\Lambda_V\right)$. Hence, $vec(\hat{V})$ never leaves Λ_V.

Case 4: $vec(\hat{W}) \in \partial\left(\Lambda_W\right)$ and $vec\left(\mu_1\right)^T vec(\hat{W})^{\perp} \leq 0$, $vec(\hat{V}) \in int\left(\Lambda_V\right)$

Similar to Case 2.

Case 5: $vec(\hat{W}) \in \partial\left(\Lambda_W\right)$ and $vec\left(\mu_1\right)^T vec(\hat{W})^{\perp} > 0$, $vec(\hat{V}) \in int\left(\Lambda_V\right)$

Similar to Case 3.

Case 6: $vec(\hat{W}) \in \partial\left(\Lambda_W\right)$ and $vec\left(\mu_1\right)^T vec(\hat{W})^{\perp} \leq 0$,
$vec(\hat{V}) \in \partial\left(\Lambda_V\right)$ and $vec\left(\mu_2\right)^T vec(\hat{V})^{\perp} \leq 0$

Similar to Case 2.

Case 7: $vec(\hat{W}) \in \partial(\Lambda_W)$ and $vec(\mu_1)^T vec(\hat{W})^{\perp} > 0$,

$vec(\hat{V}) \in \partial(\Lambda_V)$ and $vec(\mu_2)^T vec(\hat{V})^{\perp} \leq 0$

Similar to the arguments in Case 2 and Case 3.

Case 8: $vec(\hat{W}) \in \partial(\Lambda_W)$ and $vec(\mu_1)^T vec(\hat{W})^{\perp} \leq 0$,

$vec(\hat{V}) \in \partial(\Lambda_V)$ and $vec(\mu_2)^T vec(\hat{V})^{\perp} > 0$

Similar to Case 2 and Case 3.

Case 9: $vec(\hat{W}) \in \partial(\Lambda_W)$ and $vec(\mu_1)^T vec(\hat{W})^{\perp} > 0$,

$vec(\hat{V}) \in \partial(\Lambda_V)$ and $vec(\mu_2)^T vec(\hat{V})^{\perp} > 0$

Similar to Case 3. □

Lemma 5. *Proof of the decomposition in (6–55) and the inequalities in (6–56)*

Proof: The smooth projection used in (6–51) is of the form

$$\dot{\hat{W}} \triangleq proj(\varrho_1) = \begin{cases} \varrho_1 & \text{if } vec(\hat{W}) \in int(\Lambda_W) \\ \varrho_1 & \text{if } vec(\hat{W}) \in \partial(\Lambda_W) \text{ and } vec(\varrho_1)^T vec(\hat{W})^{\perp} \leq 0 \\ P^t_{Mr}(\varrho_1) & \text{if } vec(\hat{W}) \in \partial(\Lambda_W) \text{ and } vec(\varrho_1)^T vec(\hat{W})^{\perp} > 0 \end{cases}$$

where

$$\varrho_1 = \Gamma_1 \alpha_2 \hat{\sigma}' \hat{V}^T \dot{\bar{x}}_d e_2^T + \Gamma_1 \dot{\hat{\sigma}}_f \eta^T.$$

For the first two cases of the projection, we have $proj(\varrho_1) = \varrho_1$, and therefore,

$$\dot{\hat{W}} = \chi_\eta^W + \chi_{e_2}^W$$

such that

$$\chi_\eta^W = \Gamma_1 \dot{\hat{\sigma}}_f \eta^T, \qquad \chi_{e_2}^W = \Gamma_1 \alpha_2 \hat{\sigma}' \hat{V}^T \dot{\bar{x}}_d e_2^T$$

which using the fact that the NN weight estimates and input vector are bounded, can be upper bounded as

$$\left\| \chi_\eta^W \right\| \leq b_1 \|\eta\|, \qquad \left\| \chi_{e_2}^W \right\| \leq b_2 \|e_2\|.$$

For the third case of the projection, we have

$$\dot{\hat{W}} = P_{Mr}^{t}\left(\Gamma_1\alpha_2\hat{\sigma}'\hat{V}^T\dot{\bar{x}}_d e_2^T + \Gamma_1\dot{\hat{\sigma}}_f\eta^T\right).$$

Since the tangential component of the sum is the same as the sum of the tangential components, we get

$$\dot{\hat{W}} = P_{Mr}^{t}\left(\Gamma_1\alpha_2\hat{\sigma}'\hat{V}^T\dot{\bar{x}}_d e_2^T\right) + P_{Mr}^{t}\left(\Gamma_1\dot{\hat{\sigma}}_f\eta^T\right).$$

Therefore, choose

$$\chi_\eta^W = P_{Mr}^{t}\left(\Gamma_1\dot{\hat{\sigma}}_f\eta^T\right), \qquad \chi_{e_2}^W = P_{Mr}^{t}\left(\Gamma_1\alpha_2\hat{\sigma}'\hat{V}^T\dot{\bar{x}}_d e_2^T\right)$$

and the following inequalities hold

$$\left\|\chi_\eta^W\right\| \leq b_1\left\|\eta\right\|, \qquad \left\|\chi_{e_2}^W\right\| \leq b_2\left\|e_2\right\|.$$

□

REFERENCES

[1] M. Krstic, I. Kanellakopoulos, and P. Kokotovic, *Nonlinear and Adaptive Control Design*. New York: Wiley, 1995.

[2] S. Sastry and M. Bodson, *Adaptive Control: Stability, Convergence, and Robustness*. Upper Saddle River, NJ: Prentice-Hall, 1989.

[3] J. J. Slotine and W. Li, *Applied Nonlinear Control*. Upper Saddle River: Prentice-Hall, 1991.

[4] W. Lin and C. Qian, "Adaptive control of nonlinearly parameterized systems: a nonsmooth feedback framework," *IEEE Trans. Automat. Contr.*, vol. 47, no. 5, pp. 757–774, May 2002.

[5] R. Antsaklis and K. Passino, *An Introduction to Intelligent and Autonomous Control*. Kluwer Academic Publishers, 1993.

[6] R. Longman, "Iterative learning control and repetitive control for engineering practice," *Int. J. Control*, vol. 73, no. 10, pp. 930–954, 2000.

[7] R. Horowitz, "Learning control of robot manipulators," *Trans. ASME J. Dyn. Systems Measurement and Control*, vol. 115, pp. 402–402, 1993.

[8] Z. Ding, "Output regulation of uncertain nonlinear systems with nonlinear exosystems," *IEEE Trans. Automat. Contr.*, vol. 51, no. 3, pp. 498–503, 2006.

[9] L. Hunt, G. Meyer, and R. Su, "Noncausal inverses for linear systems," *IEEE Trans. Automat. Contr.*, vol. 41, no. 4, pp. 608–611, 1996.

[10] R. Marino and P. Tomei, "Robust adaptive regulation of linear time-varying systems," *IEEE Trans. Automat. Contr.*, vol. 45, no. 7, pp. 1301–1311, 2000.

[11] A. Serrani and A. Isidori, "Semiglobal nonlinear output regulation with adaptive internal model," in *Proc. IEEE Conf. on Decision and Control*, vol. 2, 2000, pp. 1649–1654.

[12] V. I. Utkin, *Sliding Modes in Control and Optimization*. New York: Springer-Verlag, 1992.

[13] Z. Qu, *Robust Control of Nonlinear Uncertain Systems*. Wiley Inc., New-York, 1998.

[14] S. Ge, T. Lee, and C. Harris, *Adaptive neural network control of robotic manipulators*. World Scientific, 1998.

[15] F. Lewis, J. Campos, and R. Selmic, *Neuro-Fuzzy Control of Industrial Systems with Actuator Nonlinearities*. SIAM, PA, 2002.

[16] C. Lin and C. Lee, "Neural-network-based fuzzy logic control and decision system," *IEEE Tran. on computers*, vol. 40, no. 12, pp. 1320–1336, 1991.

[17] W. Miller III, R. Sutton, and P. Werbos, *Neural networks for control*, 1990.

[18] L. Wang, *A course in fuzzy systems and control*. Prentice-Hall, Inc. Upper Saddle River, NJ, USA, 1996.

[19] P. M. Patre, W. MacKunis, C. Makkar, and W. E. Dixon, "Asymptotic tracking for systems with structured and unstructured uncertainties," *IEEE Trans. Contr. Syst. Technol.*, vol. 16, no. 2, pp. 373–379, 2008.

[20] ——, "Asymptotic tracking for systems with structured and unstructured uncertainties," in *Proc. IEEE Conf. on Decision and Control*, San Diego, CA, 2006, pp. 441–446.

[21] Z. Qu and J. Xu, "Model-based learning controls and their comparisons using Lyapunov direct method," *Asian Journal of Control*, vol. 4, no. 1, pp. 99–110, Mar. 2002.

[22] B. Xian, D. M. Dawson, M. S. de Queiroz, and J. Chen, "A continuous asymptotic tracking control strategy for uncertain nonlinear systems," *IEEE Trans. Automat. Contr.*, vol. 49, no. 7, pp. 1206–1211, Jul. 2004.

[23] Z. Cai, M. S. de Queiroz, and D. M. Dawson, "Robust adaptive asymptotic tracking of nonlinear systems with additive disturbance," *IEEE Trans. Automat. Contr.*, vol. 51, pp. 524–529, 2006.

[24] B. Xian, M. S. de Queiroz, D. M. Dawson, and M. McIntyre, "A discontinuous output feedback controller and velocity observer for nonlinear mechanical systems," *Automatica*, vol. 40, pp. 695–700, 2004.

[25] X. Zhang, A. Behal, D. M. Dawson, and B. Xian, "Output feedback control for a class of uncertain MIMO nonlinear systems with non-symmetric input gain matrix," in *Proc. IEEE Conf. on Decision and Control, and the European Control Conf.*, Spain, 2005, pp. 7762–7767.

[26] C. Makkar, G. Hu, W. G. Sawyer, and W. E. Dixon, "Lyapunov-based tracking control in the presence of uncertain nonlinear parameterizable friction," *IEEE Trans. Automat. Contr.*, vol. 52, no. 10, pp. 1988–1994, 2007.

[27] W. E. Dixon, Y. Fang, D. M. Dawson, and T. J. Flynn, "Range identification for perspective vision systems," *IEEE Trans. Automat. Contr.*, vol. 48, no. 12, pp. 2232–2238, Dec. 2003.

[28] S. Gupta, D. Aiken, G. Hu, and W. E. Dixon, "Lyapunov-based range and motion identification for a nonaffine perspective dynamic system," in *Proc. IEEE Amer. Control Conf.*, Minneapolis, MN, 2006, pp. 4471–4476.

[29] M. L. McIntyre, W. E. Dixon, D. M. Dawson, and I. D. Walker, "Fault identification for robot manipulators," *IEEE Trans. Robot.*, vol. 21, pp. 1028–1034, 2005.

[30] K. Hornik, M. Stinchcombe, and H. White, "Multilayer feedforward networks are universal approximators," *Neural Networks*, vol. 2, pp. 359–366, 1985.

[31] F. Lewis, K. Liu, and A. Yesildirek, "Neural net robot controller with guaranteed tracking performance," *IEEE Trans. Neural Networks*, vol. 6, no. 3, pp. 703–715, 1995.

[32] F. L. Lewis, "Nonlinear network structures for feedback control," *Asian Journal of Control*, vol. 1, no. 4, pp. 205–228, 1999.

[33] S. S. Ge, C. C. Hang, and L. C. Woon, "Adaptive neural network control of robot manipulators in task space," *IEEE Trans. on Industrial Electronics*, vol. 44, no. 6, pp. 746–752, 1997.

[34] D. Y. Meddah, A. Benallegue, and A. R. Cherif, "A neural network robust controller for a class of nonlinear MIMO systems," in *Proc. IEEE Intl. Conf. on Robotics and Autom.*, Albuquerque, New Mexico, 1997, pp. 2645–2650.

[35] M. B. Cheng and C. C. Tsai, "Hybrid robust tracking control for a mobile manipulator via sliding-mode neural network," in *Proc. IEEE Intl. Conf. on Mechatronics*, Taipei, Taiwan, 2005, pp. 537–542.

[36] C. M. Kwan, D. M. Dawson, and F. L. Lewis, "Robust adaptive control of robots using neural network: Global tracking stability," in *Proc. IEEE Conf. on Decision and Control*, New Orleans, Louisiana, 1995, pp. 1846–1851.

[37] T. Hayakawa, W. Haddad, and N. Hovakimyan, "Neural network adaptive control for a class of nonlinear uncertain dynamical systems with asymptotic stability guarantees," *IEEE Trans. Neural Networks*, vol. 19, no. 1, pp. 80–89, Jan. 2008.

[38] Y. Tang and M. A. Arteaga, "Adaptive control of robot manipulators based on passivity," *IEEE Trans. Automat. Contr.*, vol. 39, no. 9, pp. 1871–1875, Sept. 1994.

[39] J. J. Slotine and W. Li, "Composite adaptive control of robot manipulators," *Automatica*, vol. 25, no. 4, pp. 509–519, Jul. 1989.

[40] W. E. Dixon, M. S. de Queiroz, D. M. Dawson, and T. J. Flynn, "Adaptive tracking and regulation of a wheeled mobile robot with controller/update law modularity," *IEEE Trans. Contr. Syst. Technol.*, vol. 12, no. 1, pp. 138–147, Jan. 2004.

[41] M. Krstic and P. V. Kokotovic, "Adaptive nonlinear design with controller-identifier separation and swapping," *IEEE Trans. Automat. Contr.*, vol. 40, no. 3, pp. 426–440, Mar. 1995.

[42] R. H. Middleton and C. G. Goodwin, "Adaptive computed torque control for rigid link manipulators," *System and Control Letters*, vol. 10, pp. 9–16, 1988.

[43] M. S. de Queiroz, D. M. Dawson, and M. Agarwal, "Adaptive control of robot manipulators with controller/update law modularity," *Automatica*, vol. 35, pp. 1379–1390, 1999.

[44] R. L. Leal and C. C. DeWit, "Passivity based adaptive control for mechanical manipulators using LS-type estimation," *IEEE Trans. Automat. Contr.*, vol. 35, no. 12, pp. 1363–1365, Dec. 1990.

[45] N. Sadegh and R. Horowitz, "An exponentially stable adaptive control law for robot manipulators," *IEEE Trans. Robot. Automat.*, vol. 6, no. 4, pp. 491–496, Aug. 1990.

[46] R. H. Middleton, "Hybrid adaptive control of robot manipulators," in *Proc. IEEE Conf. on Decision and Control*, Austin, TX, 1988, pp. 1592–1597.

[47] P. V. Kokotovic, "The joy of feedback: nonlinear and adaptive," *IEEE Control Syst. Mag.*, vol. 12, no. 3, pp. 7–17, Jun. 1992.

[48] A. Morse, "Global stability of parameter-adaptive control systems," *IEEE Trans. Automat. Contr.*, vol. 25, no. 3, pp. 433–439, Jun 1980.

[49] J.-B. Pomet and L. Praly, "Indirect adaptive nonlinear control," in *Proc. IEEE Conf. on Decision and Control*, 7–9 Dec. 1988, pp. 2414–2415.

[50] S. Sastry and A. Isidori, "Adaptive control of linearizable systems," *IEEE Trans. Automat. Contr.*, vol. 34, no. 11, pp. 1123–1131, Nov. 1989.

[51] F. Mrad and A. Majdalani, "Composite adaptive control of astable UUVs," *IEEE J. Oceanic Eng.*, vol. 28, no. 2, pp. 303–307, 2003.

[52] S. Abiko and G. Hirzinger, "An adaptive control for a free-floating space robot by using inverted chain approach," in *Proc. IEEE/RSJ Int. Conf. on Intelligent Robots and Systems*, 2007, pp. 2236–2241.

[53] E. Christoforou, "On-line parameter identification and adaptive control of rigid robots using base reaction forces/torques," in *Proc. IEEE Int. Conf. on Robotics and Autom.*, 2007, pp. 4956–4961.

[54] W.-J. Wang and J.-Y. Chen, "Composite adaptive position control of induction motor based on passivity theory approach," *IEEE Power Eng. Rev.*, vol. 21, no. 6, pp. 69–69, 2001.

[55] ——, "Compositive adaptive position control of induction motors based on passivity theory," *IEEE Trans. on Energy Conversion*, vol. 16, no. 2, pp. 180–185, 2001.

[56] E. Zergeroglu, W. Dixon, D. Haste, and D. Dawson, "A composite adaptive output feedback tracking controller for robotic manipulators," in *Proc. Amer. Control Conf.*, 1999, pp. 3013–3017.

[57] F. L. Lewis, C. Abdallah, and D. Dawson, *Control of Robot Manipulators*. New York: MacMillan Publishing Co., 1993.

[58] J. Reed and P. Ioannou, "Instability analysis and robust adaptive control of robotic manipulators," *IEEE Trans. Robot. Automat.*, vol. 5, no. 3, pp. 381–386, Jun. 1989.

[59] C. Makkar, W. E. Dixon, W. G. Sawyer, and G. Hu, "A new continuously differentiable friction model for control systems design," in *Proc. IEEE/ASME Intl. Conf. on Advanced Intelligent Mechatronics*, Monterey, CA, 2005, pp. 600–605.

[60] B. Xian, M. S. de Queiroz, and D. M. Dawson, *A Continuous Control Mechanism for Uncertain Nonlinear Systems in Optimal Control, Stabilization, and Nonsmooth Analysis*. Heidelberg, Germany: Springer-Verlag, 2004.

[61] M. M. Polycarpou and P. A. Ioannou, "On the existence and uniqueness of solutions in adaptive control systems," *IEEE Trans. Automat. Contr.*, vol. 38, no. 3, pp. 474–479, Mar 1993.

[62] S. Gutman, "Uncertain dynamical systems–a Lyapunov min-max approach," *IEEE Trans. Automat. Contr.*, vol. 24, no. 3, pp. 437–443, Jun 1979.

[63] H. K. Khalil, *Nonlinear Systems*, 3rd ed. New Jersey: Prentice-Hall, Inc., 2002.

[64] M. S. Loffler, N. P. Costescu, and D. M. Dawson, "QMotor 3.0 and the QMotor robotic toolkit: a PC-based control platform," *IEEE Control Syst. Mag.*, vol. 22, no. 3, pp. 12–26, Jun. 2002.

[65] N. Stefanovic, M. Ding, and L. Pavel, "An application of L2 nonlinear control and gain scheduling to erbium doped fiber amplifiers," *Control Eng. Practice*, vol. 15, pp. 1107–1117, 2007.

[66] T. Fujinaka, Y. Kishida, M. Yoshioka, and S. Omatu, "Stabilization of double inverted pendulum with self-tuning neuro-PID," in *Proc. IEEE-INNS-ENNS International Joint Conference on Neural Networks IJCNN 2000*, vol. 4, 24–27 July 2000, pp. 345–348.

[67] F. Nagata, K. Kuribayashi, K. Kiguchi, and K. Watanabe, "Simulation of fine gain tuning using genetic algorithms for model-based robotic servo controllers," in *Int. Sym. on Comput. Intell. in Robotics and Autom.*, June 2007, pp. 196–201.

[68] R. Kelly, V. Santibanez, and A. Loria, *Control of Robot Manipulators in Joint Space*. Springer, 2005.

[69] X. Zhang, D. M. Dawson, A. Behal, and B. Xian, "A modular controller for a class of uncertain MIMO nonlinear systems with non-symmetric input gain matrix," Clemson University, College of Engineering and Science, Control and Robotics (CRB), Tech. Rep. CU/CRB/9/10/04/1, 2004.

[70] W. E. Dixon, A. Behal, D. M. Dawson, and S. P. Nagarkatti, *Nonlinear Control of Engineering Systems: a Lyapunov-Based Approach*. Boston: Birkhuser, 2003.

[71] B. Igelnik and Y. Pao, "Stochastic choice of basis functions in adaptive function approximation and the functional-link net," *IEEE Trans. Neural Networks*, vol. 6, no. 6, pp. 1320–1329, 1995.

[72] H. D. Patino, R. Carelli, and B. R. Kuchen, "Stability analysis of neural networks based adaptive controllers for robot manipulators," in *Proc. Amer. Control Conf.*, Baltimore, Maryland, 1994, pp. 609–613.

[73] ——, "Neural networks for advanced control of robot manipulators," *IEEE Trans. Neural Networks*, vol. 13, no. 2, pp. 343–354, 2002.

[74] S. S. Ge and T. H. Lee, "Robust model reference adaptive control of robots based on neural network parametrization," in *Proc. IEEE Amer. Control Conf.*, Albuquerque, New Mexico, 1997, pp. 2006–2010.

[75] P. M. Patre, W. MacKunis, K. Kaiser, and W. E. Dixon, "Asymptotic tracking for uncertain dynamic systems via a multilayer neural network feedforward and RISE feedback control structure," *IEEE Trans. Automat. Contr.*, vol. 53, no. 9, pp. 2180 –2185, Oct. 2008.

[76] P. J. Werbos, "Back propagation: past and future," in *Proc. Int. Conf. Neural Nets*, vol. 1, 1989, pp. 1343–1353.

[77] D. O. Hebb, *The organization of behavior*. Wiley Inc., New-York, 1949.

[78] Z. Qu, R. A. Hull, and J. Wang, "Globally stabilizing adaptive control design for nonlinearly-parameterized systems," *IEEE Trans. Automat. Contr.*, vol. 51, no. 6, pp. 1073–1079, Jun. 2006.

[79] B. Xian, D. Dawson, M. de Queiroz, and J. Chen, "A continuous asymptotic tracking control strategy for uncertain multi-input nonlinear systems," Dept. of Mechanical Engineering, Louisiana State University, Tech. Rep. ME-MS1-03, February 2003.

[80] P. Patre, W. MacKunis, K. Dupree, and W. Dixon, "A new class of modular adaptive controllers, part I: Systems with linear-in-the-parameters uncertainty," in *Proc. Amer. Control Conf.*, Seattle, WA., 2008, pp. 1208–1213.

[81] P. Patre, K. Dupree, W. MacKunis, and W. Dixon, "A new class of modular adaptive controllers, part II: Neural network extension for non-LP systems," in *Proc. Amer. Control Conf.*, Seattle, WA., 2008, pp. 1214–1219.

[82] J.-J. Slotine and W. Li, "Adaptive robot control: A new perspective," in *Proc. IEEE Conf. on Decision and Control*, Dec. 1987, pp. 192–198.

[83] R. Lozano and B. Brogliato, "Adaptive control of robot manipulators with flexible joints," *IEEE Trans. Automat. Contr.*, vol. 37, no. 2, pp. 174–181, 1992.

BIOGRAPHICAL SKETCH

Parag Patre was born in Nagpur, India. He received his Bachelor of Technology degree in Mechanical Engineering from the Indian Institute of Technology Madras, India in 2004. After this he worked for a year as a Graduate Engineer Trainee in Larsen & Toubro Limited, Asia's largest engineering conglomerate. He then joined the Nonlinear Controls and Robotics (NCR) research group of the Department of Mechanical and Aerospace Engineering, University of Florida in the Fall of 2005 to pursue his doctoral research under the advisement of Dr. Warren E. Dixon.